DEVELOPMENT AND CHARACTERISATION OF INJECTABLE CALCIUM PHOSPHATE CEMENTS FOR USE IN VERTEBROPLASTY

PAR

Christian PITTET

ingénieur en sciences des matériaux diplômé EPF
de nationalité suisse et originaire de Carouge (GE)

REMERCIEMENTS

Un travail de thèse est une tâche de longue haleine dans laquelle il est important de pouvoir compter sur le soutien et les conseils des autres. L'accomplissement de ce travail a pu se faire grâce aux aides précieuses que j'ai pu recevoir pendant ce temps. C'est donc l'occasion, par ces quelques lignes, de rendre hommage à tous ceux qui m'ont aidé, sous quelque forme que ce soit.

Ce travail est le fruit d'une collaboration entre l'Hôpital Orthopédique de la Suisse Romande (HOSR) et le Laboratoire de Technologie des Poudres (LTP) à l'EPFL. J'aimerais donc remercier le Prof. Pierre-François Leyvraz et le Dr Pascal Rubin de l'HOSR, qui ont gardé un oeil critique sur mon travail, m'ont permis de prendre conscience des impératifs des cliniciens, et de concilier au mieux les attentes des uns et des autres.

Je tiens à remercier mon directeur de thèse, le Dr Jacques Lemaître, qui m'a appris à travailler de manière rigoureuse, scientifique, et qui s'est toujours montré disponible et prompt à la discussion. Je tiens aussi à adresser ma reconnaissance au Prof. Heinrich Hofmann qui m'a accueilli dans son laboratoire (LTP) et m'a soutenu financièrement quand cela s'est avéré nécessaire. Merci aussi au Dr Pascale Van Landuyt, qui m'a encadré au début de ma thèse, et m'a permis de rapidement devenir indépendant grâce à un efficace transfert de connaissances.

J'ai eu la chance de pouvoir compter sur l'aide de nombreux étudiants ayant travaillé avec moi. Les encadrer dans leur travail a toujours été pour moi source de grand plaisir, et les liens créés dans ces moments sont assurément plus que de simples liens professionnels. Qu'ils soient donc tous remerciés comme il se doit : Pierre Grasso, Cédric Barraud, Didier Falconnet, Florian Calame, Cédric von Grünigen, Delphine Marchand et David Brendlen.

Mes remerciements s'adressent aussi aux membres du LTP, avec qui mes contacts ont été aussi divers qu'enrichissants. Parmi ceux-ci, j'aimerais remercier tout particulièrement Stéphane Terrazzoni, et le Dr Paul Bowen qui m'a beaucoup appris sur la technologie des poudres.

VERSION ABRÉGÉE

L'objectif général du présent travail était de mieux comprendre comment les composants de départ des ciments brushitiques influencent des propriétés du ciment importantes en vue d'une application à la vertébroplastie. Ainsi, le travail s'est concentré sur les propriétés suivantes : la résistance mécanique, l'opacité aux rayons X, et le dégagement de chaleur lors de la prise.

Pour mener à bien cet objectif, un protocole de tests mécaniques a d'abord été développé de manière à caractériser les propriétés mécaniques de ciments phospho-calciques de la manière la plus complète possible. La représentation des cercles de Mohr a permis de comprendre que pour un matériau comme notre ciment, la contrainte à la rupture mesurée avec l'essai brésilien est inférieure à la résistance à la traction car le rapport des résistances en compression et en traction est inférieur à huit. Néanmoins, l'essai brésilien ou essai de compression diamétrale reste un test facile à utiliser avec des matériaux fragiles et requiert des géométries d'échantillons simples. C'est pourquoi nous le considérons comme un essai approprié à nos ciments. Il a donc été utilisé pour mesurer la résistance à la traction indirecte des ciments testés tout au cours de ce travail.

La réduction des tailles des particules de deux des poudres de départ, MCPM et CSH, a permis d'accroître de manière significative les résistances en compression et en traction indirecte. Le broyage de ces poudres a multiplié par cinq la résistance en compression et par trois celle en compression diamétrale. Les résistances de ces ciments, faits avec du MCPM et du CSH broyés, ont été les plus élevées parmi toutes celles mesurées lors de ce travail : 4.1 MPa en compression diamétrale, et 22.1 MPa en compression simple. Les propriétés mécaniques de ces ciments se sont montrées fortement dépendantes de la granulométrie et de la pureté de la poudre de CSH.

Un modèle mathématique a été développé pour calculer le coefficient d'atténuation linéique de tout matériau dont la composition est connue. Il a ensuite été validé par des mesures expérimentales. Le coefficient d'atténuation linéique standard qu'un ciment destiné à la vertébroplastie devrait avoir a été calculé. Il est de 2.47 cm^{-1}, dans les conditions simulées. Le calcul du coefficient d'atténuation linéique du ciment brushitique a montré que ce matériau n'est pas assez radio-opaque pour être utilisé de manière sûre en vertébroplastie. C'est pourquoi des molécules iodées ont été incorporées à une formulation de ciment brushitique, de manière à produire l'opacification aux rayons X requise. Il a été constaté que

l'incorporation d'Iopentol, un agent de contraste communément utilisé dans des applications d'imagerie aux rayons X, n'est pas néfaste aux propriétés mécaniques du ciment et n'influence pas non plus le temps de prise de la réaction.

Enfin, un calorimètre sur mesure a été développé pour la mesure de paramètres cinétiques et thermométriques des ciments. Une unique mesure permet de calculer la vitesse maximale des réactions de prise, les temps de travail et de prise des pâtes de ciment, le taux de conversion des ciments, et l'élévation de température lors de la prise. Les résultats montrent que le degré d'hydratation du sulfate de calcium ont une influence marquée sur la cinétique de la réaction de prise. La réaction est accélérée par le sulfate de calcium di-hydraté car il fournit des sites de nucléation hétérogène pour la précipitation de la brushite. Le sulfate de calcium hémi-hydraté, au contraire, ralentit la réaction de prise en relâchant des ions sulfates dans le liquide de gâchage. Comme la réaction de prise est plus rapide quand du CSD est utillisé, la production de chaleur a lieu plus rapidement et s'accumule dans le système. Ceci entraîne une élévation plus importante de la température lors de la prise.

ABSTRACT

The global objective of this thesis was to understand how the starting components of brushite cements influence the cement properties relevant for its use in vertebroplasty. Therefore, this work focussed on the following cement properties : mechanical strength, X-ray opacity and heat release upon setting.

To carry out the global objective, a test protocol was first developed to characterise the mechanical properties of calcium phosphate cements. The Mohr's circles representation allowed to understand that for a material like our cement, ultimate stress measured with the Brazilian test can only underestimate tensile strength because the compressive/tensile strength ratio is lower than 8. Nevertheless, the Brazilian test remains a test that is easy to use with brittle materials and requires simple sample shape. Therefore, it was considered as an appropriate test for our cements, and was used as a way to measure the indirect tensile strength of the cements tested in the run of this work.

Refining two of the starting powders, MCPM and CSH, allowed to increase significantly both compressive and diametral tensile strengths. Milling of these powders provided a five-fold inrease in axial compression, and a three-fold increase in diametral compression. The mechanical strengths of cements made with milled MCPM and CSH were the highest measured in this thesis work : 4.1 MPa diametral tensile strength and 22.1 MPa compressive strength. The mechanical properties of the cement were found to be strongly dependent on both CSH granulometry and chemical purity.

A computer model was developed to calculate the linear X-ray attenuation coefficient of any material of known composition. It was then validated by experimental measurements. The standard linear X-ray attenuation coefficient a cement should exhibit to be used in vertebroplasty was found to amount 2.47 cm^{-1} for the conditions simulated. It was calculated from an acrylic cement composition considered a standard in vertebroplasty. Calculation of the attenuation coefficient of a brushite cement revealed that this material is not radiopaque enough for safe use in vertebroplasty. Therefore, we added iodinated molecules to a brushite cement formulation so as to produce the required X-ray opacification. We found that incorporation of Iopentol, a contrast media commonly used in X-ray imaging applications, does not impair the mechanical properties of the cement and does not alter the setting time of the reaction either.

Finally, a custom-made calorimeter was developed for measurement of kinetic and thermometric parameters of cements. One single measurement allowed calculation of the maximum reaction rate of the setting reactions, the working and setting times of the cement pastes, the degree of conversion of the cements, and the temperature increase induced by the setting reaction. The degree of hydration of the calcium sulfate was found to have a significant influence on the kinetics of the setting reaction. The reaction is accelerated by calcium sulfate dihydrate because it provides nuclei for heterogeneous precipitation of brushite. In contrast, calcium sulfate hemihydrate was found to slow down the reaction by releasing sulfate ions in the mixing liquid. As the reaction is faster when CSD is used, heat production occurs faster and accumulates in the system. As a consequence, the temperature elevation during setting is more important.

CHAPTER 1   GENERAL INTRODUCTION.

ABSTRACT

This introductive chapter aims at presenting the clinical context and the specific problematics of vertebroplasty, the various materials used nowadays with this application, and those likely to be used in the future. The introduction starts with the presentation of osteoporosis, as vertebroplasty generally treats vertebral fractures subsequent to this disease. Then, the vertebroplasty technique is described, and the specific requirements for a material suited to vertebroplasty are enunciated. The advantages and drawbacks of acrylic cements used nowadays in vertebroplasty are then presented. Then, the numerous calcium phosphate cement formulations developed until now are reviewed, with an emphasis on brushite cements.

Finally, the objectives of the thesis are presented, along with the organisation of the chapters.

Introduction

Vertebroplasty is a minimally invasive technique consisting in injecting a bone cement into a fractured vertebra, in order to provide mechanical stabilisation. The materials used nowadays for this application are acrylic cements. However, they present several drawbacks that will be discussed later. Calcium phosphate cements might replace acrylic cements for vertebroplasty on osteoporotic vertebrae in the near future, but they still need to be developed so as to fulfill the specific requirements for this application. This is what we propose to do in this thesis.

Osteoporosis

With the aging of the population, an increasing number of elderly people suffer osteoporosis, with symptomatic evidence or not. Osteoporosis is a widely spread disease in western countries, but the possible lack of evident and disabling symptoms makes it difficult to define: over the years, lots of various definitions of osteoporosis have been given. In 1991, a consensus development conference statement defined osteoporosis as "a disease characterized by low bone mass and microarchitectural deterioration of bone tissue, leading to enhanced bone fragility and a consequent increase in fracture risk".[1] This definition is rather conceptual, and more technical definitions have been proposed for clinical use since then.[2] However, it is sufficient for the present context.

Osteoporosis is one of the major public health problems facing postmenopausal women and aging individuals of both sexes. In the USA, about 1.5 million fractures per year can be ascribed to osteoporosis, 700'000 of them being vertebral fractures, 250'000 distal forearm fractures, 250'000 hip fractures, the remaining 300'000 concerning other limb sites.[3] The prevalence of radiographic vertebral compression fractures (VCFs) was found to be as high as 26% in women 50 years old or older (VCFs assessed radiographically are not necessarily painful).[4] Considered in its globality, the annual cost of osteoporosis to the US healthcare system is estimated to amount at least $5-$10 billion.[3] Statistics are more difficult to find for European countries. In France, 50'000 VCFs per year are diagnosed.[5]

Standard management of vertebral compression fractures includes back bracing, bed rest, narcotic administration, or spine surgery. The latter was always considered a heavy, risky procedure. However, since the middle of the eighties, a new minimally invasive procedure

was developed and is being more and more commonly used to treat osteoporotic vertebral fractures : this procedure is called vertebroplasty.

Vertebroplasty

Vertebroplasty is a minimally invasive procedure aiming at stabilizing and strengthening fragilized collapsing vertebral bodies. It consists in injecting percutaneously a bone cement into the vertebral body. The goal of the intervention is to reinforce mechanically the vertebra and to alleviate pain caused by the pathologic vertebral compression fracture of the vertebral body. The first vertebroplasty (VP) was performed in France in 1984 by Deramond and Galibert. They injected acrylic cement (PMMA) into a cervical vertebra weakened by an aggressive spinal angioma.[6] Since then, percutaneous VP has become more and more popular, and is about to become a standard of care for the treatment of pathologic VCFs in the US.[7]

There are various indications for VP, but the necessary indication is pain subsequent to VCF, whatever its etiology. VP has been performed for three indications in France : osteoporosis,[8,9] angiomas,[6,10] and tumors.[11,12,13] Since its introduction in the US in 1997,[14] the procedure tends to become more and more used for osteoporotic VBs, which is not surprising regarding the importance of this pathology in western countries. Many american surgeons consider the possibility to use VP as a prophylactic procedure, to reinforce osteoporotic VBs at risk of fracture. Currently, data likely to support prophylactic use of percutaneous VP are lacking. However, if minimally invasive VP is perfected, prophylactic prevention of osteoporotic VB collapse would be concevable.[15] Mathis et al[7] consider that prophylactic intervention could evolve if more physiological cements stimulating bone remodeling would become available. This shows clearly that clinicians consider seriously the possibility of using VP as a prophylactic procedure, but are not keen on doing it with acrylic cement, the biological behaviour of this product being not safe enough for such cases.

For thoracic and lumbar vertebrae, the approach[16] preferred is a postero-lateral transpedicular way (Figure 1) : needles are forced through one or both pedicles into the collapsed VB. The patient lies prone on a table, provided with conscious sedation and local anesthesia. As the procedure is percutaneous, the clinician must have a means to visualize needle positioning and cement flow into the VB. This is why VP is performed using fluoroscopic guidance (live X-ray imaging). The fluoroscopic equipment can be a biplane or a C-arm type. It is important to be aware that clear visualization of the cement during injection and careful monitoring for cement extravasation are the keys to making percutaneous VP a safe procedure.

a)   b)
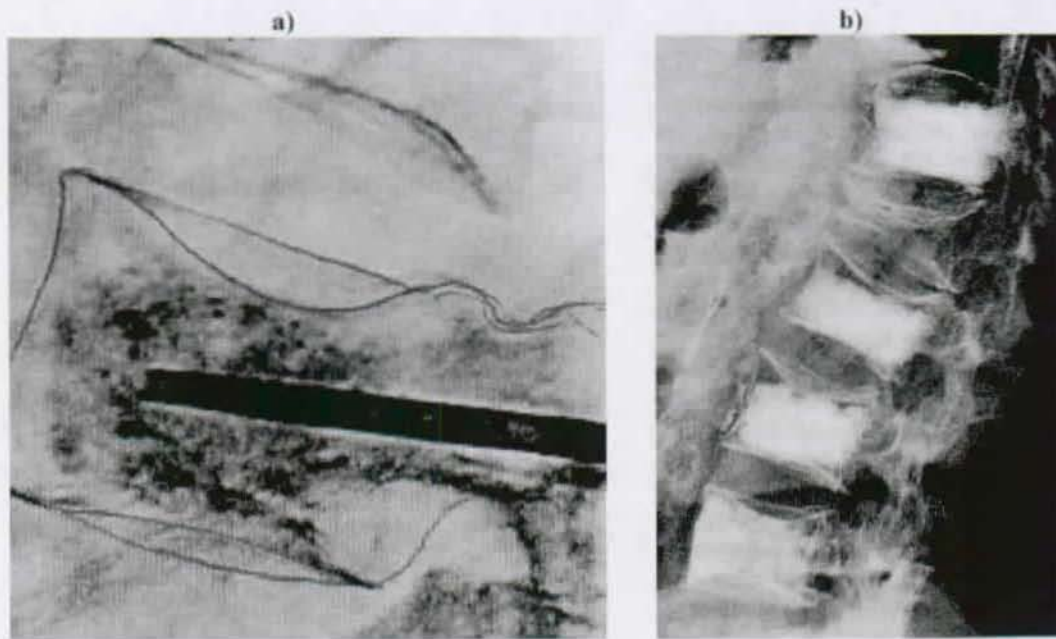
Figure 1 : a) X-ray lateral view of a posterolateral transpedicular injection. b) Injected osteoporotic fractured vertebrae.

The potential complications encountered after VP are radiculopathy,[13] rib fractures,[14] cement pulmonary embolism,[17] and spinal cord compression. The latter is always cited as a potentially hazardous complication, and explains why cement leakage out of the vertebra is to be avoided at any cost. However, to our knowledge, no such case was ever reported in the literature. The rate of complications depends on the indication treated : in the case of osteoporotic fractures, complications are few (1 to 2%) and most of the time transient and nonneurologic, whereas they are more frequent and sometimes persistent in cases of tumors.[7] Although the results regarding pain alleviation look excellent, the mechanism responsible for pain relief is still unknown.[15] It is still unclear whether it has to be attributed to monomer toxicity towards nervous tissue,[18] to thermal damage,[23] or to mechanical stabilization reducing fracture-site micro-motions.[19] Nevertheless, if VP were to be used prophylactically, one would expect good adhesion to bone tissue to allow bone remodeling at the implant surface. This implies that thermal necrosis would have to be avoided, which means that the cement to be used should not produce too much heat upon setting. Such requirements would necessarily preclude the use of acrylic cements.

In view of the considerations discussed above, it appears that, in the near future, vertebroplasty may well become a prophylactic procedure to stabilize osteoporotic vertebrae before painful symptoms occur. However, the patients to be treated will be individuals with longer life expectancy, at risk of vertebral fracture, but not complaining about any pain. Therefore, if a clinical intervention would be performed prophylactically, the risk to impair

patient's health should be minimal. To perform safe and efficient vertebroplasty, the material to be used in the future will have to fulfil various specifications :

- ✓ injectability,
- ✓ sufficient mechanical strength,
- ✓ sufficient X-ray opacity,
- ✓ limited heat release upon setting,
- ✓ biodegradability,
- ✓ osteoconductive properties (allowing recolonization by new bone).

Acrylic cements

Use of acrylic cement (PMMA) in orthopedic surgery goes back to the beginning of the 1960s, when Charnley used it to anchor a femoral head prosthesis to the shaft of a femur.[20] Despite its name ("cement"), this material is actually a polymeric material. Mixing pre-polymerized polymethyl-methacrylate (PMMA) powder to methyl-methacrylate liquid in presence of a polymerization initiator (like N,N-dimethyl-p-toluidine) produces a soft, dough-like mass that hardens as the polymerization reaction progresses. This is a mere exothermic polymerization process, but the fact that it consolids through mixing of a powder and a liquid to give a paste and finally a hardened product is the reason why it has been called "cement" by surgeons. Thus, the widespread use of acrylic cement for anchoring orthopedic prostheses to osseous sites is only due to a historical fact, and it is important to keep in mind that this material now considered as a biomaterial was in fact never developed in that sense. It is doubtful that this material would still be considered the material of choice for implantation into osseous sites if the situation would be reconsidered in the light of the materials at hand nowadays. The use of acrylic cement in percutaneous VP comes from the choice of Deramond and Galibert, who chose, logically, to use the material commonly used by surgeons as a bone cement.[6] However, the requirements for such a procedure are different from those used for cementing orthopedic prostheses : the main difference lies in the diameter of the cannula through which the cement is injected. As it is smaller in vertebroplasty, the cement viscosity has to be decreased to ensure easy flow through the needle and the trabecular pattern of bone. However, these changes may strongly influence the cement properties, as will be seen later. PMMA cements used in vertebroplasty are generally Simplex® P or Cranioplastic.[27,14]

Beside their "cementitious" behaviour, acrylic cements present the advantage of having high mechanical properties. Tensile and compressive strengths range from 25 to 30 MPa, and 60 to 80 MPa respectively, depending on the brand considered and the way it has been prepared.[21,22]

Drawbacks reported from clinical experience with acrylic cements are monomer toxicity[15] and high exothermicity[23] inducing thermal contact necrosis.[15,24] VP practicioners commonly alter the cement Solid/Liquid ratio to increase the setting time and decrease the viscosity.[16,14] However, these changes increase the heat produced by the polymerization reaction, decrease the mechanical properties of the hardened cement[25] and enhance the risk of leaving unreacted toxic monomer after setting. The polymeric character of acrylic cements makes them very radiolucent. Thus, addition of a radiopacifying agent is also a common operation prior to using PMMA for vertebroplasty. Barium sulphate can be used to enhance the cement radiopacity, but this addition was also found to be deleterious to the mechanical properties of the hardened product.[26] In practice, tungsten or tantalum powders are added as opacifiers for PMMA cements,[27] but addition of a heavy metal to a biomaterial is a risky procedure.

A new polymeric cement, Orthocomp (Orthovita Inc.), is being developed specifically for vertebroplasty, to overcome the deficiencies of PMMA cements. It is actually a glass-ceramic reinforced composite material with a matrix of Bis-phenol glycidyl dimethacrylate (BisGMA), Bis-phenol ethoxy dimethacrylate (BisEMA), and triethyleneglycol dimethacrylate (TEGDMA). The fillers, depicted as bioactive and inert, were found to promote direct contact between bone tissue and implant at the cement-bone interface.[28] This was never reported for PMMA cements, that tend to be encapsulated by a fibrous tissue. In a comparative in vitro study, Simplex® P and Orthocomp were injected into cadaveric human osteoporotic vertebrae, precrushed to simulate VCF. Vertebral bodies augmented with Orthocomp were significantly stronger than the controls and those augmented with Simplex® P.[29] In addition, Orthocomp presents the advantage of being less exothermic than PMMA cements.[23] However, even though Orthocomp seems to effectively overcome the main drawbacks of PMMA cements, it remains a non resorbable material and consequently cannot be replaced by newly grown bone.

In short, acrylic cements presented in this introduction possess mechanical properties sufficient for strengthening vertebral bodies. However, Cranioplastic and Simplex must be altered to meet the radiopacity requirements. Orthocomp is supposed to be more radiopaque than Simplex, but there is no evidence that its intrinsic radiopacity suits the needs of VP practicioners. Furthermore, all acrylic cements are, by their chemical nature, more or less

toxic and non degradable. In addition, the heat they produce upon setting may damage the surrounding bone tissue, impairing osseointegration of the implant. There is no discussion that these drawbacks cannot be accepted in the perspective of a use for prophylactic VP.

The numerous drawbacks associated with use of acrylic cements in vertebroplasty would be a sufficient reason to promote the use of another biomaterial, best suited to the specific requirements of percutaneous VP. Unfortunately, acrylic cements are the only materials presently at hand for surgeons. However, a new class of bone substitutes are being developed currently, presenting numerous advantages on PMMA cements : the calcium phosphate cements.

Calcium phosphate cements

Calcium phosphate cements (CPCs) were first developed by Brown and Chow to serve as remineralizing dental cements or as bone implant materials. The inventors foresaw very soon the potential interest these materials could present for the clinicians and the biomedical companies, and therefore patented their invention in 1985.[30]

This type of material is suited for applications where bone has to be reconstructed, like canal sealing and filling,[31] repair of alveolar bone defects,[32] reconstruction of frontal sinus,[33] cranioplasty,[34] or facial skeletal augmentation.[35]

Calcium phosphate formulations proposed by Brown and Chow consist in mixtures of TTCP with DCPD, DCP, OCP or TCP, that dissolve upon mixing in water to give rise to HAP precipitation (acronyms, see Table I). The hardened material is very well tolerated by the body since HAP is actually the mineral phase present in natural bone. Numerous studies conducted by various research groups have been done on this type of cement, dealing with physico-chemical properties, as well as in vitro and in vivo properties.[36,37] One of the numerous possible formulations described by Brown and Chow in their patent is now registered as a trademark : Bone Source™. The starting components consist in TTCP and DCP. This cement is indicated for use in the "repair of neurosurgical burr holes, contiguous craniotomy cuts and other cranial defects with a surface area no larger than 25 cm² per defect" (according to the product notice), which are all low stress-bearing applications.[38] This cement seems to be a clinical success, although no prospective clinical study is available at the moment. However, according to Chow himself, this product is too expensive because of the production cost of the TTCP powder. This is why he has now patented a new formulation without TTCP.[39] To our knowledge, only the physico-chemistry of this cement was studied,[40] and nothing was published until now about its in vitro or in vivo behaviours.

Table I : Acronyms, formulae and Ca/P ratios of calcium phosphate compounds.

Compound	Formula	Name	Ca/P
MCPM	$Ca(H_2PO_4)_2.H_2O$	Monocalcium Phosphate Monohydrate	0.50
CPP	Ca_2P_2O	Calcium Pyrophosphate	1.00
DCP	$CaHPO_4$	Dicalcium Phosphate Anhydrous (*Monetite*)	1.00
DCPD	$CaHPO_4.2H_2O$	Dicalcium Phosphate Dihydrate (*Brushite*)	1.00
OCP	$Ca_8H_2(PO_4)_6.5H_2O$	Octacalcium Phosphate	1.33
α, β-TCP	α, β-$Ca_3(PO_4)_2$	α, β-Tricalcium Phosphate	1.50
CDHA	$Ca_9H(PO_4)_6OH$	Calcium Deficient Hydroxyapatite	1.50
HAP	$Ca_5(PO_4)_3OH$	Hydroxyapatite	1.67
CHAP	$Ca_{18}(PO_4)_9(CO_3)_3(OH)_3$	Carbonated Hydroxyapatite	2.00
TTCP	$Ca_4(PO_4)_2O$	Tetracalcium Phosphate	2.00

Another CPC formulation consisting of MCPM, α-TCP and calcium carbonate was developed by Constantz et al.[41] The final product is carbonated apatite (dahllite). This formulation is patented in the USA[42] and is sold under the two following registered names : Norian SRS® (Skeletal Repair System) and CRS® (Craniofacial Repair System). This system seems to have been quite thoroughly studied, but relatively few data concerning its physico-chemical[43] or in vivo[44] properties were published. On the other hand, numerous clinical results have been published : Norian cements have been used, mainly in the US, in clinical indications like distal radius fractures,[45,46,47] hip fractures,[48] and craniofacial repair.[49]

ETEX Corporation has launched its own calcium phosphate cement, α-BSM™, announcing superior resorptive and osseointegrative properties compared to existing brands like Norian SRS® or Bone Source™. The starting components are HAP and DCPD, reacting with a saline isotonic solution to precipitate poorly crystalline apatite. An in vivo study where canine femoral slot defects were filled with this cement showed that new bone formation occurs in the implantation site. The biodegradability was clearly demonstrated, as 99% material resorption had occurred within 26 weeks.[50] In 1999, an in vitro study was conducted, aiming at comparing the strengthening effect on osteoporotic VBs of injected α-BSM™ with that of acrylic Simplex cement. Both cements were found to produce a two-fold increase in vertebral fracture strengths, and no significant difference was found between the two cements.[51] To allow easy injection, the S/L ratio had to be lowered compared with the S/L recommended by

ETEX Corporation, passing from 1.5 down to 1.1 g/cc. This S/L decrease surely has a negative effect on the mechanical properties of the cement. The compressive strength of α-BSM™ used with the recommended S/L is about 10 MPa (dry samples), which is rather low in comparison with other calcium phosphate cements like Norian SRS® or Bone Source™.[52] However, it is highly interesting to state that a cement exhibiting a compressive strength much lower than acrylic cements (60 to 80 MPa) can produce a comparable strengthening once injected in an osteoporotic vertebra. This finding is very encouraging for use of CPCs in vertebroplasty, and shows clearly that a CPC meant to be used in VP will not necessarily have to exhibit mechanical properties as high as those of acrylic cements.

Brushite cements

The calcium phosphate cement of interest in this work is the only one among CPCs whose final product is not HAP, but brushite (DCPD), another calcium phosphate phase, more soluble than HAP, hence undergoing faster biodegradation. To understand what was done in this thesis work, it is essential to be aware of the development history of this cement, since the composition evolved significantly throughout the past years. This is why a brief review of this cement development is presented here.

At the time this cement was first described (1987), many studies had been done on β-TCP based biomaterials.[53,54] As their biocompatibility and their resorbable character were demonstrated, Lemaître et al.[55] thought of combining the excellent biocompatibility of β-TCP with the advantages of calcium phosphate cements by proposing a new cement whose main final phase would be β-TCP. The proposed reaction was the following :[56]

$$Ca_3(PO_4)_2 + CaH_4(PO_4)_2.H_2O + 7H_2O \rightarrow 4CaHPO_4.2H_2O \qquad (1)$$

$$\beta\text{-TCP} \quad + \quad \text{MCPM} \quad + \text{water} \quad \rightarrow \quad \text{DCPD}$$
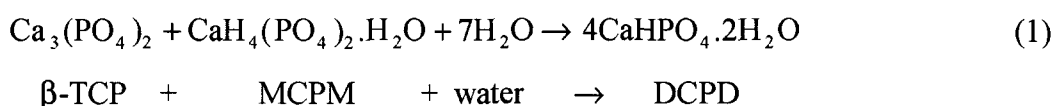
where the DCPD phase acts as a binder, forming bridges between the β-TCP aggregates. One of the factors studied was the amount of MCPM mixed to β-TCP, and it appeared that the higher this amount, the higher the diametral tensile strength (concentrations studied : between 5 and 20 wt% MCPM). This study showed the feasibility of such a calcium phosphate cement, but it also pointed out some problems that would have to be solved to make the cement usable in clinical conditions : a very short setting time (less than 30 seconds) and a very low diametral tensile strength (highest strength measured : 1 MPa, measured on dry samples). The second step consisted logically in incorporating potential setting regulators to

the cement.[57] The additives tested were calcium pyrophosphate (CPP), calcium sulfate dihydrate (CSD) and calcium sulfate hemihydrate (CSH). The setting time could be increased up to 10 minutes with CSD, but this compound was found to have a negative effect on the mechanical properties of the cement. On the other hand, CSH appeared to increase the mechanical properties as well as the setting time. The best cement produced in this study was one made of 64 wt% β-TCP, 16 wt% MCPM, 15 wt% CSH and 5 wt% CPP, with a setting time of 5 minutes and a diametral tensile stength of 3.2 MPa (mechanical tests made on dry samples). From a microstructural viewpoint, CSH was found to favour a needle-like shape of DCPD crystals, probably accounting for the benefits in terms of mechanical properties. It appeared only later that the relevant factor regarding setting time was the concentration in sulfate anions, with few effect of the counter-ion.[58] CSD particles were suspected to act as heterogeneous nuclei for DCPD crystals, due to their similar crystallographic properties.

The setting time being controllable and the mechanical properties increased, this composition (β-TCP – MCPM – CSH – CPP) was tested in vivo in metaphysial bone defects of dogs.[59] The implant was very well tolerated and incorporated by bone (absence of soft tissue between the resorbing material and the ingrowing bone), it resorbed slowly and showed osteoconductive properties, since the structural pattern of bone appeared to be restored 7 months after implantation. The main phase was unreacted β-TCP, binded by brushite. A second in vivo study was conducted with practically the same composition, but with another animal model : the cement was implanted in rabbit femoral condyles. Microradiography of bone tissue slices showed new bone apposition after 4 weeks, resorption of the brushitic phase, recolonisation by bone tissue after 8 weeks, and formation of a trabecular pattern after 16 weeks, confirming the adequate resorption rate and the osteoinductive character of the cement.[60]

Although this cement formulation provided excellent in vivo results, its composition was rather complex, and the number of starting components to be mixed together was too large to allow easy cement preparation. In an attempt to simplifiy the mixing gesture, a new formulation incorporating sulfate ions under the form of sulfuric acid rather than calcium sulfate powder was developed. A study was conducted to assess the influences of sulfuric acid concentration, initial MCPM content, and Solid/Liquid ratio (S/L) on setting time and diametral tensile strength.[61] The composition giving the best results was one made of 40 wt% MCPM, a 0.1 M sulfuric acid solution as mixing liquid, and a S/L of 2.5 g/cc. The mechanical tests were performed on wet samples, and the strengths observed (3 MPa) appeared to be

higher than those ever measured until then with CSH-containing cements. This new formulation differed from the previous ones not only by its starting components, but also by the proportion of final phases in the set cement. From that time, the β-TCP/MCPM cements could be named "brushite cements", this phase becoming the major phase in the hardened cement.

Objectives and chapters organization

Calcium phosphate cements are most likely to be used some day as the material of choice for prophylactic vertebroplasty, or even for standard vertebroplasty on painful osteoporotic vertebrae. However, their mechanical properties are low in comparison with those of acrylic cements, and their radiopacity has never been assessed. Furthermore, even though calcium phosphate cements are known to release less heat than acrylic ones, their thermodynamic properties need to be documented in more details.

The objective of this thesis is to understand how the starting components of the brushite cement influence the properties relevant for its use in vertebroplasty. Therefore, this work focusses on the following cement properties :

✓ mechanical strength,

✓ X-ray opacity,

✓ heat release upon setting.

Before the start of this work, mechanical properties of the brushite cement were always measured with the diametral compression test. This test produced poorly reproducible results, and the way it compared to direct tension test was still unclear. Thus, the aim of the first part of this work is to develop an improved test protocol to characterise as fully as possible the mechanical properties of calcium phosphate cements. We also intend to get a better insight into cement strength when submitted to multi-dimensional stresses. This study is presented in chapter 2, entitled "Mechanical characterization of brushite cements: A Mohr circles' approach".

The second part deals with the granulometric properties of the starting powders, as it was suspected to be an important factor affecting the mechanical properties of brushite cements. The test protocol developed in chapter 2 is used to measure the compressive and diametral tensile strengths of the cements. This study is presented in chapter 3, entitled "Influence of the starting powders granulometry on the mechanical strength of a calcium phosphate brushite cement".

X-ray opacity of cements used in vertebroplasty has been adapted in the field by VP practicioners. However, no specification regarding this cement property is available, and each group adds its specific radiopacifier to its cement, as to suit its needs. Therefore, we propose to define the appropriate degree of radiopacity needed for cements to be used in VP. A simple computer model allowing calculation of X-ray attenuation coefficients of cements is presented and evaluated in chapter 4, entitled "A model for calculations of bone cements radiopacity : Development and validation".

As X-ray opacity of the brushite cement has been found not to be sufficient for safe use of brushite cements in VP, we have developed a new formulation and measured the effect of various opacifiers on the mechanical properties of the opacified cement. These results are presented in chapter 5, "Radiopacification of calcium phosphate brushite cements with iodine-containing additives".

Then, a custom-designed calorimeter for setting reaction heat measurement has been developed. It allows to clarify how the starting components properties influence the heat released during setting and the kinetics of the setting reaction. This study is presented in chapter 6, entitled "Thermometric study of a calcium phosphate brushite cement".

Finally, a general conclusion, chapter 7, points out the main results obtained in this work and presents the remaining hurdles for use of brushite cement in vertebroplasty. The chapters of the thesis are organized the following way :

- **Chapter 1 :** General introduction.
- **Chapter 2 :** Mechanical characterization of brushite cements: A Mohr circles' approach.
- **Chapter 3 :** Influence of the starting powders granulometry on the mechanical strength of a calcium phosphate brushite cement.
- **Chapter 4 :** A model for calculations of bone cements radiopacity : Development and validation.
- **Chapter 5 :** Radiopacification of calcium phosphate brushite cements with iodine-containing additives.
- **Chapter 6 :** Influence of the starting compositions on kinetic and thermometric properties of brushite cements.
- **Chapter 7 :** General conclusions.

References

[1] Consensus development conference, 1991. Prophylaxis and treatment of osteoporosis. Am J Med 1991;90:107-110.

[2] Kanis JA, Milton LJ, Chrisitiansen C, Johnston CC, Khaltaev N. The diagnosis of osteoporosis. J Bone Miner Res 1994;9:1137-1141.

[3] Riggs BL, Melton LJ. The worldwide problem of osteoporosis: Insights afforded by epidemiology. Bone 1995;17:505S-511S.

[4] Melton LJ, Kan SH, Frye MA, Wahner HW, O' Fallon WM, Riggs BL. Epidemiology of vertebral fractures in women. Am J Epidemiol 1989;129:1000-1011.

[5] Cortet B. Oral communication. 10 années de vertébroplastie. Amiens (F), june 1998.

[6] Galibert P, Deramond H, Rosat P, Le Gars D. Note préliminaire sur le traitement des angiomes vertébraux par vertébroplastie acrylique percutanée. Neurochirurgie 1987;33:166-168.

[7] Mathis JM, Barr JD, Belkoff SM, Barr MS, Jensen ME, Deramond H. Percutaneous vertebroplasty: a developing standard of care for vertebral compression fractures. Am J Neuroradiol 2001;22:373-381.

[8] Debussche-Depriester C, Deramond H, Fardellone P, Heleg A, Sebert JL, Cartz L, Galibert P. Percutaneous vertebroplasty with acrylic cement in the treatment of osteoporotic vertebral crush fracture syndrome. Neuroradiol 1991;33:149-152.

[9] Cortet B, Cotten A, Boutry N, Flipo R-M, Duquesnoy B, Chastanet P, Delcambre B. Percutaneous vertebroplasty in the treatment of osteoporotic vertebral compression fractures: An open prospective study. J Rheumatol 1999;26:2222-2228.

[10] Deramond H, Darrasson R, Galibert P. Percutaneous vertebroplasty with acrylic cement in the treatment of aggressive spinal angiomas [in french]. Rachis 1989;1:143-153.

[11] Kaemmerlen P, Thiesse P, Bouvard H, Biron P, Mornex F, Jonas P. Vertébroplastie percutanée dans le traitement des métastases: Technique et résultats. J Radiol 1989;70:557-562.

[12] Weill A, Chiras J, Simon JM, Rose M, Sola-Martinez T, Enkaoua E. Spinal metastases: Indications for and results of percutaneous injection of acrylic surgical cement. Radiol 1996;199:241-247.

[13] Cotten A, Dewatre F, Cortet B, Assaker R, Leblond D, Duquesnoy B, Chastanet P, Clarisse J. Percutaneous vertebroplasty for osteolytic metastases and myeloma: Effects of the percentage of lesion filling and the leakage of methyl methacrylate at clinical follow-up. Radiol 1996;200:525-530.

[14] Jensen ME, Evans AJ, Mathis JM, Kallmes DF, Cloft HJ, Dion JE. Percutaneous polymethylmethacrylate vertebroplasty in the treatment of osteoporotic vertebral body compression fractures: Technical aspects. Am J Neuroradiol 1997;18:1897-1904.

[15] Bostrom MPG, Lane JM. Future directions: augmentation of osteoporotic vertebral bodies. Spine 1997;22:38S-42S.

[16] Deramond H, Depriester C, Toussaint P, Galibert P. Percutaneous vertebroplasty. Semin Musculoskel Radiol 1997;1:285-295.

[17] Padovani B, Kasriel O, Brunner P, Peretti-Viton P. Pulmonary embolism caused by acrylic cement: A rare complication of percutaneous vertebroplasty. Am J Neuroradiol 1999;20:375-377.

[18] Dahl OE, Garvick LJ, Lyberg T. Toxic effects of methylmethacrylate monomer on leukocytes and endothelial cells in vitro. Acta Orthop Scand 1994;65:147-153.

[19] Belkoff SM, Maroney M, Fenton DC, Mathis JM. An in vitro biomechanical evaluation of bone cements used in percutaneous vertebroplasty. Bone 1999;25:23S-26S.

[20] Charnley J. Anchorage of the femoral head prosthesis to the shaft of the femur. J Bone and Joint Surg 1960;42:28.

[21] Saha S, Pal S. Mechanical properties of bone cement: A review. J Biomed Mater Res 1984;18:435-462.

[22] Davies JP, O' Connor DO, Greer JA, Harris WH. Comparison of the mechanical properties of Simplex P, Zimmer Regular, and LVC bone cements. J Biomed Mater Res 1987;21:719-730.

[23] Deramond H, Wright NT, Belkoff SM. Temperature elevation caused by bone cement polymerization during vertebroplasty. Bone 1999;25:17S-21S.

[24] Jeffries CD, Lee AJC, Ling RSM. Thermal aspects of self-curing polymethacrylate. J Bone Joint Surg 1975;57B:511-518.

[25] Jasper LE, Deramond H, Mathis JM, Belkoff SM. The effect of monomer-to-powder ratio on the material properties of Cranioplastic. Bone 1999;25:27S-29S.

[26] de Wijn JR, Slooff TJ, Driessens FC. Characterization of bone cements. Acta Orthop Scand 1975;46:38-51.

[27] Deramond H, Depriester C, Galibert P, Le Gars D. Percutaneous vertebroplasty with polymethylmethacrylate: Technique, indications, and results. Radiol Clin North Am 1998;36:533-546.

[28] Fujita H, Nakamura T, Tamura J, Kobayashi M, Katsura Y, Kokubo T, Kikutani T. Bioactive bone cement: Effect of the amount of glass-ceramic powder on bone-bonding strength. J Biomed Mater Res 1998;40:145-152.

[29] Belkoff SM, Mathis JM, Erbe EM, Fenton DC. Biomechanical evaluation of a new bone cement for use in vertebroplasty. Spine 2000;25:1061-1064.

[30] Brown WE, Chow LC. Dental restorative cement pastes, US Patent 4,518,430, 1985.

[31] Hong YC, Wang JT, Hong CY, Brown WE, Chow LC. The periapical tissue reaction to a calcium phosphate cement in the teeth of monkeys. J Biomed Mater Res 1991;25:485-498.

[32] Sugawara A, Nishiyama M, Kusama K, Moro I, Nishimura S, Kudo I, Chow LC, Takagi S. Histological reactions of calcium phosphate cement. Dent Mater 1992;11:11-16.

[33] Friedman CD, Costantino PD, Jones K, Chow LC, Pelzer HJ, Sisson GA. Hydroxyapatite cement II. Obliteration and reconstruction of the cat frontal sinus. Arch Otolaryngol, Head Neck Surg 1991;117:379-384.

[34] Costantino PD, Friedman CD, Jones K, Chow LC, Sisson GA. Experimental hydroxyapatite cement cranioplasty. Plast Reconstr Surg 1992;90:174-191.

[35] Shindo ML, Costantino PD, Friedman CD, Chow LC. Facial skeletal augmentation using hydroxyapatite cement. Arch Otolaryngol, Head Neck Surg 1993;119:185-190.

[36] Chow LC, Takagi S. Calcium phosphate cements. Cem Res Prog 1994, ed. by Struble LJ, Am Ceram Soc. 189-202.

[37] Lemaître J. Injectable calcium phosphate hydraulic cements: New developments and potential applications. Innov Tech Biol Med 1995;16(S1):109-120.

[38] Friedman CD, Costantino PD, Takagi S, Chow LC. Bone Source™ hydroxyapatite cement: a novel biomaterial for craniofacial skeletal tissue engineering and reconstruction. J Biomed Mater Res (Appl Biomater) 1998;43:428-432.

[39] Chow LC, Takagi S. Self-setting calcium phosphate cements and methods for preparing and using them. US Patent 5,525,148, 1996.

[40] Takagi S, Chow LC, Ishikawa K. Formation of hydroxyapatite in new calcium phosphate cements. Biomater 1998;19:1593-1599.

[41] Constantz B R, Ison I C, Fulmer M T, Poser R D, Smith S T, Van Wagoner M, Ross J, Goldstein S A, Jupiter J B, Rosenthal D I. Skeletal repair by in situ formation of the mineral phase of bone. Science 1995;267:1796-1799.

[42] Constantz BR. Methods for in situ prepared calcium phosphate minerals. US Patent 5,129,905, 1992.

[43] Morgan EF, Yetkinler DN., Constantz BR., Dauskardt RH. Mechanical properties of carbonated apatite bone mineral substitute: strength, fracture and fatigue behaviour. J Mater Sci Mater Med 1997;8:559-570.

[44] Constantz BR, Barr BM, Ison IC, Fulmer MT, Baker J, McKinney L, Goodman SB, Gunasekaren S, Delaney DC, Ross J, Poser RD. Histological, chemical, and crystallographic analysis of four calcium phosphate cements in different rabbit osseous sites. J Biomed Mater Res 1998;43:451-461.

[45] Kopylov P, Runnqvist K, Jonsson K, Aspenberg P. Norian SRS versus external fixation in redisplaced distal radial fractures. A randomized study in 40 patients. Acta Orthop Scand 1999;70:1-5.

[46] Cohen MS, Whitman K. Calcium phosphate bone cement--the Norian skeletal repair system in orthopedic surgery. AORN J. 1997;65:958-962.

[47] Sanchez-Sotelo J, Munuera L, Madero R. Treatment of fractures of the distal radius with a remodellable bone cement: a prospective, randomised study using Norian SRS. J Bone Joint Surg Br 2000;82:856-863.

[48] Goodman SB, Bauer TW, Carter D, Casteleyn PP, Goldstein SA, Kyle RF, Larsson S, Stankewich CJ, Swiontkowski MF, Tencer AF, Yetkinler DN, Poser RD. Norian SRS cement augmentation in hip fracture treatment. Laboratory and initial clinical results. Clin Orthop 1998;348:42-50.

[49] Mahr MA, Bartley GB, Bite U, Clay RP, Kasperbauer JL, Holmes JM. Norian craniofacial repair system bone cement for the repair of craniofacial skeletal defects. Ophthal Plast Reconstr Surg 2000;16:393-398.

[50] Knaack D, Goad MEP, Aiolova M, Rey C, Tofighi A, Chakravarthy P, Duke Lee D. Resorbable calcium phosphate bone substitute. J Biomed Mater Res (Appl Biomater) 1998;43:399-409.

[51] Bai B, Jazrrawi LM, Kummer FJ, Spivak JM. The use of an injectable, biodegradable calcium phosphate bone substitute for the prophylactic augmentation of osteoporotic vertebrae and the management of vertebral compression fractures. Spine 1999;24:1521-1526.

[52] Pittet C, Van Landuyt P, Lemaître J. Unpublished results.

[53] Klein CPAT, Driessen AA, De Groot K, Van den Hoff A. Biodegradation of various calcium phosphate materials in bone tissue. J Biomed Mater Res 1983;17:769-784.

[54] Akao M, Aoki H, Kato K, Sato A. Dense polycrystalline b-tricalcium phosphate for prosthetic application. J Mater Sci 1982;17:343-346.

[55] Lemaître J, Mirtchi AA, Mortier A. Calcium phosphate cements for medical use: State of the art and perspectives of development. Silic Ind 1987;9-10:141-146.

[56] Mirtchi AA, Lemaître J, Terao N, Calcium phosphate cements: study of the β-tricalcium phosphate-monocalcium phosphate system. Biomater 1989;10:475-480.

[57] Mirtchi AA, Lemaître J, Munting E. Calcium phosphate cements: action of setting regulators on the properties of the β-tricalcium phosphate – monocalcium phosphate cements. Biomater 1989;10:634-638.

[58] Bohner M, Lemaître J, Ohura K, Hardouin P. Effects of sulfate ions on the in vitro properties of β-TCP – MCPM – water mixtures. Preliminary in vivo results. Bioceramics : Materials and Applications. pp. 245-259. Ed. by Fishma G, Clare A, and Hench L. American Ceramic Society, Westerville, OH, 1995.

[59] Munting E, Mirtchi AA, Lemaître J. Bone repair of defects filled with a phosphocalcic hydraulic cement : an in vivo study. J Mater Sci Mater Med 1993;4:337-344.

[60] Ohura K, Bohner M, Hardouin P, Lemaître J, Pasquier G, Flautre B. Resorption of, and bone formation from, new β-tricalcium phosphate-monocalcium phosphate cements: an in vivo study. J Biomed Mater Res 1996;30:193-200.

[61] Van Landuyt P, Lowe C, Lemaître J. Optimization of setting time and mechanical strength of β-TCP/MCPM cements. Bioceramics 10:477-480. Ed. by L. Sedel and C. Rey, 1997.

CHAPTER 2   MECHANICAL CHARACTERIZATION OF

BRUSHITE CEMENTS: A MOHR CIRCLES'

APPROACH.

ABSTRACT

Dry and wet brushite cements with various solid/liquid ratios were tested in compression and
tension. Two different testing techniques were used to determine tensile strength : Direct
Tensile test (DT) and Diametral Compression test (DC) (Brazilian test), which is an indirect
way of measuring tensile strength on brittle materials. Statistical analysis of the results
obtained on dry cements points to a constant ratio between the values measured by DT and
Brazilian tests (DC/DT = 85%).

The Mohr's circles representation allows to understand that for a material like our cement, the
ultimate stress measured with the Brazilian test is an underestimate of the tensile strength
because the compressive/tensile strength ratio is lower than 8. The second consequence of
this low ratio is that in the Brazilian test, the plane along which fracture initiates undergoes
not only a normal tensile stress, but also a tangential stress component. Thus, the state of
stress on the fracture plane differs from the one taking place in the direct tensile test.
Consequently, with such a material ($\sigma_c/\sigma_t < 8$), the Brazilian test does not allow to estimate
the true tensile strength.

INTRODUCTION

Calcium phosphate cements are bone filling materials whose biocompatibility, resorption and capacity of osteoconduction have been shown in previous *in vivo* studies.[1,2] The cement can be injected directly into a bone defect and hardens *in situ*. Its mechanical properties develop during the setting reaction.

The calcium phosphate cement used in this study is a modification of the brushite cement developed by Mirtchi *et al.* in 1989.[3] Since no systematic study of the mechanical resistance of this cement has been done yet, there is a lack of data concerning its mechanical properties. As this cement is meant to be used as a bone graft, and as one of bone's first functions is to support body weight, characterisation of the mechanical resistance of the cement is a priority. Measurement of the mechanical resistance can be done by various testing methods. This is particularly true for the tensile strength, for which numerous mechanical tests have been developed. This property can thus be determined by direct tensile, indirect tensile, 3- or 4-point bending, or biaxial bending tests. Although all these tests allow measurement of tensile strength, they do not necessarily all give the same results, because stress distribution or effective volume are not the same in all these tests. This is the reason why information about the testing method and specimen dimensions should always be indicated along with the reported results.

Diametral compression test, also named Brazilian test or indirect tension test, is routinely used for brittle materials like ceramics or concrete. In the literature concerned with biocements, tensile strength data are very often derived from the Brazilian test. It allows the use of an experimental setup similar to the one used for axial compression, to keep simple sample shape, and to avoid the problem of mounting specimens on the universal testing machine. The advantage of the diametral compression test is that fracture starts within the specimen, and the measured value is, therefore, not dependent on the surface state.

Although calcium phosphate cements are viewed as promising bone grafting materials, their mechanical resistance is too weak to allow their application in high-load conditions. Many studies have reported diametral tensile and uni-axial compressive strengths of various calcium phosphate cements. Martin and Brown[4] measured tensile and compressive strengths of 13.1 and 173 MPa, respectively, for a Ca-deficient apatite. Strengths of carbonated apatite

were 10.1 MPa in tension and 63.8 MPa in compression.[4] The samples were kept wet until the tests were performed. Diametral compression tests on wet specimens of TTCP-DCPA cements forming hydroxyapatite upon setting showed ultimate strengths varying between 1.5 and 7.5 MPa, according to the solid/liquid ratio of the starting components.[5] The same type of cement tested in compression shows 50 MPa strength.[6] Bermudez et al. performed strength measurements of most types of calcium phosphate developed around the world. They tested 26 cement formulations in diametral and uni-axial compression and found ultimate strengths largely lower than those presented in the literature, the stronger cement withstanding 2.8 and 12 MPa in tension and compression, respectively.[7] This statement shows that comparisons are difficult since conditions et sample preparation are not necessarily identical in different studies.

Although ultimate strength values measured in diametral compression are usually considered as representative of the direct tensile strength, comparison between direct tensile and diametral tensile strengths has (to our knowledge) never been done for biocements. This is why we propose to better understand how the two tests compare. To achieve this goal, we discuss the obtained results with help of the Mohr circles representation. In this study, diametral compression, uni-axial compression and direct tension tests were performed on dry and wet brushite cements prepared with different solid/liquid ratios.

EXPERIMENTAL

Experimental design

The following factors were tested to evaluate their influence on the mechanical properties : type of test, solid/liquid ratio, aging conditions. To determine the tensile strength of the cements, we used the direct tension test and the diametral compression test. Compression strength was measured with the uni-axial compression test. Solid/liquid ratios were made to vary between 2.0 and 3.5 g/mL, by increments of 0.5. Solid/liquid ratio does in fact determine the final compacity of the specimens. Table I gives the mean porosity of the cements in relation with their solid/liquid ratio.

Table I : Open porosity of brushite cements vs. Solid/liquid ratio.

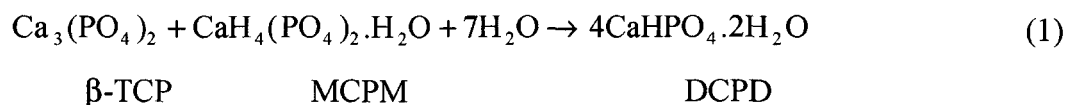| Solid/Liquid (g/mL)	2.0	2.5	3.0	3.5
Porosity (%)	41.9	35.3	30.7	25.8

Prior to testing, the specimens were placed 24 hours in ambient atmosphere (dry conditioning) or in a water-saturated atmosphere (wet conditioning). Table II summarizes the factors and the levels at which they were tested.

Table II : Factors tested and their levels.

Test	Conditioning	Sol./Liq. (g/mL)
Diametral compression		2.0
	Dry	2.5
Direct tension		
	Wet	3.0
Uni-axial compression		
		3.5

Sample preparation

The starting powders are β-tricalcium phosphate (β-TCP, synthesized in the laboratory) and monocalcium phosphate monohydrate (MCPM, Albright&Wilson), reacting in presence of water to form brushite (dicalcium phosphate dihydrate, DCPD) according to reaction 1. Small amounts of sodium pyrophosphate (Na2H2P2O7, Fluka) is added to the starting powders as a setting regulator. Mixing of the powders is made in a sulfuric acid solution (0.1M):

$$Ca_3(PO_4)_2 + CaH_4(PO_4)_2.H_2O + 7H_2O \rightarrow 4CaHPO_4.2H_2O \tag{1}$$

$$\text{β-TCP} \qquad\qquad \text{MCPM} \qquad\qquad\qquad\qquad \text{DCPD}$$

The cement paste was prepared in a mortar and introduced with a spatula in a 2mL syringe whose extremity was previously cut. After each cement addition into the syringe, the paste was vibrated to eliminate entrapped air bubbles. Hardened cement was expelled from the syringe by pushing on its plug. The so-obtained cylinders had a 8.7 mm diameter. Their faces were then ground (SiC paper 120) in order to obtain the desired height and parallelism between the faces. The height of the cylinders varied depending on the test to which the specimen was destinated.

Direct tension test and uni-axial compression test

The direct tension test consists of applying a tensile load on a specimen along a given axis. The applied force on a plane normal to the load axis must be uniform on the whole section. Direct tension test is rarely used on brittle materials, since misalignement problems are difficult to avoid. As brittle materials do not deform until rupture, misalignment of the specimen may induce a tangential stress component that may lower the measured strength of the material.

Another difficulty encountered with direct tension tests on brittle samples is how to fix them on the testing machine. Various fixation systems have been developed[9], but the easiest way seems to be the use of a glue since it allows to keep a simple specimen shape. However, use of a glue implies that the glued interfaces are more resistant than the tested specimens.

Direct tension tests were performed on an Adamel Lhomargy DY31 universal testing machine with a 2 kN load cell. Loading rate was 1 mm/min. We used a mechanical joint allowing auto-alignment of the system to avoid stresses outside the loading axis. Specimens were cylindrical, with 8.7 mm diameter and 12 mm length. Each treatment was repeated 4 times.

Fixation of the specimen on the testing apparatus was made by cementing both faces of the cylinder on aluminium cylinders screwed on the testing device. The glue was actually a mortar (Sikadur®30, Sika®). Before cementing, the aluminium cylinders' faces were ground on a polishing machine and sanded to improve the mechanical resistance of the mortar-metal interface.

Axial compression tests were performed on an Instron 4467 universal testing machine with a 30 kN load cell. The compressive load rate was 0.2 kN/min. Specimens were cylindrical, with 8.7 mm diameter and 18 mm length. Each treatment was repeated 4 times.

Diametral compression test (Brazilian test)

The diametral compression test was developed in Brazil in 1952 by Carneiro and Barcellos.[10] It allows measurement of brittle materials' tensile strength by applying a compressive load along two opposite generators of a cylinder, as shown in Figure. 1a. Failure takes place along the plane defined by the two generators (diametral plane). Even though this test allows measurement of brittle materials' tensile strength, the stress distribution strongly differs from

the one taking place in the direct tension test. It is uni-axial in the direct tension test, whereas it is biaxial in the case of the Brazilian test.
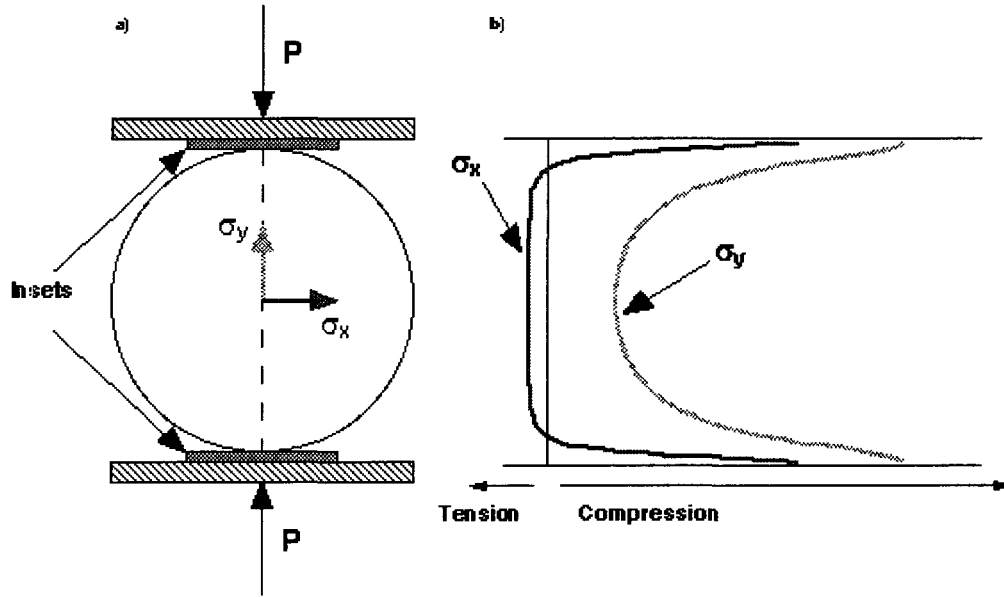

Figure 1 : Diagram showing (a) the Brazilian test setup and (b) the stress distribution along the vertical diametral plane.

The Brazilian test is thus an indirect method for measuring tensile strength. One generally only considers the vertical diametral plane of the tested specimen, since stresses are highest on this plane.[11] Calculation of the applied stress at failure is made with help of equation (4). Principal stresses σ_x and σ_y acting on the loaded diametral plane are expressed in the following manner (with the assumption : $a \le 0.1$ D)[12] :

$$\sigma_x = \frac{-2P}{\pi DL}\left[1 - \frac{D}{2a}(\varphi - \sin\varphi)\right] \tag{2}$$

$$\sigma_y = \frac{-2P}{\pi DL}\left(1 - \frac{D}{2a}(\varphi + \sin\varphi) - \frac{1}{1 - r/D}\right) \tag{3}$$

where P is the applied force, D the cylinder diameter, L its length, r the distance between the considered point and the closest generator, and a the width of the insets ($\varphi = 2$ arctg(a/2r)). These symbols are represented in Figure 2, where M is the point on which stresses are calculated. σ_x and σ_y variations along the diametral plane, calculated after (2) and (3), are shown in Figure 1b. The horizontal stress σ_x is constant and in tension over about three quarters of the diameter and becomes compressive when approaching the contact points,

whereas the vertical stress σ_y is compressive on the whole diameter, increasing from the centre (where $\sigma_y = -3\ \sigma_x$) to the edges of the diametral plane. The stress distribution in the specimen depends on the width of the insets. The wider the inset, the lower the compressive stress near the contact points, and the shorter the portion of the diametral plane submitted to tension. But whatever the width of the inset, the σ_x/σ_y ratio remains constant in the middle of the plane. At the centre of the diameter, on the diametral plane, equation (2) for the horizontal stress σ_x simplifies in the following way :

$$\sigma_x = \frac{-2P}{\pi D L} \tag{4}$$

This equation is used for calculating the stress at failure from the applied force. It assumes that failure starts at the centre of the loaded diameter. If this is the case, the specimens break down into two half-cylinders, due to the tensile stress σ_x.
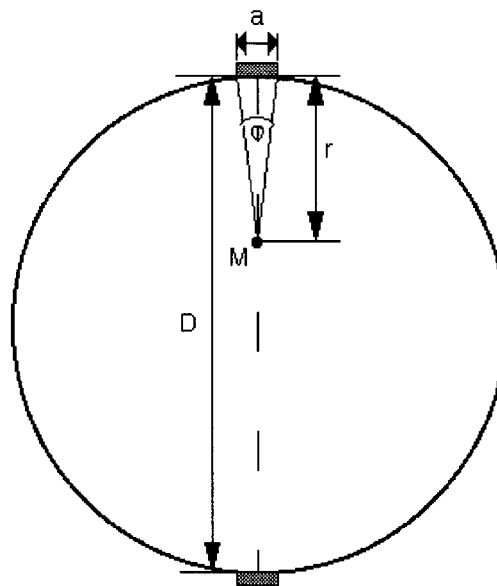
Figure 2 : Diagram showing the symbols used for stress calculations.

Measurements were made with an Adamel Lhomargy DY31 universal testing machine equipped with a 2 kN load cell. The steel platens of the press were covered with a cardboard to insure contact along the whole cylinder and to distribute the applied force on a certain width. The inset width was not defined *a priori* since they covered the whole platen surface. The effective inset width depends on how deep the specimen went into the inset. That width may be estimated by measuring the prints left on the cardboard by the cylinder after fracture. Each test was performed on an intact region of the insets.

Specimens were cylindrical, 8.7 mm in diameter and 6 mm in height. Loading rate was 1 mm/min. Each treatment was repeated 4 times. Cardboard pads covering the steel platens of the press were used to reduce the compressive stress along the contact line between the cylinder and the platens.

RESULTS

Diametral tensile strength

The experiment was organised in a 2×4 experimental design (with 4 replicates) and analysed with the Anova technique.[13] Results of ultimate stress versus S/L ratio for dry and wet brushite cements are presented in Figure 3. Within the range of tested S/L ratios, dry cements are more resistant than the wet ones. Such a difference between dry and wet specimens has been observed in previous studies.[14]
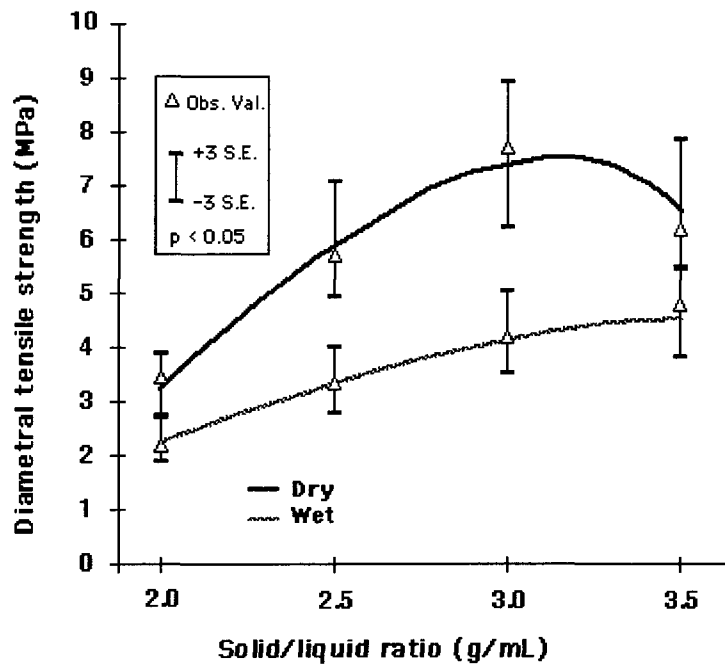
Figure 3 : Diametral tensile strengths of dry and wet brushite cements vs. solid/liquid ratio.

The highest ultimate strength was measured on the 3 g/mL-cements, which are nevertheless not the most compact specimens (see Table I). The ultimate stress goes through a maximum at 3 g/mL, and decreases for higher S/L ratios. Difficulty to eliminate air bubbles entrapped in the 3.5 g/mL-cement paste when mixing may explain the decrease in strength measured on

these cements. Air bubbles entrapped within the structure may cause local stress concentrations leading to failure at a lower apparent stress than what a macropore-free cement could withstand. Elimination of these air bubbles when moulding the cement paste would result in an ultimate stress higher than the one of the 3 g/mL-cements. Thus, the tensile strength decrease at high S/L ratios (>3 g/mL) can be ascribed to cement preparation and is therefore not directly related to the specimen's apparent density.

Comparison between direct and indirect tension tests

The experiment was organised in a 2 × 4 experimental design (with 4 replicates) and analysed with the Anova technique. Figure 4 presents results of ultimate tensile stress as a function of the S/L ratio for dry brushite cements tested with the indirect (Brazilian) and direct tension tests. Statistical analysis of the measured values shows that the strength ratio remains constant over the whole investigated S/L range : tensile strength as measured with the Brazilian test equals 85% of the strength determined with the direct tension test.
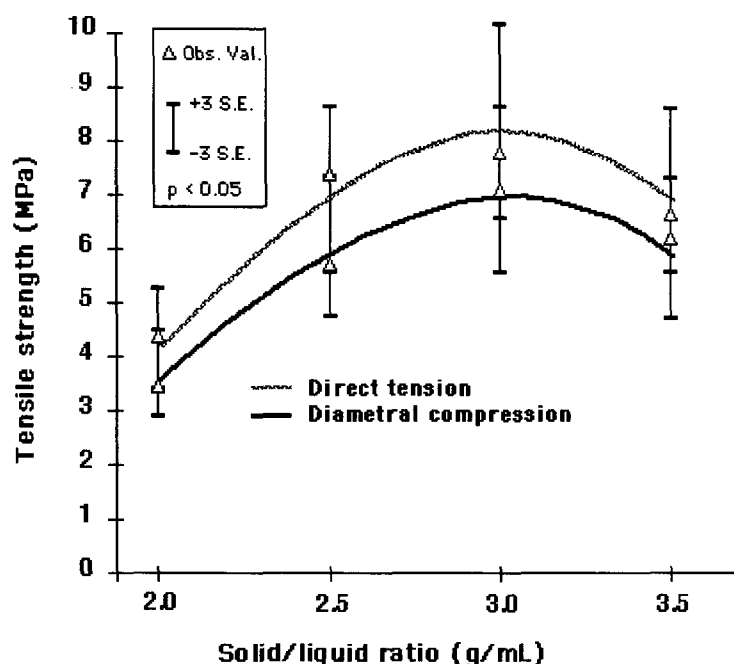

Figure 4 : Direct and indirect tensile strengths of dry brushite cements vs. solid/liquid ratio.

Compressive strength

The experiment was organised in a 2 × 4 experimental design (with 4 replicates) and analysed with the Anova technique. The compressive strength was found to increase linearly with the

S/L ratio, for both wet and dry cements, as shown in Figure 5. The highest compressive strengths were obtained on the 3.5 g/mL-cements. Monotonous increase of compressive strength with S/L ratio indicates that the defects (air bubbles) introduced into the cement structure when mixing do not have a detrimental effect on the compressive strength.
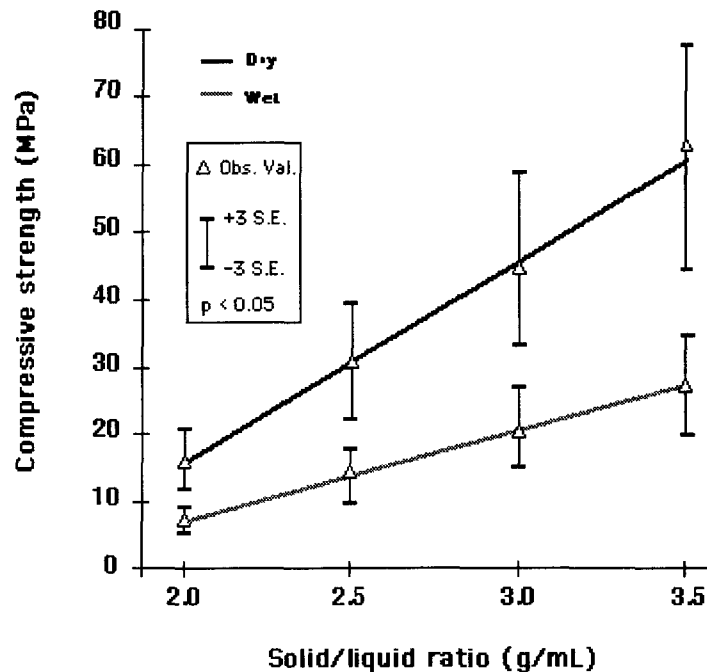
Figure 5 : Compressive strength of dry and wet brushite cements vs. solid/liquid ratio.

Contrary to tensile loading, failure starting at a defect does not lead alone to catastrophic failure of the whole specimen. This might be the reason why such defects are less detrimental to compressive strength. Observation of the fractured specimens shows that the orientation of fracture surfaces is always diagonal, leaving a conic shape at the bottom of the specimen (see Figure 6). This is typical of shear failure.
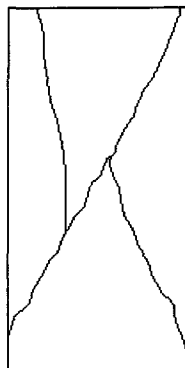
Figure 6 : Schematic representation of a typical failure obtained in compression.

DISCUSSION

Homogeneity of the specimens

Calculation of the ultimate tensile strength in diametral compression (Eq. 4) is based on hypotheses that are not necessarily fulfilled in the case of brushite cements, like homogeneity and continuity. When mixing and moulding the cement paste, it is difficult to eliminate bubbles completely from the paste, which eventually form spherical defects (macropores) in the hardened cement. Thus, the cement samples contain randomly distributed macroscopic defects which are likely to affect strength measurements.

It was sometimes observed in our diametral compression experiments that the fracture surface did not coincide with the vertical diametral plane. On these surfaces, one could often see a large pore that most probably initiated fracture. As this defect is not situated on the vertical diametral plane, fracture is initiated at a lower stress value than the one acting on the diametral plane. Since Eq.4 gives the stress on the latter, the mechanical resistance of the sample is thus underestimated.

In the diametral compression test, the volume actually tested represents only a fraction of the total sample volume. If the spherical macropores in the cement are not too numerous, as in the case of the less compact cements, the probability to find such a pore within the tested volume is low. Therefore, the average strength of such a cement measured with this test would be higher than the strength measured with the direct tension test.

These two considerations about the presence of air bubbles in the cement explain why contradictory effects on the tensile strength may be observed, depending on the testing procedure.

General remarks on the tests

Ultimate strengths measured in tension and compression in this study are significantly higher than those measured by Bermudez et al.[7] on various calcium phosphate cements. However, the experimental conditions being not rigorously identical, it would be risky to draw conclusions from this comparison.

The evolution of strength with S/L ratio was found to be different whether tested in tension or in compression. This might be a consequence of the differences in fracture modes. In simple

tension, a single crack (normal to the load axis) leads alone to catastrophic failure of the whole specimen. Therefore, a defect initiating a crack is responsible for the breakdown of the whole sample. On the other hand, in compression, the first initiated crack does not propagate alone until fracture of the specimen. Total breakdown of a specimen loaded in compression takes place as soon as many cracks have met to form the fracture surface. Therefore, the presence of macropores is less damageable for strength in compression than in tension. Tension loading can be viewed as a way to measure the internal cohesion of a material, whereas compression loading is representative of the resistance of the material to internal friction between planes subitted to both compressive and shearing stresses.

On wet cements, the direct tensile test did not give any handable results, for fracture always took place at the mortar-metal interface. The measured interface strength was 3.2 ± 0.9 MPa. Though disappointing, this result can be accepted as the lower limit of the tensile strength for wet brushite cements.

Statistical analysis of the results shows a constant ratio between direct and indirect strengths. Diametral tensile strength amounts to 85% of the strength measured with the direct tension test. For practical purpose, this observation can be used to avoid having to test the cements in direct tension. However, it is important to be aware of the limits of this result. In fact, this ratio is only valid for dry brushite cement, since indirect/direct tension measurement ratios also depend on the compressive/tensile strength ratio.

Considerations about insets

Brazilian tests were performed with cardboard pads used as insets to lower the compressive stresses near the contact points between specimen and platens. It is generally admitted[8] that the pad's width should not exceed one tenth of the cylinder's diameter to avoid producing a stress distribution that would differ too much from the one predicted by the theory, and to avoid fracture modes other than pure tension. On the other hand, Peltier, the only author to our knowledge who published a thorough theoretical study of the Brazilian test, recommends a ratio of 0.2 (pad width/cylinder's diameter) for a material whose compressive strength is nine times higher than tensile strength. In our experiments, the pad width was not fixed *a priori*. Many published experiments on concrete were made using pad width/cylinder's diameter ratios varying between 0.05 and 0.3 : use of pads wider than one tenth of the cylinder's diameter did not significantly change the measured ultimate stresses.[8]

The width of the prints left on the cardboards after specimen fracture was measured and appeared to vary between 0.11 and 0.23 times the cylinder's diameter. With small samples like the ones used in our study (8.7 mm diameter), it was much easier to use insets as wide as the whole press platens. The advantage of this set-up is to avoid the technical problem of aligning perfectly a cylinder 8.7 mm in diameter and 6 mm in length along an inset as narrow as 1 mm. On the other hand, its main drawback is that, the pad width being not fixed, the actual stress distribution within the specimen can not be calculated accurately. According to the available literature dealing with the Brazilian test on concrete, the width of the insets does not influence the measured stress values at failure[8]. However, the type of fracture seems to be dependent on that width[16]. In the present study, as the width of the prints left on the cardboards by the specimens was not systematically measured, it was not possible to correlate the type of fracture with the effective width of the insets.

Mitchell observed different fracture types depending on the insets width (Figure 7).[16] Without insets, he reported a compressive type of failure starting beneath the contact points between the cylinder and the press platens. With very wide insets, the specimen breaks as shown on the right-hand side of Figure 7. For insets narrower than the latter case, a clean break typical of pure cleavage, resulting in two identical half-cylinders, is obtained. This is the kind of failure that is expected in the diametral compression test. However, Mitchell's conclusions about the relation between inset's width and fracture type seems to be oversimplified. Careful examination of his results shows that, for a given inset width, the same type of fracture is not obtained systematically. Although compressive fracture effectively seems to take place preferentially with extremely narrow or no insets at all, and shearing fracture with very wide insets, one cannot predict that a given type of fracture will systematically take place at a given pad width.

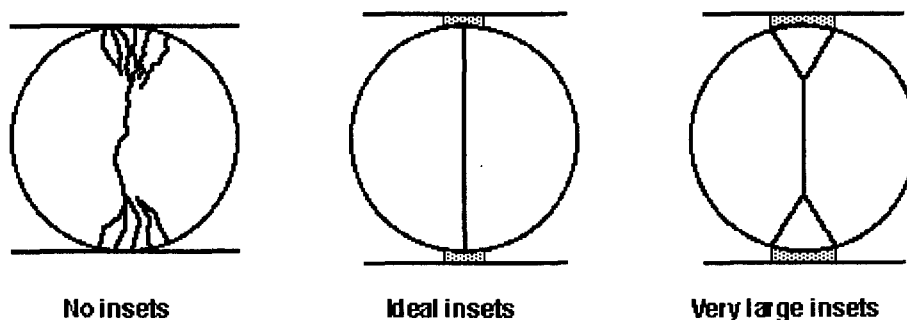No insets   Ideal insets   Very large insets

Figure 7 : Types of rupture obtained with different inset widths, adapted from Ref. 16.

Some studies on the diametral compression test of concrete used various types of insets and have shown that the measured values of ultimate stress could be statistically different if the materials used as insets mechanically behave in a very different way.[12,17] The ideal inset must be deformable enough as to match the shape of possible irregularities on the cylinder surface. In addition, it must not break before the specimen fracture occurs. The soft cardboards used in our experiments fulfill both conditions.

The difficulty to obtain systematically a given type of fracture with the Brazilian test was confirmed by our experiments on brushite cements. However, it seems that, as already reported by studies on concrete, the type of fracture is not correlated with the measured ultimate stress. Given the scatter of the results, it is doubtful that such a correlation could ever be found with the Brazilian test.

Brazilian test - Mohr's fracture criterion

In order to get a good insight into the Brazilian test limitations, it is necessary to consider carefully the stress distribution within the loaded cement cylinders. One- to three-dimensional states of stress can be represented graphically in a two-dimensional diagram called Mohr circle's representation[15], which allows determination of the stresses acting on a given point of a specimen in the three directions of space. The two axis of the diagram represent the normal stresses (abscissa) and the tangential stresses (ordinate). The stresses actually acting in all directions of a given plane all stand on a circle called Mohr's circle. The coordinates of each point of the circle give the values of stress components, normal and tangential to the considered plane. A more extensive explanation of the Mohr's representation can be found in Appendix A.

Mohr's circles describing the state of stress in the middle of the diameter are easy to construct. Two principal stresses σ_x and σ_y act on a point located in the middle of the diameter. Being normal to each other, their representative points lie on the abscissa of the Mohr's diagram, the compressive stress on the positive side, the tensile stress on the negative side of the abscissa. In the Brazilian test, the σ_x/σ_y ratio is equal to 3 (see Figure 1b and Eqs. 1 and 2), and the Mohr's circle of this two-dimensional state of stress passes through these points on the abscissa. Increase of the applied force induces the increase of the principal stresses, but their ratio remains the same until fracture.

We used Mohr's fracture criterion, which only takes into account the two extreme principal stresses. Fracture occurs when the Mohr's circle becomes tangent to a specific curve of the (σ, τ) plane, called intrinsic curve of the material. This curve characterises the mechanical resistance of a material submitted to two-dimensional state of stress. The shape of the curve can be characterised by the τ_0/σ_0 ratio (see Figure 8). The higher this ratio, the higher the σ_c/σ_t ratio. Equations used to calculate intrinsic curves from the results of the tension, compression and Brazilian tests are presented in Appendix B.
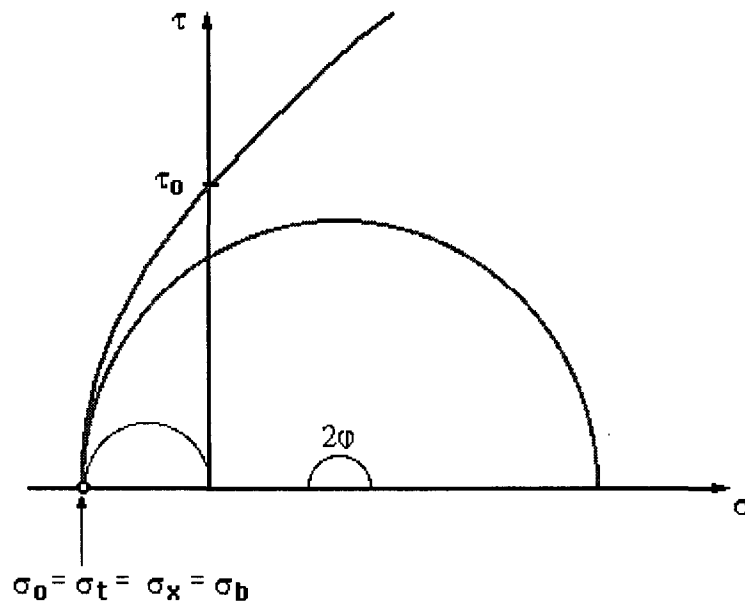
Figure 8 : Mohr's diagram representing the state of stress in the center of the specimen. High ratio τ_0/σ_0.

It is easy to see on a Mohr's diagram that the slope of the intrinsic curve can have a marked effect on the Brazilian test. Figures 8 and 9 show the intrinsic curves of two materials, whose compressive/tensile strength ratios are different. For each material, the Mohr's circle of the state of stress in the Brazilian test is represented (middle of the specimen). The contact point between the intrinsic curve and the Mohr's circle gives the normal and tangential stress components acting on the fracture plane. The angle between the fracture plane and the vertical diametral plane is found by dividing by two the angle 2φ on Figs. 8 and 9. The diagrams show that, in the Brazilian test, fracture of a specimen whose σ_c/σ_t ratio is low will take place under a stress value lower than the tensile strength measured by direct tension test. Theoretically, 8 is the minimum σ_c/σ_t ratio allowing pure cleavage in the Brazilian test (point of tangency on the abscissa). With a σ_c/σ_t ratio of 5, the ultimate stress measured with the

diametral compression test should theoretically amount to 82% of the direct tensile strength. Thus, it is obvious that the ultimate indirect tensile stress does not equal the ultimate stress this material can withstand in the direct tension test. In addition, the stress acting on the fracture plane decomposes into a normal and a tangential components, whereas in the direct tension test the stress is normal to the fracture plane. Thus, with materials whose σ_c/σ_t ratio does not exceed 8, fracture should theoretically start on a plane forming an angle φ with the horizontal diametral plane, and on which the stress also has a tangential component. On the contrary, if the σ_c/σ_t ratio is higher than 8, the tensile stress (σ_x) at rupture calculated with Eq.3 should correspond to the ultimate stress measured with the direct tensile test. As the σ_c/σ_b ratio of our 2- to 3-g/mL cements was found to vary between 3 and 7 (i.e. lower than 8), this cement submitted to the two-dimensional state of stress can not exhibit the same ultimate strength as with the direct tensile test and the fracture that takes place cannot be pure cleavage. Thus, for such a material, the Brazilian test can not be considered as a way to determine tensile strength.
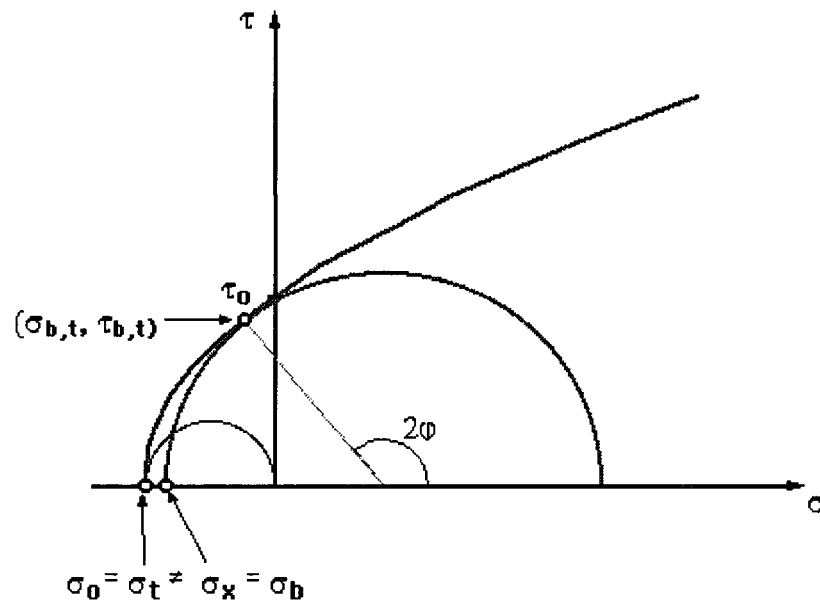
Figure 9 : Mohr's diagram representing the state of stress in the center of the specimen. Low ratio τ_0/σ_0.

Concrete and ceramics $(\sigma_c/\sigma_t > 8)$ generally have a higher ultimate strength when tested with the Brazilian test than with the direct tension test.[8] This case can not be drawn on a Mohr's diagram since the Mohr's circle of the state of stress of the Brazilian test would intersect the intrinsic curve determined with the direct tension and compression tests. The reason for this

discrepancy between experiment and theory stems from the fact that the volume effectively tested in the Brazilian test is smaller than the one tested in direct tension.

Determination of the intrinsic curve of the brushite cement

Results obtained with the three mechanical tests used in this study give strengths of materials in loading conditions that are those defined by each test. However, the loading conditions tested in laboratories are simplified and poorly representative of the actual mechanical loading the material could undergo when implanted in a bone defect. The implant geometry, as well as the nature of forces acting on the skeleton, give rise to complex and heterogeneous stress distributions within the implanted material. Such conditions being difficult or impossible to reproduce in the laboratory, we attempted to link the results of the different simple tests used here to be able to predict the strength of our material under more complex loading conditions.

If the intrinsic curve is assumed to be a parabola, then only two Mohr's circles suffice to determine the equation of such a curve. It means that two different mechanical tests allow to calculate the intrinsic curve of our cements. Uni-axial and diametral compression tests being the easier tests to perform, we decided to calculate the intrinsic curves by considering the strengths measured with these two tests. Equations allowing calculation of these curves are presented in Appendix B.

The determined intrinsic curve intersects the abscissa and ordinate at points called σ_0 and τ_0, representing the intrinsic tensile and shearing strengths, respectively. The σ_c, σ_t and σ_b parameters represent failure stresses in uni-axial compression, direct tension and Brazilian test respectively. ($\sigma_{b,t}$, $\tau_{b,t}$) is the point of tangency between the intrinsic curve and the Mohr's circle of failure state of stress in the Brazilian test. These symbols are shown on the Mohr's diagram in Figure 9. For the point of tangency ($\sigma_{b,t}$, $\tau_{b,t}$) to be located on the abscissa of the Mohr's diagram (case of cleavage failure in the Brazilian test), the σ_c/σ_b ratio must be higher than 8 (see Appendix B for details). Now these ratios are lower than 8 for most of our cements, as shown in Table III. Thus, the points of tangency ($\sigma_{b,t}$, $\tau_{b,t}$) on the Mohr's diagram are not located on the abscissa. This means that the plane on which fracture initiates is not the vertical diametral plane and that the state of stress acting on this plane is not only tension, but a combination of tension and shear, as mentioned earlier. As a consequence of this ($\tau_{b,t} \neq$ 0), the intrinsic curve intersects the abscissa at a more negative value than $-\sigma_t$. If the intrinsic

curve calculated from the compression and Brazilian test results (CB curve) and the Mohr's circle of stress at rupture in direct tension are drawn on the same Mohr's diagram, it appears that the circle does not intersect the intrinsic curve. Thus, there is some incompatibility between the curve determined from the two tests (uni-axial and diametral compression) and the results obtained with the third test (direct tension). Moreover, it would not be possible to make the direct tension Mohr's circles be tangent with the CB curve on the abscissa. Now direct tension experiments showed that fracture surfaces were normal to the load axis, and should therefore correspond to a point of tangency located on the abscissa of the Mohr's diagram.

Table III : Compressive strength/Diametral strength ratios of brushite cements (mean ± 1 SE).

S/L [g/mL]	σ_c/σ_b	
	Dry	Wet
2	4.5 ± 0.5	3.2 ± 0.4
2.5	5.1 ± 0.6	4.1 ± 0.4
3	6.7 ± 0.8	5.0 ± 0.6
3.5	10.3 ± 1.2	6.0 ± 0.7

As the standard error on measurements was fairly high, it was propagated in our calculations in order to determine how precise the determination of σ_0 and τ_0 can be. These parameters are shown in Figs. 10 and 11. They were determined by combining the test results by pairs : compression-Brazilian (CB), compression-tension (CT) and tension-Brazilian (TB).
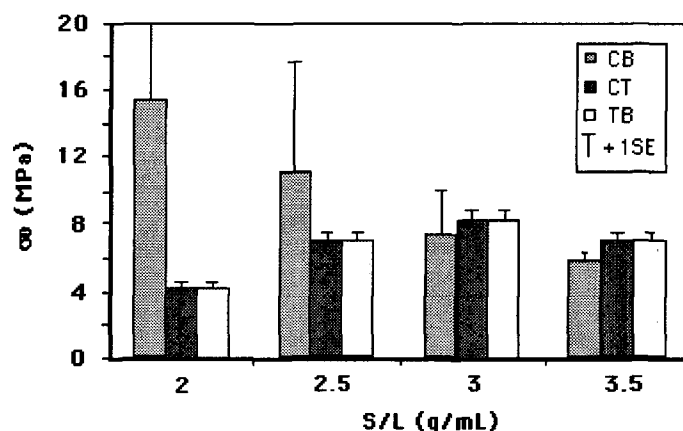
Figure 10 : σ_0 **parameters determined after combination of compression and Brazilian tests (CB), compression-tension (CT), and tension-Brazilian (TB) for dry brushite cements with various solid/liquid ratios.**

Figure 11 : τ_0 **parameters determined after combination of compression and Brazilian tests (CB), compression-tension (CT), and tension-Brazilian (TB) for dry brushite cements with various solid/liquid ratios.**
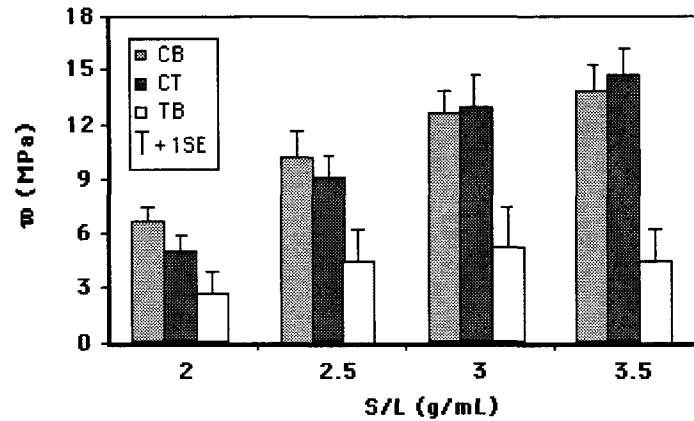
According to our calculations, for the CT curve to be tangent on the abscissa with the direct tension Mohr's circle, σ_c/σ_t ratio has to be higher than 3. For the TB curve, σ_b/σ_t has to be higher than 0.58. In Figure 10, the σ_0 values determined by CT and TB curves correspond to direct tensile strength (σ_t) since the σ_c/σ_t and σ_b/σ_t ratios are higher than 3 and 0.58 respectively. If the CB curve was to allow prediction of direct tensile strength, it should intersect the abscissa at $-\sigma_t$. It can be seen in Figure 10 that σ_0 values predicted by CB curves are always different from σ_t, and that the lower the S/L ratio, the higher the standard error. For 2- to 3-g/mL cements, the confidence interval is so large that it encompasses the results obtained with the CT and TB curves. Thus, use of only compression and Brazilian tests does not allow a precise estimate of σ_0. Hence, it seems not possible to determine a coherent σ_0 value without help of the direct tension test.

In Figure 11, one can see that the τ_0 values determined by CB and CT curves are close to each other and standard error on these values is always smaller than the one on τ_0 determined by the TB curve. In addition, the latter gives τ_0 values that are systematically lower than those determined by the CT and CB curves. From these comparisons, it appears that the compression test is necessary to determine τ_0. This is not surprising since the shear stress component on the failure plane is much more important in compression than in tension tests.

Finally, the intrinsic curve that gives the more coherent σ_0 and τ_0 values is the curve determined by the compression and tension tests. Nevertheless, the direct tension test cannot be contemplated as a routine test for wet cement specimens, as no glue sufficiently resistant in wet conditions is available.

CT curve gives correct σ_0 values since these correspond to the direct tensile strength. From this curve, it is possible to calculate what should theoretically be the strength measured in diametral compression (assuming a unique point of tangency between the curve and the Mohr's circle of the Brazilian test). Results of these calculations are presented in Table IV.

Table IV : Experimental and theoretical (calculated from CT curves) indirect tensile strengths of cements with different Solid/Liquid ratios.

S/L [g/mL]	σ_b [MPa]		
	measured	recalculated (from CT)	difference
2	3.6	2.9	- 0.7
2.5	5.9	5.2	- 0.7
3	6.9	7.3	0.4
3.5	5.9	6.9	1.1

The differences between experimental and theoretical σ_b values (recalculated from CT curves) are significant at a 5% error risk, except for the 3 g/mL-cement. This confirms that the Brazilian test results can not be used to define a correct intrinsic curve of our cements.

For the two cements with the lower S/L ratios, the strength measured with the Brazilian test is higher than the one predicted by the CT curve. Since these cements probably have less macroporosity (due to air bubbles) than the 3 and 3.5 g/mL cements, the probability of finding a macropore on the diametral plane is lower for these cements. Hence, it seems logical that the resistance measured with the Brazilian test is higher than the one predicted on the basis of simple tension tests.

Domain of applicability of the intrinsic curves

The calculations of the intrinsic curves were based on the hypothesis that the intrinsic curve has a parabolic shape. However, it is evident that such a curve can not predict the mechanical

resistance of a porous material undergoing biaxial compressive loads. It would predict an infinite resistance to biaxial compression when σ_1 equals σ_2, which is has no physical meaning. To predict the biaxial compression behaviour, the curve should therefore have an elliptical shape. Hence, the applicability of the parabola does not extend much further from the point of tangency with the compression Mohr's circle. Given the actual knowledge of the mechanical resistance of the brushite cement, it is not possible to quantify the domain of validity of the parabolic curve in the biaxial compression region.

CONCLUSIONS

Uni-axial compression, direct tension and diametral compression tests allowed measurement of the compressive and tensile strengths of brushite cements. Diametral tensile strength appeared to be systematically lower than direct tensile strength of dry cements, whatever their solid/liquid ratio.

The Mohr's circles representation of the failure states of stress as well as calculation of intrinsic curves allowed to understand that the fracture mode in the Brazilian test is not comparable to the one in a direct tension test. Theoretically, as the σ_c/σ_b ratio is lower than 8, failure can not possibly take place in a pure tension mode in the Brazilian test. Nevertheless, the Brazilian test remains a test that is easy to use with brittle materials and requires simple specimen's shape. Hence, even though the measured strength is systematically lower than the one obtained with the direct tension test, the Brazilian test can be used as a way of comparing different brushite cement compositions. On the other hand, use of the Brazilian test results to determine the intrinsic curve of the cements is not possible, since the so-determined σ_o value does not correspond to the strength measured with the direct tension test.

APPENDIX A

The Mohr circles diagram allows representation on a plane of the three-dimensionnal state of stress acting on a given point of a mechanically loaded structure. The state of stress at this point is represented by three circles in the (σ, τ) plane. The abcissa axis represents normal

stresses, the ordinate tangential stresses acting on the considered plane. Compressive stresses are defined as positive, whereas tensile stresses are negative.

Let us consider a point of the loaded specimen. There are always at least three orthogonal planes on which tangential stresses equal zero and the normal stresses are extrema. These plane are called principal planes and the stresses acting on them are principal stresses.

Let us consider a point B in the middle of the diametral plane and the horizontal plane passing through it (Figure 12).
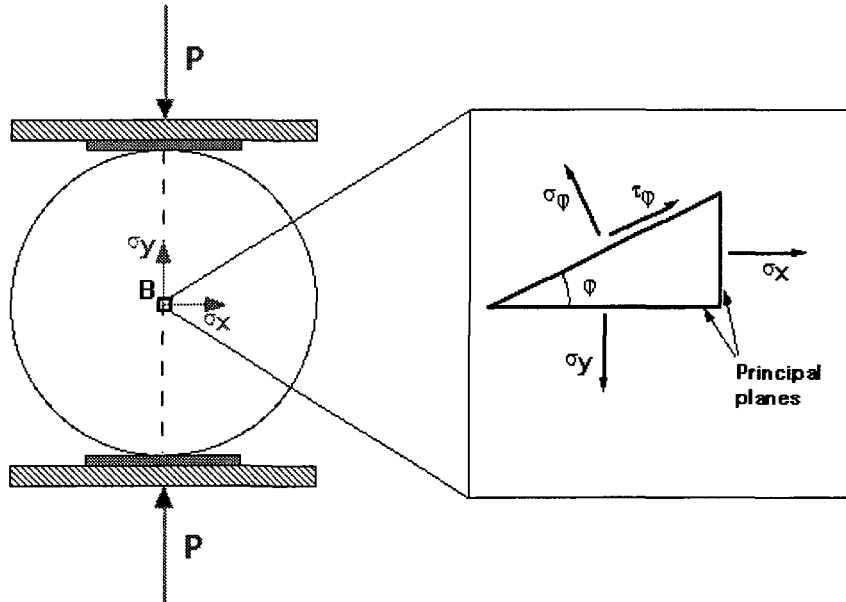

Figure 12 : Schematic representation of the Brazilian test and the stresses acting in the middle of the specimen.

Only a normal stress acts on this plane, the tangential component being equal to zero. Thus, this plane is a principal plane. The normal stress acting on this plane is compressive, the point of the (σ, τ) plane representing the stress acting on this plane is located on the positive side of the abscissa (σ-axis). By rotating the considered plane 90° around B, a new situation occurs where only a tensile stress acts on the vertical plane. The point representing this stress on the (σ, τ) plane is located on the negative side of the abscissa.

It can be shown that the normal and tangential components σ and τ vary with the angle between the considered plane and the principal plane, in the following manner :

$$\sigma_\varphi = \frac{\sigma_x + \sigma_y}{2} + \frac{\sigma_x - \sigma_y}{2} \cdot \cos(2\varphi) \qquad (1A)$$

$$\tau_\varphi = -\frac{\sigma_x - \sigma_y}{2} \cdot \sin(2\varphi)$$
(2A)

According to this, all the (σ, τ) points are located on a circle centered on $(\frac{\sigma_x + \sigma_y}{2}, 0)$, whose diameter is $\sigma_x - \sigma_y$. Each point of the circle corresponds to the stress acting on a plane forming an angle φ with the principal plane, compared with the horizontal. The angle φ between these two planes is represented by an angle 2φ on the Mohr's representation. The principal stresses are thus at $180°$ in this representation.

In the case of mono-dimensional states of stress, only one principal stress differs from zero. Such a state of stress is therefore drawn as a single circle. As the two other principal stresses equal zero, the circle passes through the $(0,0)$ point of the Mohr's diagram. Compressive and tensile states of stress at rupture are represented in Figure 13.
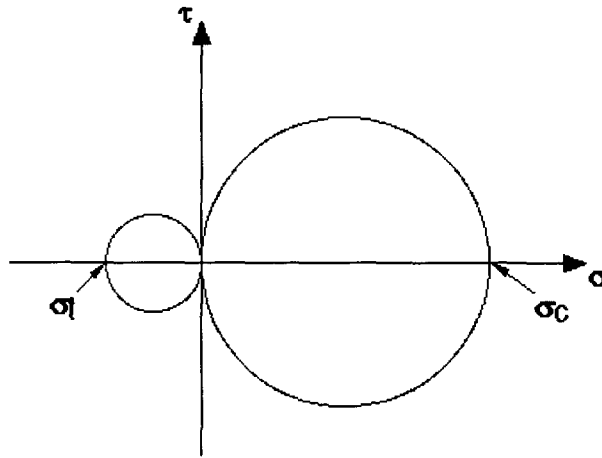
Figure 13 : Mohr circles of the failure states of stress in direct tension and uni-axial compression.

If failure states of stress (determined experimentally) are reported on the diagram, it is possible to draw the intrinsic curve, which characterises the material's resistance for any state of stress. According to Mohr's failure criterion, fracture takes place as soon as a Mohr circle becomes tangent to the intrinsic curve. Hence, this curve must be tangent to the Mohr's circles representing the failure states of stress and can be approximated by a parabola of the type $\tau^2 = k\sigma + a$, where $-a/k$ is the position of the apex of the parabola on the abscissa. To determine this parabolic curve, only two states of stress at failure must be known. Figure 14 shows an intrinsic curve tangent to three Mohr circles determined with different tests.
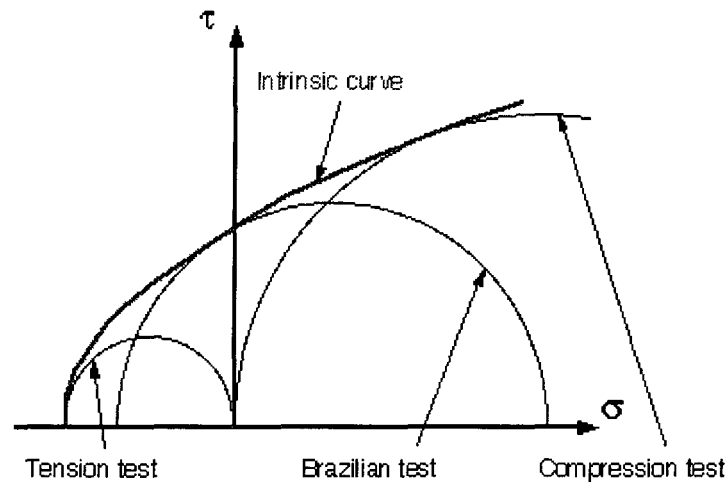
Figure 14 : Mohr's diagram with the Mohr circles of failure states of stress of compression, tension, and Brazilian tests, and the intrinsic curve tangent to these circles.

The point of tangency between the Mohr's circle of failure state of stress and the intrinsic curve can be used to determine the orientation of the fracture plane compared to the principal plane (angle φ), as well as the normal ($\sigma_{2\varphi}$) and tangential ($\tau_{2\varphi}$) components acting on the fracture plane (Figure 15).
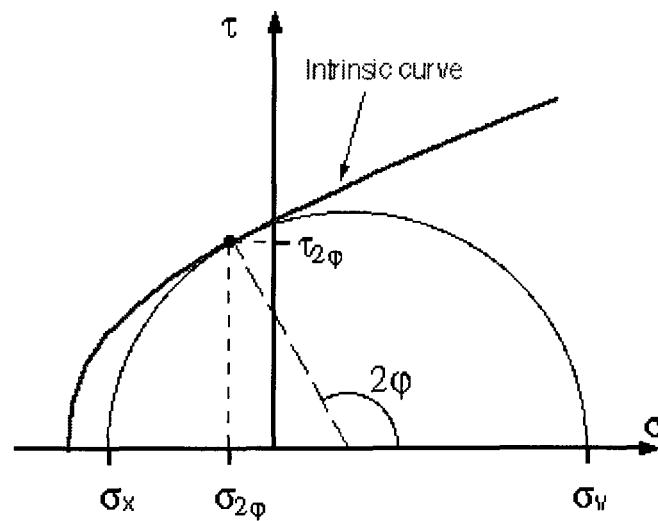
Figure 15 : Mohr's diagram allowing determination of the stress components on the fracture plane and the orientation of this plane.

APPENDIX B

CALCULATION OF THE INTRINSIC CURVE

General case

The intrinsic curve is assumed to be parabolic :

$$y^2 = kx + a \qquad (1B)$$

and must be simultaneously tangent to two circles given by the following general expression :

$$y^2 = r_i^2 - (x - c_i)^2, (i = 1,2) \qquad (2B)$$

The r_i are the radii of the circles, the c_i the abscissae of their centers, with $r_1 \leq r_2$ and $c_1 \leq c_2$. The abscissae of the intersections between the parabola (1B) and the circles i are solutions of the second order equations :

$$x^2 - (2c_i - k)x + (c_i^2 + a - r_i^2) = 0, (i = 1,2) \qquad (3B)$$

The parabola is tangent to the circle i if the discriminant of Equ. 3B is zero. Thus, the parabola will be simultaneously tangent to the two circles for values a and k respecting the following equations :

$$\frac{k^2}{4} - c_i k - a + r_i^2 = 0, (i = 1,2) \qquad (4B)$$

Solving this system of two equations with to unknowns gives :

$$k = \frac{r_2^2 - r_1^2}{c_2 - c_1} \qquad (5B)$$

$$a = \frac{c_2 r_1^2 - c_1 r_2^2}{c_2 - c_1} + \frac{k^2}{4} \qquad (6B)$$

The parabola is best described by two parameters, σ_0 and τ_0, which are the values of resistance to pure tension and pure shearing stresses :

$$\tau_0 = \sqrt{a} \qquad (7B)$$

$$\sigma_0 = a/k \qquad (8B)$$

Compression and Brazilian tests (CB)

In this case, the radii and centres of the circles are given by $c_1 = \sigma_b$, $r_1 = 2\,\sigma_b$, $c_2 = \sigma_c / 2$, $r_2 = \sigma_c / 2$, where σ_b is the indirect tensile strength, and σ_c the compressive strength.

Case 1 : $\sigma_c < 8\,\sigma_b$. By replacing the r_i and c_i in Eqs. 5B and 6B, the expressions of k and a become :

$$k = \frac{\sigma_c^2 - 16\sigma_b^2}{2(\sigma_c - \sigma_b)} \qquad (9B)$$

$$a = \frac{\sigma_b \sigma_c (8\sigma_b - \sigma_c)}{2(\sigma_c - 2\sigma_b)} + \frac{k^2}{4} \qquad (10B)$$

Case 2 : $\sigma_c \geq 8\,\sigma_b$. In this case, Eqs. 7B and 8B give :

$$\tau_0 = \sqrt{k\sigma_b} \qquad (11B)$$

$$\sigma_0 = \sigma_b \qquad (12B)$$

where k, calculated with Eq. 4B by introducing $a = k\,\sigma_b$, is given by :

$$k = (\sigma_c + 2\sigma_b) - 2\sqrt{\sigma_b(\sigma_c + \sigma_b)} \qquad (13B)$$

Compression and tension tests (CT)

In this case, the radii and centers of the circles are given by $c_1 = -\sigma_t / 2$, $r_1 = \sigma_t / 2$, $c_2 = \sigma_c / 2$, $r_2 = \sigma_c / 2$, where σ_t is the direct tensile strength, and σ_c the compressive strength.

Case 1 : $\sigma_c < 3\,\sigma_t$. By replacing the r_i and c_i in Eqs. 5B and 6B, the expressions of k and a become :

$$k = \frac{\sigma_c - \sigma_t}{2} \qquad (14B)$$

$$a = \frac{(\sigma_c + \sigma_t)^2}{16} \qquad (15B)$$

Case 2 : $\sigma_c \geq 3\ \sigma_t$. In this case, Eqs. 7B and 8B give :

$$\tau_0 = \sqrt{k\sigma_t} \qquad\qquad\qquad (16B)$$

$$\sigma_0 = \sigma_t \qquad\qquad\qquad (17B)$$

where k, calculated with Eq. 4B by introducing a = k σ_b, is given by :

$$k = (\sigma_c + 2\sigma_t) - 2\sqrt{\sigma_t(\sigma_c + \sigma_t)} \qquad\qquad (18B)$$

Tension and Brazilian tests (TB)

In this case, the radii and centers of the circles are given by $c_1 = -\sigma_t / 2$, $r_1 = \sigma_t / 2$, $c_2 = \sigma_b$, $r_2 = 2\sigma_b$, where σ_t is the direct tensile strength, and σ_b the indirect tensile strength.

Case 1 : $\sigma_b < 0.58\ \sigma_t$. By replacing the r_i and c_i in Eqs. 5B and 6B, the expressions of k and a become :

$$k = \frac{16\sigma_b^2 - \sigma_t^2}{2(2\sigma_b + \sigma_t)} \qquad\qquad (19B)$$

$$a = \frac{\sigma_b\sigma_t(\sigma_t + 8\sigma_b)}{2(2\sigma_b + \sigma_t)} + \frac{k^2}{4} \qquad\qquad (20B)$$

Case 2 : $\sigma_b \geq 0.58\ \sigma_t$. In this case, Eqs. 7B and 8B give :

$$\tau_0 = \sqrt{k\sigma_t} \qquad\qquad\qquad (21B)$$

$$\sigma_0 = \sigma_t \qquad\qquad\qquad (22B)$$

where k, calculated with Eq. 4B by introducing a = k σ_b, is given by :

$$k = (\sigma_c + 2\sigma_t) - 2\sqrt{\sigma_t(\sigma_c + \sigma_t)} \qquad\qquad (23B)$$

REFERENCES

[1] Munting E, Mirtchi A A and Lemaître J. Bone repair of defects filled with a phosphocalcic hydraulic cement : an *in vivo* study. J Mater Sci Mater Med 1993;4:337-344.

[2] Ohura K, Bohner M, Hardouin P, Lemaître J, Pasquier G, and Flautre B. Resorption of, and bone formation from, new β-tricalcium phosphate-monocalcium phospate cements: an *in vivo* study. J Biomed Mater Res 1996;30:193-200.

[3] Mirtchi A A, Lemaître J, Terao N. Calcium phosphate cements: study of the β-tricalcium phosphate-monocalcium phosphate system. Biomaterials 1989;10:634-638.

[4] Martin R I and Brown P W. Mechanical properties of hydroxyapatite formed at physiological temperature. J Mater Sci Mater Med 1995;6:138-143.

[5] Ishikawa K and Asaoka K. Estimation of ideal mechanical strength and critical porosity of calcium phosphate cement. J Biomed Mater Res 1995;29:1537-1543.

[6] Liu C, Shen W, Gu Y, and Hu L. Mechanism of the hardening process for a hydroxyapatite cement. J Biomed Mater Res 1997;35:75-80.

[7] Bermudez O, Boltong MG, Driessens FCM, Planell JA. Compressive strength and diametral tensile strength of some calcium-orthophosphate cements: a pilot study. J Mater Sci Mater Med 1993;4:389-393.

[8] Bonzel J. Ueber die Spaltzugfestigkeit des Betons. Beton 1964;3:108-114, and 4:150-157.

[9] Direct tensile test of concrete. Rilem Bulletin 1963;20:83-90.

[10] Carneiro FLLB and Barcellos A. Résistance à la traction des bétons. Rilem Bulletin 1953;13:97-126.

[11] Peltier R. Theoretical investigation of the Brazilian test. Rilem Bulletin 1954;19:29-69.

[12] Wright PJF. Comments on an indirect tensile test on concrete cylinders. Mag Concrete Res 1955;7:87-96.

[13] Montgomery DC. Design and analysis of experiments. 3rd Ed. New York: Wiley; 1991.

[14] De With G, Van Dijk HJA, Hattu N, Prijs K. Preparation, microstructure and mechanical properties of dense polycrystalline hydroxyapatite. J Mater Sci 1993;16:1592-1598.

[15] Sandor BI. Strength of materials. Englewood Cliffs, NJ: Prentice-Hall;1978. p.18.

[16] Mitchell NB. The indirect tension test of concrete. Mater Res Stand ASTM 1961;1,780-788.

[17] Sell R. Einfluss der Zwischenlage auf Streuung und Grösse der Spaltzugfestigkeit von Beton. Berlin: DeutscherAusschuss fuer Stahlbeton, 155, Verlag von W. Ernst & Sohn; 1963. p 35-47.

CHAPTER 3   INFLUENCE OF THE STARTING POWDERS

GRANULOMETRY ON THE MECHANICAL

STRENGTH OF A CALCIUM PHOSPHATE

BRUSHITE CEMENT.

ABSTRACT

The objective of this work is to try to increase the mechanical strength of a brushite cement by refining the starting powders granulometry. The three starting powders (MCPM, CSH and β-TCP) were milled, and the effect of their granulometry on compressive and diametral strengths was studied.

All three powders were milled and freeze-dried. The median diameters passed from 70.5 down to 6.2 μm for MCPM, 27.2 down to 1.1 μm for CSH, 2.4 to 1.5 μm for β-TCP. Specific surface areas of the powders increased on milling.

Milling of MCPM and CSH appeared to be beneficial to the maximum stresses the hardened cement can withstand. Cements prepared with raw powders showed 1.4 MPa indirect tensile strength and 4.4 MPa compressive strength. With milled MCPM and CSH, those values reached 4.1 and 22.1 MPa respectively, i.e. a three-fold increase in diametral compression and a five-fold increase in axial compression. β-TCP milling did not bring any benefits to the mechanical strength of the cements, mainly because the Solid/Liquid ratio had to be drastically decreased to produce a paste with the same rheology as the one made with raw β-TCP.

INTRODUCTION

Calcium phosphate bone cements have been developed in the 1980s to serve as bone substitutes. Since then, numerous formulations have been studied.[1,2,3,4,5] Calcium phosphate cements might replace acrylic bone cements in the future because they are biodegradable and osteoconductive. However, their mechanical properties remain well under those of acrylic cements. Their relatively low mechanical strength limit their application to osseous sites undergoing moderate physiological loads.

Mechanical properties of hardened cements are known to depend on numerous factors regarding sample preparation, like powder/liquid ratio, packing pressure during molding, and storage conditions. In general, an increase of the powder/liquid ratio provides higher compressive and diametral tensile strengths.[6,7,8] Applying pressure during setting is a way of enhancing the mechanical properties of the hardened cement,[8,9] but it does probably not reflect real conditions of use. Storage conditions are also of great importance (nature of the storage liquid, storage time).[10] All these factors seem to have the same effects on the mechanical properties of cements, whatever the system studied. However, a factor like granularity of the starting powders is very much more system-dependent. The effect of particle size on the mechanical properties of some calcium phosphate cements has been studied by various authors studying different systems.[5,11,12] As the reactants and their reaction kinetics differ in each system, it seems to be illusory to find a general rule linking powder granulometry to the mechanical strength of cements. As all hydraulic calcium phosphate cement systems involve more than one starting powder, the granulometries of individual powders should be studied together, because interactions between the granulometries may occur.

Brushite cement is obtained by mixing two calcium phosphate powders : β-tricalcium phosphate (β-TCP) and monocalcium phosphate monohydrate (MCPM) in water. A third granular component is plaster of Paris (calcium sulfate hemihydrate, CSH), converting to gypsum (calcium sulfate dihydrate, CSD) during setting. This third component is not necessary for the completion of the brushite-forming reaction. It was first used as a setting regulator,[13] and happened later to be beneficial to the in vivo behaviour of the set cement.[14] However, the addition of CSH to the β-TCP-MCPM cement appeared to be deleterious to the

mechanical properties of the cement.[15] This is why we proposed to modify its granulometry to try to enhance the mechanical properties of the cement. As the effect of the two other powders granulometry (β-TCP and MCPM) was still unclear to us at that time, we attempted to clarify their role by refining the particle sizes of the three starting powders, hoping to obtain finer microstructures and better mechanical properties. This study was divided into two parts : first MCPM and CSH were milled, then β-TCP. The effect of their granulometries on the mechanical properties of the cements was studied. Mechanical strengths were measured with two different tests : axial compression and diametral compression.

MATERIALS AND METHODS

Cement studied, sample preparation

The starting powders are β-tricalcium phosphate (β-TCP), monocalcium phosphate monohydrate (MCPM) and calcium sulfate hemihydrate (CSH). They react in presence of water to form brushite (dicalcium phosphate dihydrate, DCPD) and gypsum (calcium sulfate dihydrate, CSD) according to reaction 1. A small amount of sodium dihydrogen pyrophosphate (NaHPP, $Na_2H_2P_2O_7$, Fluka) is added to the starting powders as a setting regulator.

$$Ca_3(PO_4)_2 + Ca(H_2PO_4)_2.H_2O + CaSO_4.\frac{1}{2}H_2O + 8.5H_2O \rightarrow 4CaHPO_4.2H_2O + CaSO_4.2H_2O \quad (1)$$

β-TCP   +   MCPM   +   CSH   +   water   →   DCPD   +   CSD
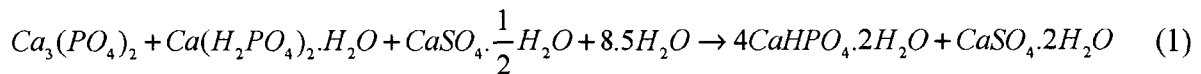
The cement paste is prepared in a mortar and mixed with a stainless steel spatula. MCPM and NaHPP are poured first in the mortar containing water, and mixed with help of the spatula. After 30 seconds, CSH is added and mixed for another 30 seconds. Then β-TCP is added, activating the setting reaction. The mix becomes pasty, and the paste must be thoroughly mixed for 1 minute. Then it is introduced with help of the spatula into a 2mL-syringe whose extremity was previously cut. After each cement addition into the syringe, the paste is vibrated to eliminate entrapped air bubbles. Hardened cement is expelled from the syringe by pushing on its plug. Immediatly after demolding, specimens are wrapped in a paper soaked with demineralized water, and stored individually in watertight snap caps at 37°C for 24

hours. The so-obtained cylinders have a diameter of 8.7 mm. Their faces are then polished (SiC paper 120) in order to obtain the desired height and parallelism between the faces. The height of the cylinders varies depending on the mechanical test to which the specimens are destinated.

Experimental design

The study was divided into two steps. First the effects of MCPM and CSH milling (attrition) on the mechanical properties (axial and diametral compressions) were studied ("MCPM/CSH milling"). The experiments were organized in a 2^2 x 4 factorial design (raw and milled CSH and MCPM powders, four replicates) and the results were analyzed with the Anova technique.[16] In the second phase, raw and milled β-TCP powders were used to study their effect on the mechanical properties ("β-TCP milling").

Starting powders

Milled powders were obtained by attrition. It took place in an attritor (Netzsch, Germany) at a rotary speed of 1500 rpm, with zirconia balls. Quantities put in the attritor were 800 g zirconia balls, 100 g aqueous attrition medium, 50 g powder.

MCPM/CSH milling

MCPM. Two batches of MCPM were used. The original one (raw) and the milled one. The raw powder was Ibex® monocalcium phosphate (Albright & Wilson, UK). A part of this batch was milled for 30 minutes with an attrition mill. The attrition liquid was an MCPM-saturated aqueous solution (to prevent dissolution of the powder during milling). After milling, the suspension was freeze-dried for 24 hours (Alpha 1-4, Christ, Germany).

CSH. Two batches of CSH were used. The original one (raw) and the milled one. The raw powder was from Merck, cat. no 102162. As CSH tends to hydrate in water, milled CSH was obtained by attriting a CSD powder (Merck, cat. no 102160) in a CSD-saturated aqueous solution and by dehydrating the milled powder after freeze-drying. Attrition conditions were the same as for MCPM, except for the time which was 60 minutes. After milling, the suspension was freeze-dried in the same conditions as for MCPM. The powder was then de-hydrated into its half-hydrate form at 105°C for 8 hours in a drying oven.

β-TCP. The granulometric characteristics of the β-TCP, synthesized in our laboratory, stand in Table I, along with those of the other powders.

β-TCP milling

β-TCP. Two batches of β-TCP were used. The original one (raw) and the milled one. The raw powder was synthesized in the laboratory. Attrition and freeze-drying conditions were the same as for MCPM, except for attrition medium : an aqueous solution of 1 wt% polyacrylic acid (PAA). After drying, the milled powder was heated at 800°C for 10 hours to eliminate the PAA from the surface of particles.

MCPM and CSH. The granulometric characteristics of MCPM and CSH are presented in Table I.

Table I : Granulometric characteristics of the starting powders used in the first and second parts of the study.

	MCPM/CSH milling		β-TCP milling	
	d_{50} [μm]	S_{BET} [m^2/g]	d_{50} [μm]	S_{BET} [m^2/g]
CSH				
raw	27.2	2.5		
attrited	1.1	10.3	1.9	5.0
MCPM				
raw	70.5	0.3		
attrited	6.2	2.1	14.0	3.1
β-TCP				
raw	2.4	1.7	2.4	1.7
attrited			1.5	2.0

Cement compositions

The powder masses used were the same for the two sets of experiments and are presented in Table II. The quantity of setting regulator NaHPP is 0.100 g, except for the cement with three raw starting powders, where the mass used was 0.080 g. All quantities were weighed with a +/- 0.001 g precision.

Table II : Starting solid components, quantities.

Powder	mass [g]	wt%
MCPM	0.781	33.6
CSH	0.339	14.6
β-TCP	1.201	51.7

The amount of water varied with the composition, resulting in cements with different Solid/Liquid ratios (see Table III). The reasons for this modification will be discussed later. β-TCP is used in excess over the stoichiometric β-TCP/ MCPM ratio (Eq. 1), so that residual unreacted β-TCP remains in the set cement to slow down in vivo dissolution of the cement.

Table III : Solid/Liquid ratios of the cements prepared.

	MCPM/CSH milling	β-TCP milling	
		raw TCP	milled TCP
S/L [g/cc]	2.2	2.2	1.4

Characterization techniques

PSD. Particle size distributions of the powders were measured by liquid-phase sedimentation (forced with centrifugation) with a Horiba Capa-700 analyzer. Raw MCPM and CSH powders were measured in a methanol-glycerol mix (25-75wt%), whereas their milled forms were measured in isopropanol. Both raw and milled β-TCP powders were measured in an aqueous 1wt% PAA solution. Before measurement, each dispersion was ultrasonicated for 10 minutes.

Specific surface area. Specific surface areas of the powders were measured by nitrogen adsorption at liquid nitrogen temperature (BET method), with a Gemini 2375 Surface Area Analyzer (Micromeritics). The powders were kept at least 24 hours at room temperature and low relative humidity (RH < 20%) before measurement.

Porosity. Porosity of the hardened cements was determined by the Archimede's method.

X-Rays Diffraction. XRD were performed with a Kristalloflex 805 (Siemens) diffractometer (Kα-Cu radiation), using the coupled θ/2θ method. They were performed on samples tested with the diametral compression test. To estimate the completion of the reactions taking place during setting, intensities of the β-TCP, DCPD and CSH diffraction peaks were measured.

The peaks retained for analysis are located at $2\theta = 27.77°$ (h k l = 2 1 4) for β-TCP, $2\theta = 20.93°$ (h k l = 0 2 1) for DCPD and $2\theta = 14.73°$ (h k l = 1 0 0) for CSH. They were chosen for their high intensity and absence of overlapping with other peaks. The amount of CSD formed cannot be estimated since its diffraction peaks systematically overlap with peaks of the other cement compounds.

Thermogravimetry. CSH powders were checked for purity by thermogravimetry. The powders were put in dessicator for 24 hours until their mass was constant. After weighing, they were calcined at 500°C for 6 hours to obtain CS, and then weighed again. Then further calcination at 1000°C was performed to eliminate impurities. Weighing of the calcined powder allowed calculation of the weight percentage of impurities.

Mechanical testing. Two types of mechanical tests were performed on the cement specimens : Diametral and axial compression tests. Diametral compression test allows indirect measurement of brittle specimen's tensile strength. The limitations in the interpretation of the results obtained on brushite cements were studied in detail in a previous study.[6] Diametral compression tests were made with an Adamel Lhomargy DY31 universal testing machine equipped with a 2 kN load cell. The steel platens of the press were covered with a cardboard to ensure contact along the whole cylinder and to distribute the applied force on a certain width. The inset width was not defined *a priori* since they covered the whole platen surface. Specimens were cylindrical, 8.7 mm in diameter and 6 mm in height. Loading rate was 0.3 mm/min. The horizontal stress in the middle of the diametral plane of the specimen (supposed to be responsible for fracture) is calculated the following way :

$$\sigma = \frac{2P}{\pi DL} \tag{2}$$

where P is the applied force, D the cylinder diameter, L its length.

Axial compression tests were performed on an Instron 4467 universal testing machine with a 30 kN load cell. The compressive load rate was 0.3 mm/min. Specimens were cylindrical, with 8.7 mm diameter and 18 mm length.

RESULTS

Powders properties

MCPM / CSH milling

MCPM. The median diameter of the MCPM powder was lowered by attrition, from 70.5 down to 6.2 µm. Particle size distributions are shown in Figure 1. PSDs are always presented as cumulated volume distributions here. The increase of the specific surface area (0.32 to 2.1 m^2/g) indicates that primary particles were broken upon milling.
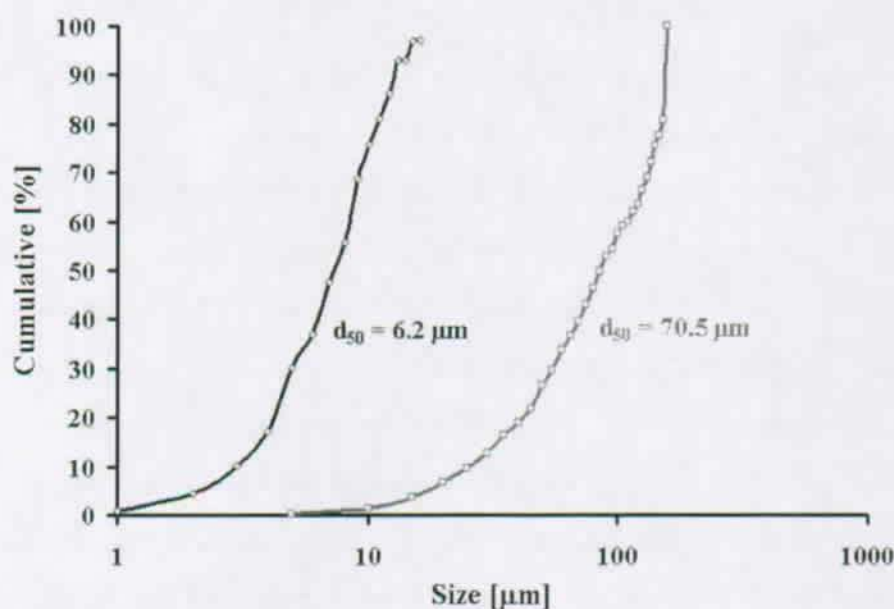

Figure 1 : Cumulative particle size distributions of raw and attrited MCPM.

SEM photographs of the raw and milled MCPM powders are shown in Figure 2. The shape of the raw powder is typical of a spray-dried powder. After milling, plate-like primary particles become visible. The two particle size distributions do practically not overlap.
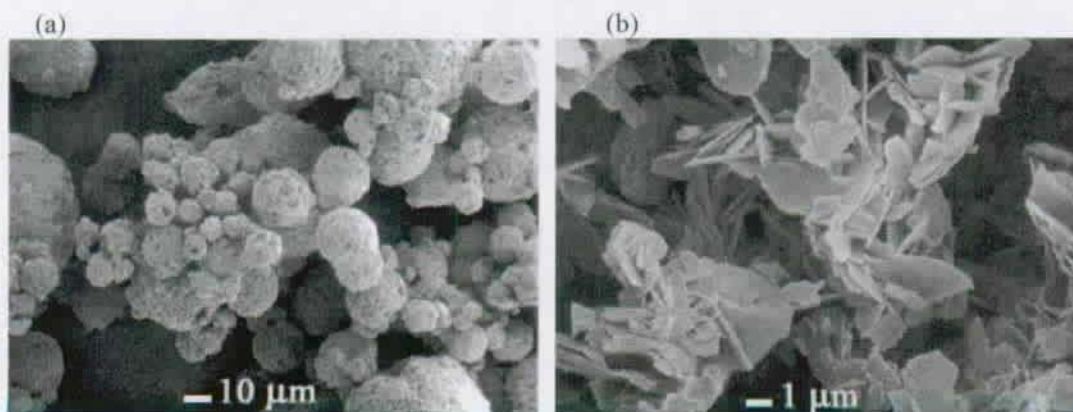
Figure 2 : SEM micrographs of (a) raw and (b) attrited MCPM.

CSH. Particle size distributions of raw and milled CSH powders are presented in Figure 3. The milled batch is not the result of attrition of the raw batch. The median diameters are 27.2 and 1.1 μm for the raw and milled powders respectively. The specific surface areas of the raw and milled powders were 2.5 and 10.3 m^2/g, respectively. SEM photographs of CSH are shown in Figure 4.
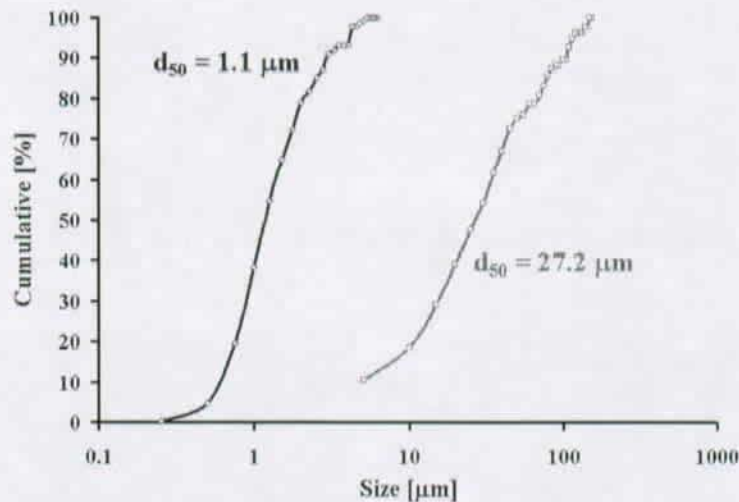

Figure 3 : Cumulative particle size distributions of raw and attrited CSH.

(a)   (b)
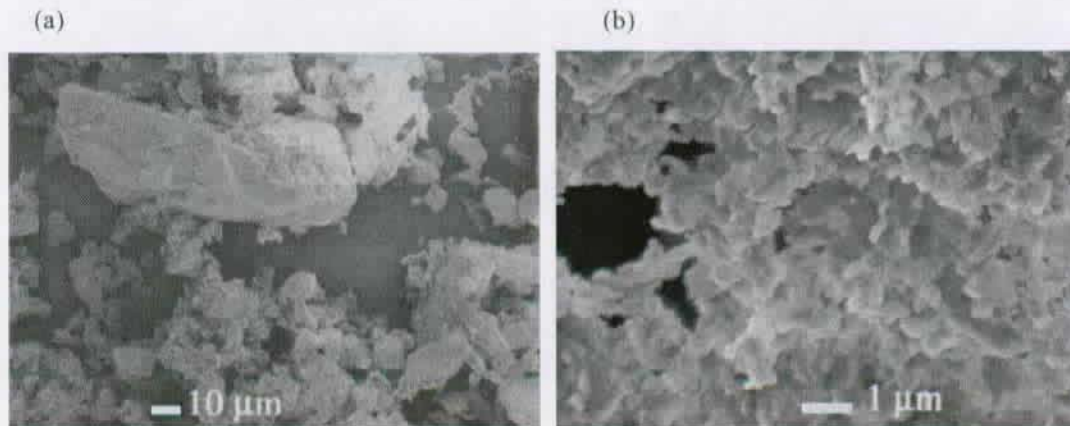
Figure 4 : SEM micrographs of (a) raw and (b) attrited CSH.

β-TCP milling

β-TCP. Particle size distributions of raw and milled β-TCP are presented in Figure 5. The decrease in median diameter is much lower than in the cases of MCPM and CSH. The median diameters are 2.4 and 1.5 μm for the raw and milled powders respectively. The specific surface areas of the raw and milled powders were 1.7 and 2.0 m^2/g respectively. SEM photographs of raw and milled β-TCP are shown in Figure 6.

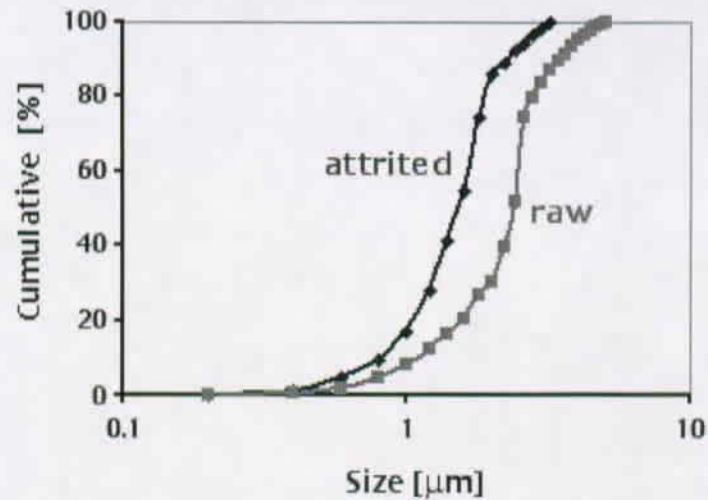**Figure 5 : Cumulative particle size distributions of raw and attrited β-TCP.**

(a)   (b)
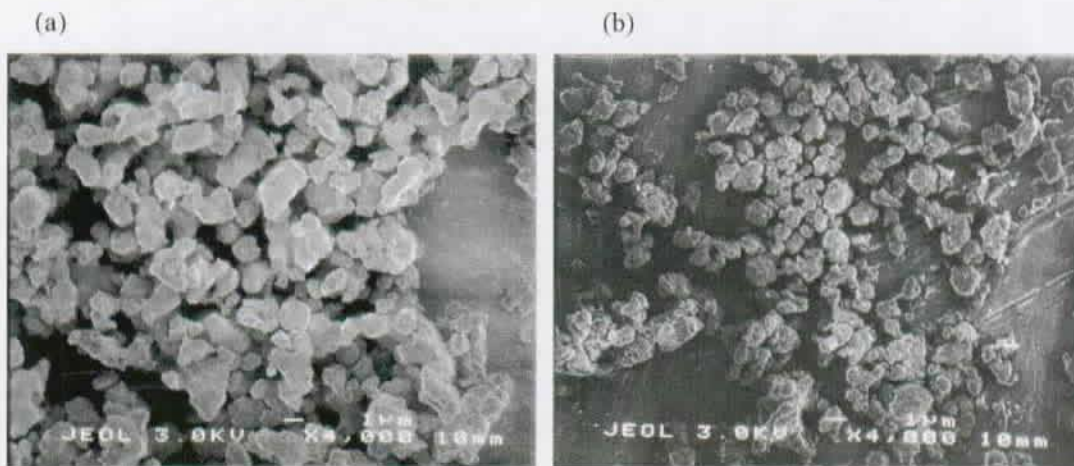
Figure 6 : SEM micrographs of (a) raw and (b) attrited β-TCP.

Cements properties

MCPM / CSH milling

Attrition of the powders appears to enhance the mechanical properties of the cement, both in tension (diametral compression test) and compression. Compressive and diametral tensile strengths are shown in Figure 7 and Figure 8. Cements made up of the raw powders show an indirect tensile strength of 1.4 MPa. It increases up to 4.1 MPa when the two milled powders are used, representing a three-fold increase. The compressive strength increase appears to be even more substantial, passing from 4.4 to 22.1 MPa (five-fold increase). It can be seen from

Figure 7 that the benefit gained from CSH attrition is much more important than that from MCPM attrition.
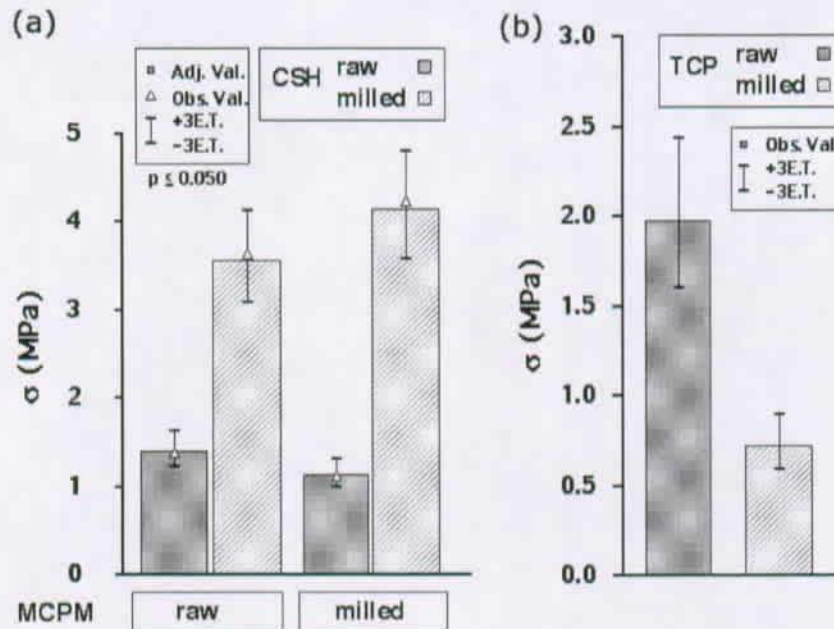
Figure 7 : Diametral tensile strengths of the cements : (a) MCPM/CSH milling, and (b) β-TCP milling.

Axial Compression
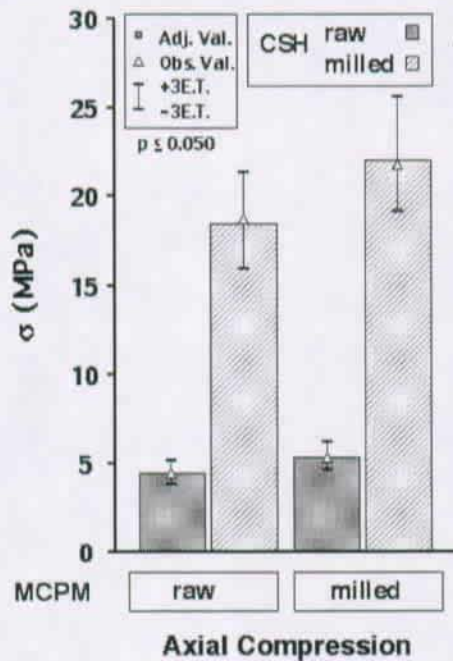
Figure 8 : Compressive strengths of the cements.

A marked decrease in porosity occurs when both MCPM and CSH are milled, passing from 52.4 to 42.1% (Figure 9). SEM photographs (Figure 10) show the microstructure of the hardened cements. Low magnification photographs show that numerous large spherical

defects (20 to 200 microns) are present in the cement made of raw powders. These defects were seen only in cements made with raw CSH.
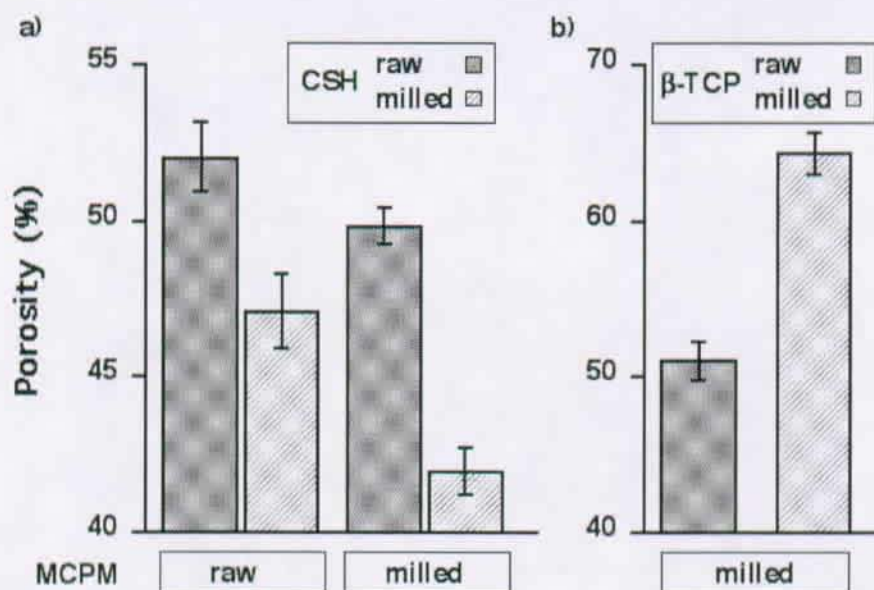
Figure 9 : Porosities of the cements (a : MCPM/CSH milling, b : β-TCP milling).

Figure 10 : SEM micrographs of (a) a cement with raw MCPM and CSH, and (b) a cement with attrited MCPM and CSH.

The completion of the DCPD- and CSD- forming reactions was assessed semi-quantitatively by X-rays diffraction. Peak ratios calculated from the diffractograms are summarized in Table

IV (intensity ratios of β-TCP/DCPD and CSH/Tot, where Tot means the sum of the intensities of the three peaks considered). This table shows that the conversion rate of β-TCP into brushite is enhanced when MCPM is milled, whereas it is lowered when fine CSH is used. Attrition of any one of the two powders enhances the hydration of CSH into CSD, which contributes to decreasing the porosity of the cement.
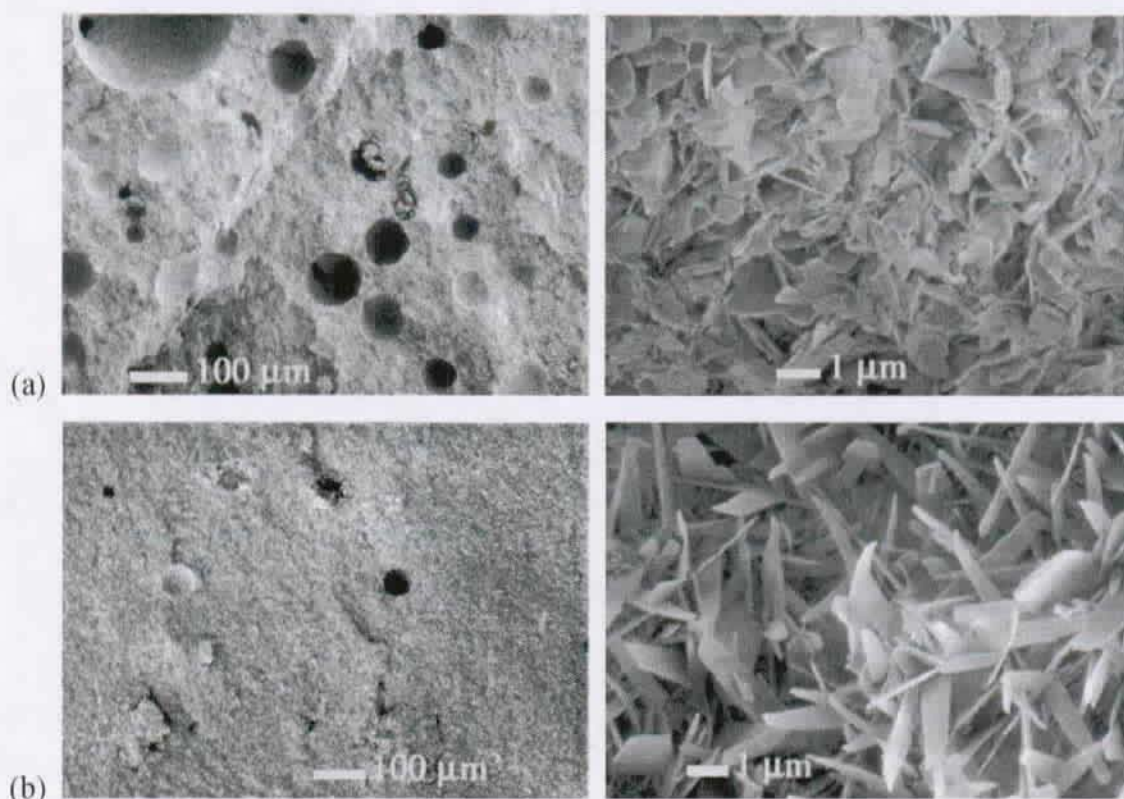
Table IV : Peak ratios calculated from the XRD diffractograms. (a) MCPM/CSH milling, (b) TCP milling.

(a)	β-TCP/DCPD [-]		CSH/Tot [-]	
	raw MCPM	milled MCPM	raw MCPM	milled MCPM
raw CSH	0.30	0.17	0.19	0.15
milled CSH	0.37	0.23	0.07	0.07

(b)	β-TCP/DCPD [-]	CSH/Tot [-]
raw TCP	0.42	0.08
milled TCP	0.83	0.11

β-TCP milling

Diametral tensile strengths of cements made of raw β-TCP is 2.0 MPa, and those made with milled β-TCP have a 0.7 MPa strength (Figure 7). Porosities are 51.0 and 64.2% for the cements made of raw and milled β-TCP, respectively (Figure 9b). The completion of the reaction is poor, as can be seen in Table IVb. All the properties measured on these cements are poor compared to the previous set of experiments. This will be discussed later. Given the bad results obtained with these cements, compression tests were not performed.

DISCUSSION

Powders properties

All powders were characterized with respect to their particle size distributions and their specific surface areas. With the median diameter and the specific surface area, it is possible to calculate a value reflecting the degree of agglomeration of the powder : the agglomeration factor. It is defined as the ratio between the median diameter and the diameter derived from the BET specific surface area measurement (d_{50}/d_{BET}).[17] This factor amounts 23.5 and 14.5 for the raw and milled MCPMs respectively, 81.6 and 13.9 for raw and milled CSHs, and 2.1 and 1.6 for raw and milled β-TCPs. It shows that the milled powders are better de-agglomerated than the raw ones. However, this finding needs to be commented. The median diameters were measured in dispersants that do not provide the same interfacial properties as those encountered in the mixing liquid. The pH of the liquid is different from the working conditions, and consequently the surface charges on the particles are not the same either. This means that the electrostatic forces acting between particles are also different, and consequently the stability of the suspension also differs. This shows a great difficulty in estimating the actual state of agglomeration of the starting powders in the liquid during mixing of the paste. However, measuring the particle size distribution in the same conditions as those of use would be misleading, since the system evolves during mixing and setting : dissolution of some species takes place, precipitation of others as well, causing the pH of the liquid to vary throughout the mixing and setting steps.[18] Before measurement of a particle size distribution, the suspensions are de-agglomerated with an ultrasonic horn. This treatment is a necessary precaution before particle size measurement to obtain reproducible measurements. However, it differs again from the actual conditions of use, and it is likely that large agglomerates form in the paste. Nevertheless, although this ultrasonic energy is not present in the paste, powders in the paste during mixing are submitted to shear stresses due to the mixing gesture with the spatula. Hence, agglomeration is hindered by these stresses. These stresses cannot be reproduced when measuring the particles size distribution. This reinforces the fact that agglomeration state during mixing might differ from that during measurement. This may explain why it is so difficult to find a relationship between the granulometric properties of the powders − measured in their own "measurement conditions" − and the mechanical properties of the cements.

Cements composition

Solid/Liquid ratios (S/L) had to be adjusted in the second part of the study, dealing with β-TCP granulometry. The milled form of the β-TCP requires more water to produce a suspension. Therefore, S/L cannot be as high as the one used with raw β-TCP in the first set of experiments. For this second part, we first intended to make cements with the same S/L ratio. It was found possible to make cements with a 1.7 g/cc S/L ratio. However, viscosities of the pastes were, as expected, very different and consequently shear stresses during mixing also differed greatly. The cement paste made with raw TCP was very liquid, whereas that made with milled TCP was very thick. Large agglomerates of unreacted raw β-TCP were found in the matrix of the hardened cement. This was suspected to be a consequence of the lack of shear stresses during mixing. On the other hand, the cement paste made with milled β-TCP was very thick, and efficient mixing was difficult to achieve. This shows that shear stresses produced during mixing are very important to help de-agglomerating the powders and that both too high and too low S/L ratios do not provide the necessary conditions to get an ideal behaviour of the powders in suspension.

As a consequence, we decided to produce two cement pastes with similar rheologies (suited for easy injectability). S/L ratios were 2.2 and 1.4 g/cc for cements with raw and milled β-TCP powders, respectively. The S/L ratio of the cement with raw β-TCP was the same as that used in the first set of experiments (see Table III).

Cements properties

MCPM / CSH milling

The mechanical strength of a calcium phosphate cement is generally related to its porosity and the fineness and homogeneity of its microstructure. As can be seen in Figure 7, use of milled MCPM generally enhances the mechanical properties of the hardened cement. Cement samples made with milled MCPM had a lower porosity and better conversion of β-TCP into brushite and CSH into CSD (Table IV). This appears to be in agreement with the knowledge that the better converted the stronger a cement becomes, and that low porosity provides good mechanical properties. Usually, porosity decreases as the setting reaction progresses.

The effect of using milled CSH is also beneficial to the mechanical properties of the cements. Porosity is significantly lowered, but conversion into brushite appears to be hindered, compared to cements prepared with raw CSH. Raw CSH appears to convert much more slowly into CSD than milled CSH. Hydration of CSH into CSD should in principle enhance the mechanical properties.

Clearly, better mechanical properties should be obtained when the porosity is lower and TCP conversion is more complete. These two properties are linked, since the specific volume of DCPD is larger than that of the original reactants. Hence, the better the conversion the lower the porosity. However, in our case, air bubbles also contribute to porosity (see Figure 10, top left). As formation of these bubbles only occurred when using raw CSH, it is suspected that calcium carbonate may be present as a contaminant, remaining from the synthesis of the calcium sulfate powder. The carbonate may evolve according to Eq. 3 to produce gaseous carbon dioxide, eventually forming spherical defects in the microstructure of the hardened cement.

$$CaCO_3(s) + 2H^+(aq) \rightarrow Ca^{2+}(aq) + \uparrow CO_2(g) + H_2O(liq) \qquad (3)$$
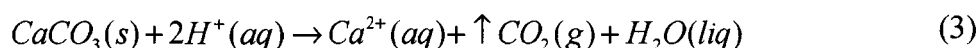
The purity of CSH powders was checked by thermogravimetry at 1000°C. Weight losses were 1.20 % for raw CSH, and 0.20% for milled CSH. Even though this measurement does not give any information about the chemical nature of the lost species, it shows that raw CSH has a much larger amount of impurities than milled CSH. Supposing that the 10% discrepancy in porosities is only due to the spherical defects produced by gaseous CO_2, then only 0.26 wt% $CaCO_3$ (100 = CSH mass) would be necessary to produce such an additional amount of porosity. Upon mixing with water, raw CSH appeared to produce bubbles. It is probable that most of the carbon dioxide produced escapes the cement paste, and that some part remains in the structure once the latter is solid enough to entrap bubbles.

This fact actually masks the effect of β-TCP conversion : cements made with milled CSH have a lower TCP conversion than those with raw CSH, but despite this their mechanical properties are much higher. This implies that the comparatively low mechanical properties of the cements made with raw CSH are mainly due to these defects. Their presence increases the effective stress acting on the cement matrix, and may partially explain the lower strength observed.

The shape of the brushite crystals is also influenced by the granulometric properties of CSH. SEM micrographs show that needle-like shape of brushite crystals is favored when fine CSH

is used, whereas raw CSH seems to promote the formation of tabular crystals (Figure 10, right-hand side). A previous study showed that needle-shaped brushite crystallization was beneficial to the diametral strength of these cements.[12]

β-TCP milling

Cements made with milled β-TCP have a much lower diametral tensile strength than those made with raw β-TCP. Values of porosity (Figure 9) and TCP/DCPD ratio (Table IVb) explain clearly this difference. Cements made with milled β-TCP have a very high porosity and a very poor conversion of TCP into brushite (DCPD). In contrast to the first part of the study (MCPM/CSH milling), the higher porosity seems to be directly related to the poor TCP conversion. Indeed, very few air bubbles were entrapped in the cement matrix.

Compared with the first part of this work, TCP to brushite conversion was much lower, and the porosity was much higher (51.0% instead of 42.1%). The porosity is comparable to that obtained with raw CSH in the first set of experiments, but this time it is likely due to the poor TCP conversion rather than to air bubbles. TCP conversion was even worse than the worst case found in the first part. Table V allows comparison of the characteristics of the cements made in this part of the study with those of the one made in the first part with milled MCPM and CSH, and raw β-TCP. Although MCPM and CSH powders were milled and freeze-dried the same way as in the first part of the study (MCPM/CSH milling), they appeared to have different granulometric characteristics. The way the drying step was performed is clearly not reproducible enough to ensure constant granulometric properties of the powders. Therefore, additional studies are needed to find a more robust way of drying our powders.

Table V : Characteristics of cements made with milled MCPM and CSH (Porosities and strength : mean±1 SD).

Study	MCPM/CSH milling	β-TCP milling	
β-TCP	raw	raw	attrited
S/L [g/cc]	2.23	2.20	1.35
TCP/DCPD	0.23	0.42	0.83
Porosity [%]	42.1±1.5	51.0±2.5	64.2±2.7
σ_{DTS} [MPa]	4.1±0.2	2.0±0.2	0.7±0.1

The large discrepancies in diametral compressive strengths between the first and the second part of the study show that the mechanical properties are very sensitive to the starting

powders granulometries. Previous studies have shown that the influence of granulometric characteristics of the sarting powders on the hardened cement properties is not easy to assess. Andrianjatovo et al[12] used a model cement with only one starting powder, but could not make a conclusive statement as to which granulometry would promote the highest mechanical properties. Furthermore, the knowledge gained from a specific study does not necessarily remain valid when changes, even minor, are made to the system. Chow et al[5] showed that high strengths were obtained when using large (d_{50} = 12 µm) TTCP particles and fine DCP (d_{50} = 0.9 µm), whereas Otsuka et al[11] reported extremely low mechanical properties with similar starting powders granulometries, but with additional HAP seed crystals.

CONCLUSIONS

Milling the starting powders is an efficient way to reduce the particle sizes and deagglomerate the powders. The attrition of MCPM and CSH was found to be beneficial both to the compressive strength and the diametral tensile strength of the cements, providing a five-fold inrease in axial compression, and a three-fold increase in diametral compression. The large difference between these values is mainly explainable by the difference in porosity of the cements. Porosity itself was found to be systematically higher when raw CSH was used. The large porosity is mainly due to the presence of large spherical defects in cements made with raw CSH. It is suspected that this powder is contaminated with some calcium carbonate, probably dissolving and producing gaseous carbon dioxide forming bubbles in the cement structure. Thermogravimetry has confirmed the presence of some impurities in the raw CSH powder. β-TCP milling did not bring any benefits to the mechanical properties of the cements, mainly because the Solid/Liquid ratio had to be drastically decreased to produce a paste with the same rheology as the one made with raw β-TCP. Thus, the granulometry of our raw β-TCP powder appears to be adapted to our needs. On the other hand, attrition of MCPM and CSH seems to be a necessary step to produce cements with enhanced mechanical properties. However, the mechanical properties of the cements are strongly dependent on the granulometry of these powders, especially CSH, which means that milling and drying routes must be under full control in order to ensure constant and precise granulometries of the resulting powders. This happens not to be the case presently, and fine tuning of these routes will be necessary to produce powders ensuring reproducible cement properties.

REFERENCES

[1] Brown W E, Chow L C. A new calcium phosphate, water-setting cement. Cem Res Prog 1986;351-379.

[2] Driessens F C M, Boltong M G, Planell J A, Bermudez O, Ginebra M P, Fernandez E. A new apatitic calcium phosphate bone cement : Preliminary results. Bioceramics 1993;6:469-473.

[3] Constantz B R, Ison I C, Fulmer M T, Poser R D, Smith S T, Van Wagoner M, Ross J, Goldstein S A, Jupiter J B, Rosenthal D I. Skeletal repair by in situ formation of the mineral phase of bone. Science 1995;267:1796-1798.

[4] Mirtchi A A, Lemaître J, Terao N. Calcium phosphate cements: study of the b-tricalcium phosphate – monocalcium phosphate system. Biomaterials 1989;10:475-480.

[5] Chow L C, Takagi S, Constantino P D, Friedman C D. Self-setting calcium phosphate cements. Mater Res Symp Proc 1991;179:3-24.

[6] Pittet C, Lemaître J. Mechanical characterization of brushite cements : A Mohr circles' approach. J Biomed Mater Res (Appl Biomater) 2000;53:769-780.

[7] Markovic M, Takagi S, Sieck B, Chow L C. Characteristic of calcium phosphate cement products in non-pressed specimens. J Dent Res 1997;76:420.

[8] Ishikawa K, Asaoka K. Estimation of ideal mechanical strength and critical porosity of calcium phosphate cement. J Biomed Mater Res 1995;29:1537-1543.

[9] Chow LC, Hirayama S, Takagi S, Parry E. Diametral tensile strength and compressive strength of a calcium phosphate cement: Effect of applied pressure. J Biomed Mater Res (Appl Biomater) 2000;53:511-517.

[10] Morgan E F, Yetkinler D N, Constantz B R, Dauskardt R H. Mechanical properties of carbonated apatite bone mineral substitute: strength, fracture and fatigue behaviour. J Mater Sci Mater Med 1997;8:559-570.

[11] Otsuka M, Matsuda Y, Suwa Y, Fox J L, Higuchi W I. Effect of particle size of metastable calcium phosphates on mechanical strength of a novel self-setting bioactive calcium phosphate cement. J Biomed Mater Res 1995;29:25-32.

[12] Andrianjatovo H, Jose F, Lemaître J. Effect of β-TCP granularity on setting time and strength of calcium phosphate hydraulic cements. J Mater Sci Mater Med 1996;7:34-39.

[13] Mirtchi A A, Lemaître J, Munting E. Calcium phosphate cements : action of setting regulators on the properties of the β-tricalcium phosphate – monocalcium phosphate cements. Biomaterials 1989;10:634-638.

[14] Ikenaga M, Hardouin P, Lemaître J, Andrianjatovo H, Flautre B. Biomechanical characterization of a biodegradable calcium phosphate hydraulic cement : A comparison with porous biphasic calcium phosphate ceramics. J Biomed Mater Res 1998;40:139-144.

[15] Van Landuyt P, Lowe C, Lemaître J. Optimization of setting time and mechanical strength of b-TCP/MCPM cements. Bioceramics 10, 1997;477-480.

[16] Montgomery DC. Design and analysis of experiments. 3rd Ed. New York: Wiley; 1991.

[17] Staiger M, Flatt RJ, Bowen P, Hofmann H. Colloidal processing of nanosized ceramic dispersions: Particle size distributions and their effect on colloid stability calculations and rheological behaviour. Ceramic Processing Science VI, Ceram Trans 2001;112:173-178.

[18] Bohner M, Van Landuyt P, Merkle H P, Lemaître J. Composition effects on the pH of a hydraulic calcium phosphate cement. J Mater Sci Mater Med 1997;8:675-681.

CHAPTER 4   A MODEL FOR CALCULATION OF BONE CEMENTS RADIOPACITY : DEVELOPMENT AND VALIDATION.

ABSTRACT

The objective of this work is to assess the X-ray opacification a bone cement should have to be used safely in fluoroscopic image-guided vertebroplasty, and to be able to calculate the radiopacification a bone cement of known composition would exhibit.

A computer model has been developed to calculate the linear X-ray attenuation coefficient of any material of known composition. It has been validated by experimental measurements on brushite cements of various porosities. The discrepancies observed between calculated and experimental attenuation coefficients was found not to exceed 15%, with the calculated values always lower than the measured values.

The standard attenuation coefficient a cement should exhibit to be used in vertebroplasty has been found to amount 2.47 cm^{-1} for the conditions simulated here. It was calculated from an acrylic cement composition considered a standard in vertebroplasty.

Linear attenuation coefficients were calculated for various calcium phosphate formulations : four commercial cements (Bone Source^{TM}, α–BSM^{TM}, Cementek$^{\circledR}$, Norian SRS$^{\circledR}$) and two brushite cements produced in our laboratroy. None of these cements was found to exhibit an attenuation coefficient as high as that of the standard one.

Finally, attenuation coefficients of brushite cements mixed to various iodinated opacifying molecules were calculated. It appears that addition of such compounds to a brushite cement seems feasible, since 3 to 6 wt% would be sufficient to produce the required opacification.

INTRODUCTION

Calcium phosphate cements were developed in the 1980s to serve as bone substitutes. All the existing formulations[1,2,3,4] are characterized by the fact that they are biocompatible and resorbable to some extent. They also show osteoconductive properties, as new bone is formed when resorption takes place.[5] Most formulations can be both used as dental or surgical materials. However, the term "bone cement" still refers to acrylic cements, since those are the cements commonly used by the clinicians when injection of a biomaterial into bone is necessary. Although the use of acrylic cement is common, many drawbacks related to this material can be reported, like strong exothermicity on setting,[6,7] monomer toxicity,[8,9] and absence of resorbability. The main advantage of acrylic cements over calcium phosphate cements lies in the fact that their mechanical properties are superior. However, some clinical applications do not necessarily require biomaterials exhibiting as high a strength as that of acrylic cements. Vertebroplasty is a good example of an application where calcium phosphate cements could favourably replace acrylic cements.

Vertebroplasty is a minimally invasive percutaneous procedure consisting in injecting cement into the vertebral body of a fragilized vertebra.[10] Causes for fragilization may stem from various pathologies like osteolytic metastasis and myeloma, aggressive hemangioma or osteoporosis. The material used is always acrylic bone cement. No calcium phosphate cement has ever been used in clinical vertebroplasty. As the gesture is performed percutaneously, the cement paste flow must be visualized in order to ensure no cement leakage out of the vertebral body. Cement leakage into the foramen must be particularly avoided since it may produce spinal cord compression and induce severe complications. Live visualization of the paste flow is ensured by radiologic control (fluoroscopy), so that the clinician can stop the injection at any time if leakage starts occurring. At the moment, no minimum radiopacity is recommended for a biomaterial to be used in vertebroplasty, and each group practising vertebroplasty makes its own mix so as to obtain easy visualization of the cement paste during injection. It is fairly reasonable to consider that the modified acrylic cement used by Deramond and his team[11] is probably the one that fulfils best radiopacity requirements, since he was the pioneer in vertebroplasty in 1984,[12] and since then he has gained extensive experience in this procedure.

As acrylic cements are very radiolucent, many studies have attempted to add radiopacifiers under various forms.[13,14,15,16,17] The mineral character of calcium phosphate cements provides them with a higher intrinsic radiopacity than acrylic cements, mainly made of light elements like carbon, hydrogen or oxygen. As calcium phosphate cements are easily detectable on radiographs, it is generally thought that opacifying these cements is useless. However, radiopacity requirements for fluoroscopy during vertebroplasty are not met as easily as for images on radiographic films, and it is still unclear whether calcium phosphate cements are radiopaque enough or not for use in vertebroplasty.

This is why we propose to study the radiopacity of calcium phosphate cements to make clear whether their opacification would be a necessary condition to match the requirements of vertebroplasty. We first develop a simple mathematical model to calculate radiopacity of any material considered (linear attenuation coefficient). After validation, we use it to calculate the linear attenuation coefficient of the "Deramond cement" and of various calcium phosphate cements.

THEORY OF OPACIFICATION

The intensity transmitted through a sample exposed to polychromatic X-rays is expressed the following way :

$$I_t = \int_{E_{min}}^{E_{max}} I_0(E) \cdot \exp\left[-\sum_i \left(\frac{\mu}{\rho}(E)\right)_i \cdot \rho_i \cdot x\right] dE \qquad (1)$$

where I_t is the intensity transmitted, E_{min} and E_{max} the minimum and maximum energies of the incident spectrum, $I_0(E)$ the incident spectrum, $(\mu/\rho)_i$ and ρ_i the mass attenuation coefficient and the volumic concentration of the species i, and x the thickness of the sample.

To calculate the linear attenuation coefficient of a sample, the following equation is used :

$$\mu = \frac{1}{x} \cdot \ln\left(\frac{\int_{E_{min}}^{E_{max}} I_0(E) dE}{I_t}\right) \qquad (2)$$

The linear attenuation coefficient of an element is proportional to the atomic number Z of the element and to the wavelength of X-rays $(Z^4 \lambda^3)$. However, this proportionality is disrupted at attenuation edges. Thus, it is easy to understand why the opacifiers or contrast products

commonly used in clinical applications are barium (Z = 56, attenuation peak at 37 keV) salts, tantalum (Z = 73, attenuation peaks at 12 and 67 keV), tungsten (Z = 74, attenuation peaks at 12 and 67 keV) or iodine (Z = 53, attenuation peak at 33 keV) compounds.

Blackening of a radiographic film exposed to X-rays is normally measured using optical density. It is defined as

$$OD = \log_{10}(I_0/I_t) \tag{3}$$

This value is measured via a densitometer.

EXPERIMENTAL

Computer model

The computer model was created with Matlab$^{®}$ to calculate linear attenuation coefficients of any material of known composition. The program allows the user to enter the following input parameters : the atomic number (Z) and the volumic concentration of each element of the material considered, as well as the thickness of the specimens. Mass attenuation coefficients depend on the energy of the incident beam. Therefore, an overall attenuation coefficient is calculated for the spectrum considered : this is the output parameter given by the program. The simulated incident spectrum put in the program is that produced by a tungsten anode, with 3 mm Al filtration. It extends from 12 to 60 keV, and the intensities are given every half keV. Linear attenuation coefficients of the elements are tabulated in the "NIST X-Ray Attenuation Databases".[18] Mass attenuation coefficients used in the program are those for 10, 15, 20, 30, 40, 50 and 60 keV. The integral determining the transmitted intensity is calculated in a discrete way on these seven points of energy, plus the energies for which elements have discontinuities in the attenuation spectrum. The function of the attenuation coefficients between these points is considered linear. The integral for calculating the incident energy is also calculated in a discrete manner every half keV, and interpolation between these points is linear, too.

Validation of our model was made by exposing various samples under the same X-rays source as that simulated. Materials used for validation were brushite cement with various Solid/Liquid ratios (2 to 3.5 g/mL, by 0.5 g/mL increments) and an acrylic cement, Simplex$^{®}$ P Radiopaque. The compositions considered to get the input parameters in the computer model were the following : for brushite cements 1.20 g β-TCP ($Ca_3P_2O_8$), 0.80 g MCPM ($CaH_6P_2O_9$) and 1.00, 0.80, 0.67, 0.57 g water for the 2, 2.5, 3.0 and 3.5 g/mL cements

respectively. Measured apparent densities were 1.32, 1.48, 1.59 and 1.69 g/cc respectively. For the Simplex® P Radiopaque : 12.55 g PMMA ($C_5O_2H_8$), 15 g MMA-styrene copolymer ($C_{13}O_3H_{16}$) and 2 g barium sulfate ($BaSO_4$), with a measured density of 1.13 g/cc. The specimens (of known volume) were weighed to calculate their apparent density. For the calcium phosphate cements, the mineral phases present in the paste before setting are not the same as those found after setting. However, as the chemical form of the species does not influence the attenuation strength of the materials, only the starting components were taken into account. Moreover, in practice the cement is visualized as it is in a pasty form, i. e. mostly made out of the starting phases.

Samples were placed along with two aluminium step wedges on a cassette containing a radiosensitive film (Kodak Trimax XLA Plus), and exposed to a 60 kVp and 2 mAs X-rays source (tungsten anode and 3 mm Al filtration, distance film-source : 1 m). 60 kVp is a typical tension used in vertebroplasty for a thin patient. It may be increased up to 80 kVp for fat patients. Optical densities measured on the developed film allowed calculations of linear attenuation coefficients relative to aluminium. Measurements of optical densities of the aluminium steps allowed plotting the curve of optical density as a function of aluminium thickness (Figure 1).
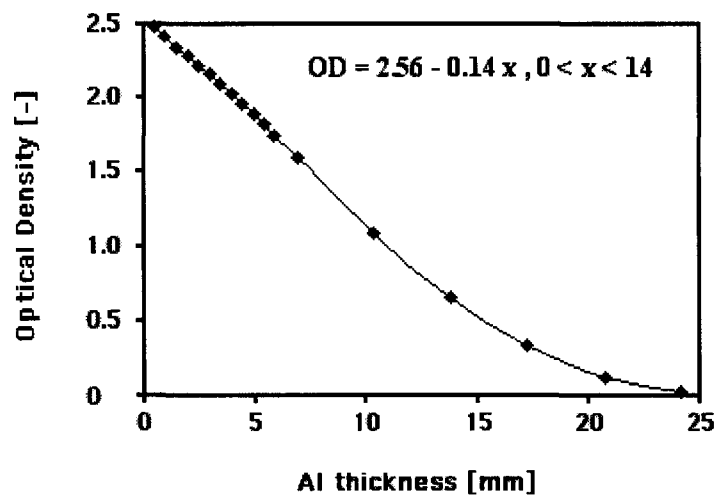

Figure 1 : Optical density versus Aluminium thickness (x).

Exposure times and specimen thicknesses were chosen so as to ensure that all optical densities measured lay in the linear part of this curve. Linear regression of the curve (for $0 \leq x_{Al} \leq 14$ mm) allowed precise determination of the equivalent aluminium thickness for every

specimen tested. For a sample of height x_s producing the same attenuation (i.e. same optical density) as x_{Al} mm of aluminium, its attenuation coefficient relative to aluminium is expressed the following way :

$$\frac{\mu_s}{\mu_{Al}} = \frac{x_{Al}}{x_s} \qquad\qquad (4)$$

Attenuation coefficients - Calculations

Linear attenuation coefficients of various calcium phosphate cements were computed with our model and compared to the calculated coefficient of the modified acrylic cement used by Deramond. The "Deramond cement" is a modified Simplex® P Radiopaque. For 10 cc liquid monomer, 13.8 g of Simplex® P Radiopaque powder and 3 grams tantalum are used.[19] The compositions entered into our program for linear attenuation coefficients calculations were : four calcium phosphate commercial cements (Bone Source™, α-BSM™, Cementek®, Norian SRS®), two calcium phosphate cements developed in our laboratory (brushite cements : LTP-A and LTP-B), one acrylic cement (Simplex® P Radiopaque) and the "Deramond cement". Compositions of the calcium phosphate cements are given in Table I (mixing liquid was always considered to be water, although it is not always the case in practice). Composition of the Simplex® P Radiopaque was the same as that given in the preceding section.

Table I : Compositions of the calcium phosphate cements entered into the calculation program.

	S/L (g/mL)	Powder 1	Powder 2	Powder 3
Bone Source™	4.0	2.29 g TTCP	1.71 g DCP	
α – BSM™	1.5	0.85 g DCPD	0.65 g HAP	
Cementek®	2.3	1.13 g TTCP	0.87 g α-TCP	0.3 g NaGP
Norian SRS®	2.0	1.53 g α-TCP	0.31 g CC	0.16 g MCPM
LTP-A	2.2	1.11 g β-TCP	0.72 g MCPM	0.31 g CSH
LTP-B	2.5	1.50 g β -TCP	1.00 g MCPM	

RESULTS AND DISCUSSIONS

Model validation

Figure 2 shows the linear attenuation coefficients expressed relative to aluminium for the four brushite cement compositions (BC x = brushite cement, x g/mL) and the acrylic cement. As the discrepancy between experimental and calculated values does not exceed 15%, the model can reasonably be used as a predictive tool for radiopacity of cements with or without opacifying additives.
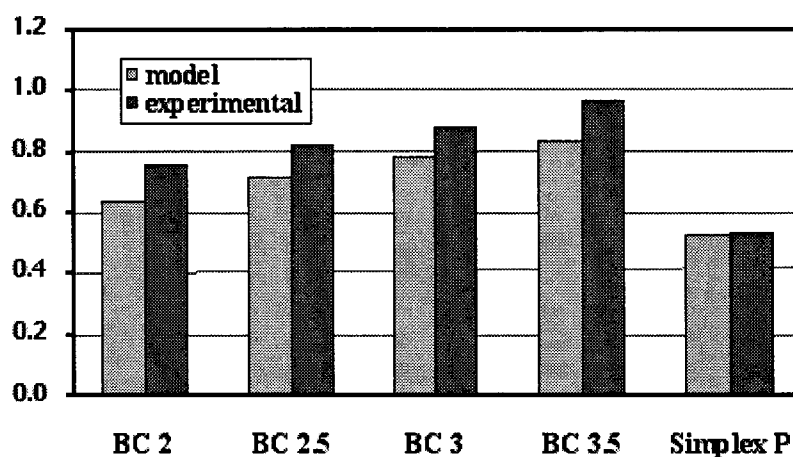

Figure 2 : Linear attenuation coefficients relative to aluminium. Experimental and calculated results.

On the basis of the materials used to test the validity of the model, it seems that the values calculated are always below those actually measured. Therefore, the model in its actual state can be considered a bit pessimistic compared to reality. There are obviously some factors limiting the degree of accuracy our model could reach. The number of points used in the integral calculations between E_{min} and E_{max} is relatively small (7 points). Increasing the number of points would refine calculations, but the intervals between tabulated attenuation coefficients in the "NIST X-Ray Attenuation Databases" are not narrower than those used here. Moreover, the interpolation between these points was considered linear for simplicity reasons, but it is a rather rough estimation of reality. The actual description of the attenuation coefficients curve would be polynomial of degree 3 at least. Another possible reason for the discrepancy observed lies in the fact that the incident spectrum "seen" by the atoms varies along the way through the sample, since all layers closer to the X-ray source filter the incident spectrum and modify it before it reaches the regions further away from the source (beam

hardening effect). In our model, the spectrum is assumed to be the same along its whole way through the material specimen. In conclusion, the discrepancies could probably be reduced by refining the model, but for its purpose of use we considered the accuracy sufficient.

Attenuation coefficients - Calculations

The calculated linear attenuation coefficient of the Deramond cement was found to amount 2.47 cm^{-1}. This value can be considered a standard value to be reached by any cement meant to be used in vertebroplasty. However, it must be kept in mind that this value is only valid in the conditions simulated in the computer model, i. e. with the same incident spectrum. As can be seen in Figure 3, all the compositions considered have an attenuation coefficient lower than that of the Deramond cement. The composition least efficient in terms of opacification is the Simplex$^{®}$ P Radiopaque, even though this acrylic cement is opacified with 10 wt% barium sulfate. The attenuation coefficients of the calcium phosphate compositions all lie between those of the Simplex$^{®}$ and of the Deramond cements. The most radiopaque calcium phosphate composition is Bone Source™, mostly because it is denser than the others (higher S/L, see Table I). However, this composition is not injectable and rendering it injectable would necessarily mean adding more water, hence lower density and opacification. All the compositions tested here do not present the required attenuation coefficient, which means that they would not produce sufficient contrast in fluoroscopy if they were to be used in their present state in vertebroplasty.
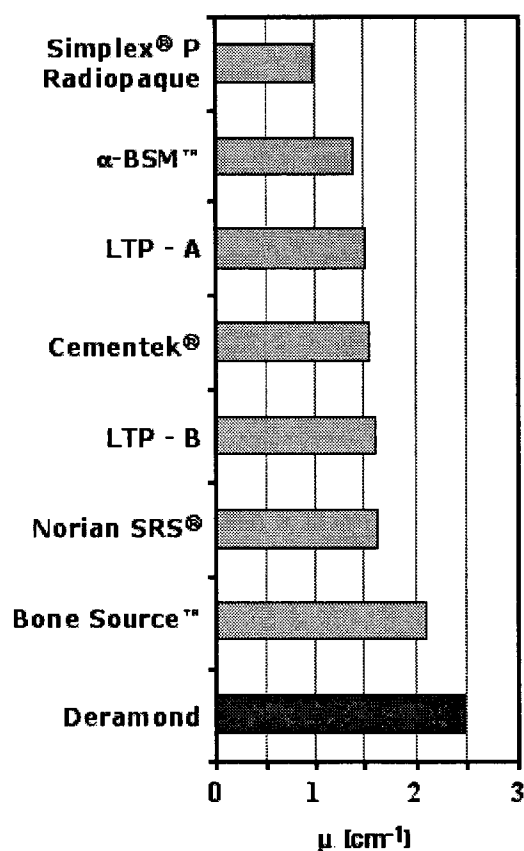
Figure 3 : Computed linear attenuation coefficients of various bone cements.

A way of improving the radiopacity of a cement is to enhance its Solid/Liquid ratio (S/L). After our calculations with LTP-A, a 62 g/mL S/L would be required to produce an attenuation coefficient equivalent to that of the Deramond cement. The amount of water added to the solid particles would be so low that this particular case practically refers to a powder blend of the starting solid components, compacted to their theoretical density, thus it is no longer a cementitious material. This shows the necessity to add radiopacifiers to calcium phosphate cements to be used safely in vertebroplasty.

Further computer calculations were made to assess the necessary amount of opacifier to be added to the LTP-A cement in order to produce the same opacification as the Deramond cement, i.e. a 2.47 cm^{-1} linear attenuation coefficient. Table II shows some examples of iodine-containing compounds and the weight percentages needed to produce the opacification required, along with the median lethal doses reported from literature.[20]

Table II : Weight percentages of various iodine-containing compounds required to produce an opacification equivalent to that of Deramond. Median lethal doses are also presented.

Name	Formula	Toxicity	wt %
Barium iodide	BaI_2	poison	3.2
Cesium iodide	CsI	LD50 ip in rats : 1.4 g/kg	3.2
Sodium iodide	NaI	LD50 iv in rats : 1.3 g/kg	3.7
Barium iodate	$Ba(IO_3)_2$	poison	3.9
Cesium iodate	$CsIO_3$	no data available	3.7
Sodium iodate	$NaIO_3$	LD50 iv in dogs : 0.2 g/kg	4.8
Iopamidol	$C_{17}H_{22}I_3N_3O_8$	LD50 iv in rats : 28.2 g/kg	6.2
Iohexol	$C_{19}H_{26}I_3N_3O_9$	LD50 iv in rats : 32.3 g/kg	6.5
Iotrolan	$C_{37}H_{48}I_6N_6O_{18}$	LD50 iv in rats : 27.1 g/kg	6.5
Iodipamide	$C_{20}H_{14}I_6N_2O_6$	LD50 iv in rats : 4.4 g/kg	4.6
Iocematic acid	$C_{12}H_{13}I_3N_2O_3$	LD50 iv in rats : 0.7 g/kg	5.0
Iomeglamic acid	$C_{17}H_{22}I_3N_3O_8$	LD50 iv in rats : 0.5 g/kg	5.0

Iodine compounds may be organic or inorganic, water soluble or not. It appears that the most efficient opacifiers are inorganic, water soluble iodine salts with a heavy cation (Ba- and Cs-iodides), but their toxicity is high. Soluble organic molecules are less efficient, but their toxicity is very much lower. In the case of resorbable calcium phosphate cements, toxicity of the opacifier is of major concern, since it is bound to be released in the body as the cement resorbs.

CONCLUSION

The computer model developed here has been validated and then used to calculate the linear attenuation coefficients of various calcium phosphate cements. The attenuation coefficient of the cement used by Deramond in vertebroplasty was also calculated and found to amount 2.47 cm^{-1} for the simulated conditions. This value can be considered now a standard value to be reached by any cement meant to be used in vertebroplasty. Results have shown that no calcium phosphate cement is radiopaque enough for a safe use, which means clearly that any such cement would have to be opacified if it were to be used in vertebroplasty. In theory, 3 to 7 wt% iodine-containing compounds would be necessary to opacify our calcium phosphate

(brushite) cement to the level of the Deramond cement. However, the influence of these opacifiers on the properties of such a cement are still unknown and now a practical study consisting in incorporating opacifiers appears to be necessary.

REFERENCES

[1] Brown W E, Chow L C. A new calcium phosphate setting cement. J Dent Res 1983;62:672.

[2] Driessens F C M, Boltong M G, Planell J A, Bermudez O, Ginebra M P, Fernandez E. A new apatitic calcium phosphate bone cement: Preliminary results. Bioceramics 1993;6:469-473.

[3] Constantz B R, Ison 1 C, Fulmer M T, Poser R D, Smith S T, Van Wagoner M, Ross J, Goldstein S A, Jupiter J B, Rosenthal D I. Skeletal repair by in situ formation of the mineral phase of bone. Science 1995;267:1796-1798.

[4] Mirtchi A A, Lemaître J, Terao N. Calcium phosphate cements: Study of the β-Tricalcium Phosphate – Monocalcium Phosphate System. Biomaterials 1989;10:635-638.

[5] Ohura K, Bohner M, Hardouin P, Lemaître J, Pasquier G, Flautre B. Resorption of, and bone formation from, new β-tricalcium phosphate-monocalcium phosphate cements: an in vivo study. J Biomed Mater Res 1996;30:193-200.

[6] Leeson M C, Lippitt S B. Thermal aspects of the use of polymethylmetacrylate in large metaphyseal defects in bone. A clinical review and laboratory study. Clin Orthop 1993;295:239-245.

[7] Deramond H, Wright N T, Belkoff S M. Temperature elevation caused by bone cement polymerization during vertebroplasty. Bone 1999;2:17S-21S.

[8] Dahl O E, Garvick L J, Lyberg T. Toxic effects of methylmethacrylate monomer on leukocytes and endothelial cells in vitro. Acta Orthop Scand 1994;65:147-153.

[9] Bostrom M P, Lane J M. Future directions. Augmentation of osteoporotic vertebral bodies. Spine 1999;22:39S-42S.

[10] Mathis J M, Barr J D, Belkoff S M, Barr M S, Jensen M E, Deramond H. Percutaneous vertebroplasty: a developing standard of care for vertebral compression fractures. Am J Neuroradiol 2001;22:373-381.

[11] Jasper L, Deramond H, Mathis J M, Belkoff S M. Evaluation of PMMA cements altered for use in vertebroplasty. Oral communication. 10th Interdisciplinary Research Conference on Injectable Biomaterials. Toulouse (F), 13-14 March 2000.

[12] Galibert P, Deramond H, Rosat P, Le Gars D. Note préliminaire sur le traitement des angiomes vertébraux par vertébroplastie acrylique percutanée. Neurochirurgie 1987;33:166-168.

[13] de Wijn JR, Slooff TJ, Driessens FC. Characterization of bone cements. Acta Orthop Scand 1975;46:38-51.

[14] Vallo C I, Cuadrado T R, Frontini P M. Mechanical and fracture behaviour evaluation of commercial acrylic bone cements. Polymer International 1997;43:260-268.

[15] Chang P. Polymer implant materials with improved X-ray opacity and biocompatibility. Biomaterials 1981;2:151-155.

[16] Nzihou A, Attias L, Sharrock P, Ricard A. A rheological, thermal and mechanical study of bone cement – from a suspension to a solid biomaterial. Powder Technology 1998;99:60-69.

[17] Vazquez B, Ginebra M P, Gil F J, Planell J A, Lopez Bravo A, San Roman J. Radiopaque acrylic cements prepared with a new acrylic derivative of iodo-quinoline. Biomaterials 1999;20:2047-2053.

[18] http://physics.nist.gov/PhysRefData/XrayMassCoef/cover.html

[19] Jasper L, Deramond H, Mathis JM, Belkoff SM. Evaluation of PMMA cements altered for use in vertebroplasty. 10th Interdisciplinary Research Conference on Injectable Biomaterials, Toulouse (F), 13-14 march 2000.

[20] The Merck Index, 11th Ed., Merck&Co. Inc., 1989.

CHAPTER 5   RADIOPACIFICATION OF CALCIUM

PHOSPHATE BRUSHITE CEMENTS WITH

IODINE-CONTAINING ADDITIVES.

ABSTRACT

Four radiopacifiers were selected to be incorporated into brushite cements. Two were organic compounds soluble in water (Iopentol and Iopamidol), commonly used as contrast enhancing media in X-ray imaging applications. The two others were inorganic molecules, one soluble (sodium iodide), the other sparingly soluble in water (sodium iodate). Their effect on the setting times and the compressive and diametral tensile strengths was studied. A control cement without opacifier was made for comparison.

A first series of five cement compositions (four opacified and one control) made with identical Solid/Liquid weight ratios was prepared. None of the opacifiers appeared to alter the setting time of the cement. Iopentol-cement was found to be the strongest if both compressive and diametral tensile strengths are taken into account. This cement was the one exhibiting the lowest porosity among the opacified cements. However, its paste was thicker than those of the other opacified cements and that of the control.

In view of these results, two cements with similar paste rheologies (one opacified with Iopentol, the other without opacifier) were compared as to their compressive and diametral tensile strengths. Their compressive and diametral tensile strengths appeared not to be significantly different. Iopentol diffusion kinetics after setting was also assessed. Within 24 hours, more than 80% of the Iopentol was released from the cement samples.

INTRODUCTION

The preceding chapter has shown clearly that X-ray opacification of calcium phosphate cements is a necessary operation prior to using them in image-guided vertebroplasty. The amount of opacifier needed to be added to a cement for safe opacification is now easy to assess, but the effects of radiopacifiers on the cement properties remain unknown. Additives of any type are known to possibly alter paste rheology, setting time and mechanical properties of the hardened cement. The effects of various radiopacifiers on the mechanical properties of acrylic bone cements have been investigated in different studies. Some of the principal radiopaque additives tested were barium sulfate[1,2] or zirconium oxide[1,2,3] as powders, or diiodo-quinolyl methacrylate[4] as a monomer.

As acrylic cements do not show any bioactive properties, practically any radiopaque additive may be used, regardless of its potential toxicity. On the contrary, porous biodegradable calcium phosphate cements should not contain any toxic compound since it is bound to be released in the body, if not during injection, at least during cement degradation. To our knowledge, no opacifying agent has ever been added to a calcium phosphate cement. Thus, there is no means to know how such additives could alter the paste or hardened cement properties.

Iodine-containing compounds produce excellent radiopacification in the kilovolt range used in image-guided vertebroplasty. They are commonly used as contrast enhancing agents for X-ray imaging applications like angiography or neuroradiology. Non-ionic water soluble tri-iodinated benzoic molecules are those most commonly used presently. Their toxicity and pharmacokinetics have been extensively studied and well documented. The main complication associated with the use of these molecules as injectable contrast media is nephrotoxicity,[5] but they are generally very well tolerated.[6] In terms of weight fraction to be added to a cement, inorganic molecules compare favourably with the organic ones, since smaller amounts are needed for the same opacification (see preceding chapter). These molecules may be soluble to a various extent. Molecules with limited solubility are not expected to interact in a significant way with the setting reaction of calcium phosphate cements.

The objective of this study is to try to make brushite cements with X-ray opacity suited for use in vertebroplasty, and to assess the effect of the opacifiers on the mechanical strength of

the cements. To achieve this goal, four iodinated compounds were selected for use as opacifying additives : sodium iodate, sodium iodide, and two tri-iodinated benzoic molecules, Iopentol® and Iopamidol®.

EXPERIMENTAL

Experimental design

The experiments were divided into two parts. First, a series of four opacifiers was added to the cements and the effects of these additives on setting time and mechanical properties were studied. All compositions had the same massic Solid/Liquid ratios, but different paste rheologies. Axial and diametral compression tests were performed to estimate compressive and diametral tensile strengths, respectively. Results were analyzed with the Anova technique.[7] The designation of the cement compositions and the types of tests performed are summarized in Table I. Each treatment was repeated four times.

Table I : Cement compositions and mechanical tests performed.

Compositions	Tests
Control	
Iopentol	Axial compression
Iopamidol	
NaI	Diametral compression
NaIO$_3$	

In a second step, two formulations were prepared : one opacified with Iopentol, the other one without opacifier (control). Solid/Liquid ratios were adapted so as to ensure the same paste rheology of the two cements. Both were tested in diametral and axial compressions, with four replicates for each composition. Results were analysed with Student's test statistical analysis.

Radiopacifiers

Four different radiopacifiers were chosen to be added to our cements. Two of them are inorganic compounds : one is soluble in water, sodium iodide (NaI, Merck, Cat. No. 106520); the other is sparingly soluble in water, sodium iodate (NaIO$_3$, Merck, Cat. No. 106525); the

two other molecules are organic and soluble in water : Iopentol® (Imagopaque®, Nycomed Imaging AS) and Iopamidol® (Iopamiro®, Bracco spa). The two latter are tri-iodinated benzoic molecules commonly used in angiographic applications.

The quantities to be added to the cement for producing a 2.47 cm⁻¹ linear attenuation coefficient (see preceding chapter) were calculated with the computer model presented in the preceding chapter. Table II shows the resulting concentrations and the weight percentages of the opacifiers. Concentrations given in mg/mL refer to the opacifier concentration within the mixing liquid. Concentrations in wt% refer to the mass fraction of the total cement weight.
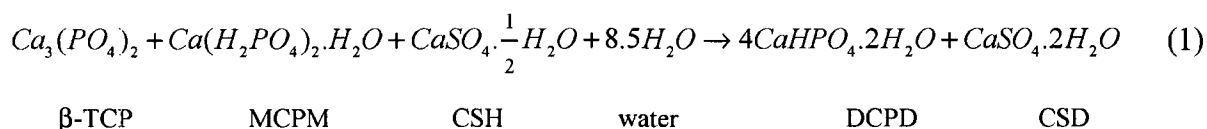
Table II : Concentrations and weight percentages of opacifiers to be added to the cement to obtain μ = 2.47 cm⁻¹.

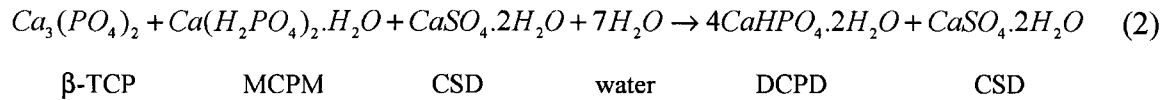| Concentration	Iopentol	Iopamidol	NaI	NaIO₃
in mg/mL	222	203	120	157
in mg(I)/mL	100	100	100	100
in wt%	6.6	6.0	3.8	4.8

The mixing liquids of cements opacified with water soluble additives are the aqueous solutions made from these opacifying molecules. As the solubility of sodium iodate is much lower (90 mg/mL in cold water), it was added to the cement in a powdery form, only partially solubilised upon addition to the mixing liquid (water in this case).

Cement compositions

The starting powders are β-tricalcium phosphate (β-TCP), monocalcium phosphate monohydrate (MCPM) and calcium sulfate, hemihydrated (CSH) or dihydrated (CSD). β-TCP and MCPM react in presence of water to form brushite (dicalcium phosphate dihydrate, DCPD). The latter phase is the main constituent of the hardened cement. Gypsum (calcium sulfate dihydrate, CSD) is also present in the final product. If CSH is used, the setting reaction takes place according to the following reaction :

$$Ca_3(PO_4)_2 + Ca(H_2PO_4)_2.H_2O + CaSO_4.\frac{1}{2}H_2O + 8.5H_2O \rightarrow 4CaHPO_4.2H_2O + CaSO_4.2H_2O \quad (1)$$

| β-TCP | MCPM | CSH | water | DCPD | CSD |

If CSD is used, this reaction becomes :

$$Ca_3(PO_4)_2 + Ca(H_2PO_4)_2.H_2O + CaSO_4.2H_2O + 7H_2O \rightarrow 4CaHPO_4.2H_2O + CaSO_4.2H_2O \quad (2)$$

β-TCP   MCPM   CSD   water   DCPD   CSD

A small amount of sodium dihydrogen pyrophosphate (NaHPP, $Na_2H_2P_2O_7$, Fluka) is added to the starting powders as a setting regulator (0.090 g). β-TCP is used in excess over the stoichiometric β-TCP/ MCPM ratio.

The starting powders, β-TCP, MCPM, CSH and CSD were prepared in our laboratory to meet the granulometric requirements. Specific surface areas and median diameters of the powders are presented in Table III.

Table III : Specific surface areas and median diameters of the starting powders.

Powder	S_{BET} $[m^2/g]$	d_{50} $[\mu m]$
β-TCP	1.5	4.7
MCPM	3.3	12.4
CSH	12.1	2.2
CSD	5.1	5.4

The cements opacified with the four iodinated compounds (see Table II) were made with CSH, according to reaction (1). The quantities mixed are the following : 1.201 g β-TCP, 0.781 g MCPM, 0.339 g CSH, 1.081 g mixing liquid. Five cements were prepared and tested : Control-, Iopentol-, Iopamidol-, NaI-, and $NaIO_3$-cements (control = without opacifier). Massic Solid/Liquid ratios are the same for the five cements (2.15 g/g).

A second series of cements was prepared, with two different compositions : one opacified with Iopentol, the other as a control, i.e. not opacified. These cements are those of reaction (2), where CSD is used instead of CSH. In order to estimate the effect of Iopentol on mechanical properties when the paste rheology is the same as that of the control cement, the quantity of mixing liquid was modified. The two cement compositions stand in Table IV.

Table IV : Compositions of the control- and Iopentol- cements with same paste rheology (Mixing liquids : control = water, Iopentol = Iopentol solution 110 mg(I)/mL).

	Control-cement	Iopentol-cement
MCPM [g]	0.781	0.781
β-TCP [g]	1.201	1.201
CSD [g]	0.339	0.339
Mixing liquid [g]	1.10	1.26
S/L [g/mL]	2.11	2.07

Sample preparation

The cement paste is prepared in a mortar and mixed with a metallic spatula. MCPM and NaHPP are poured first in the mortar containing water, and mixed with help of the spatula. After 30 seconds, CSH is added and mixed for another 30 seconds. Then β-TCP is added, activating the setting reaction. The mix becomes pasty, and the paste must be thoroughly mixed for 1 minute. Then it is introduced with help of the spatula into a 2mL-syringe whose extremity was previously cut. After each cement addition into the syringe, the paste is vibrated to eliminate entrapped air bubbles. Immediatly after demolding, specimens are stored individually in watertight snap caps in water-saturated atmosphere at 37°C for 24 hours. The resulting cylinders have a diameter of 8.7 mm. Their faces are then polished (SiC paper 120) in order to obtain the desired height and parallelism between the faces. The height of the cylinders varies depending on the test to which the specimen is destinated.

Characterizations

Setting times. Setting times were measured with a Vicat needle (98.35 g, needle diameters: 1 and 2 mm).

Porosity. Open porosity of the hardened cements (tested in diametral compression) was determined by the Archimede's method.

X-Rays Diffraction. XRD was performed with a Kristalloflex 805 (Siemens) diffractometer (Kα-Cu radiation), using the coupled θ/2θ method. It was done on crushed hardened cement samples. Relative heights of β-TCP (2θ = 27.77°) and DCPD (2θ = 20.93°) peaks were

calculated from the diffraction spectra obtained, allowing indirect estimation of the completion of the setting reactions.

Mechanical testing. Two types of mechanical tests were performed on the cement specimens : axial and diametral compression tests (the diametral compression test is also referred to as Brazilian test or indirect tension test). Diametral compression test allows indirect measurement of a specimen's tensile strength. The limitations in the interpretation of the results obtained on brushite cements were studied in detail in another study.[8] Diametral compression tests were made with an Adamel Lhomargy DY31 universal testing machine equipped with a 2 kN load cell. The steel platens of the press were covered with a cardboard to insure contact along the whole cylinder and to distribute the applied force on a larger surface. Specimens were cylindrical, 8.7 mm in diameter and 6 mm in length. Loading rate was 0.3 mm/min. The horizontal stress in the middle of the diametral plane of the specimen (supposed to be responsible for fracture) is calculated the following way :

$$\sigma = \frac{2P}{\pi D L} \tag{3}$$

where P is the applied force, D the cylinder diameter, L its length.

Axial compression tests were performed with an Instron 4467 universal testing machine with a 30 kN load cell. The compressive load rate was 0.3 mm/min. Specimens were cylindrical, with 8.7 mm diameter and 18 mm length.

Iopentol diffusion kinetics. Six samples of Iopentol-cements were prepared in silicon molds (h = 13 mm, Ø = 10 mm). They were allowed to set for 20 minutes in their molds, then unmolded and dipped in cell culture wells filled with 9.5 mL simulated body fluid (modified Hanks 9269 body fluid, composition shown in Table VII). The simulated body fluid was renewed after 1, 2, 4, 9 and 24 hours. At each of these times the solution was withdrawn for Iopentol concentration measurement by UV spectrophotometry (Perkin Elmer Lambda 900). Iopentol produces an absorbance peak at 242.5 nm, which height varies linearly with the length of optical path, the molar absorption coefficient and the concentration of the solution (Beer-Lambert law).

Table V : Composition of the modified Hanks 9269 body fluid.

Species	Conc. [mmol/L]
NaOH	144.99
Ca(OH)$_2$	1.26
HCl	144.77
H$_3$PO$_4$	0.78
NaHCO$_3$	4.17
H$_2$SO$_4$	0.81

RESULTS

Setting times of the four opacified cements and the control (measured with the Vicat needle) are all within 24±1 minutes.

Diametral tensile and compressive strengths of the cements tested are presented in Figure 1 and Figure 2, respectively. Duncan's multiple range tests show that NaI-cements exhibit a diametral tensile strength significantly higher ($p<0.05$) than that of Iopamidol-, NaIO$_3$- and control- cements. There is a 50% strength increase between the control cement and the one opacified with sodium iodide, the diametral tensile strength increasing from 2.1 up to 3.1 MPa.

Results for compressive strengths do not show the same ranking, since the strongest cement appears to be the one with Iopentol, with a compressive strength significantly higher than all other cements (Duncan's multiple range test, $p<0.05$). Iopentol-cements are 40% stronger in compression than the control ones (14.7 vs. 10.7 MPa). As Iopentol-cement's diametral tensile strength is not significantly lower than that of the NaI-cement, it can be considered the globally strongest cement when both compression and indirect tension are taken into account.
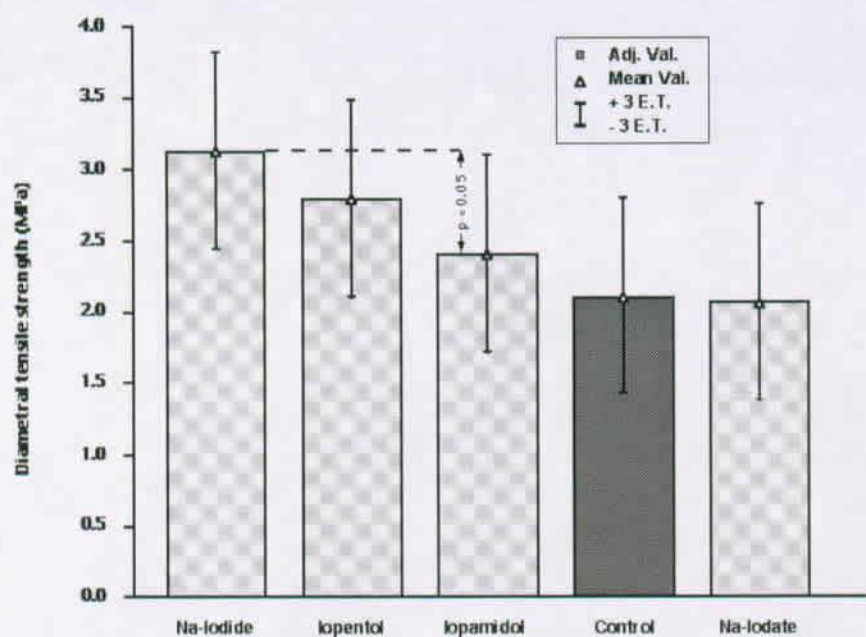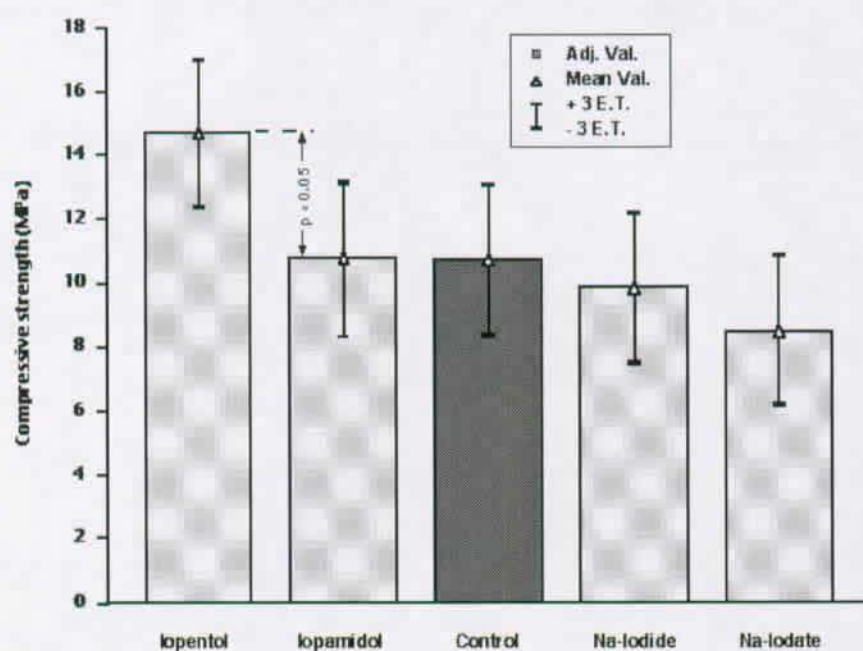
Figure 1 : Diametral tensile strengths of cements.

Figure 2 : Compressive strengths of cements.

β-TCP/DCPD peak height ratios measured from X-ray diffractograms are presented in Table VI, along with porosities.

Table VI : β-TCP/DCPD peak height ratios from XRD, and porosities of the cements. Porosities are means of 4 measurements (expressed as mean ± standard deviation).

Cement	TCP/DCPD [-]	P [%]
Control	0.37	50.3 ± 5.5
Iopentol	0.43	39.0 ± 2.3
Iopamidol	0.48	40.2 ± 1.3
NaI	0.55	44.2 ± 2.4
NaIO₃	0.62	49.0 ± 2.3

Results of diametral and axial compression tests performed on the two cements with the same paste rheology (Iopentol and control, see Table IV) are displayed in Table VII. There is no significant difference (Student's test, n = 4, p<0.01) between the two cements in terms of mechanical strength. Setting times appear to be the same (6 minutes) with or without Iopentol.

Table VII : Compressive and diametral tensile strengths of control- and Iopentol-cements (mean±3SD).

	Control	Iopentol
Compressive Strength [MPa]	11.03±0.85	10.81±1.33
Diametral Tensile Strength [MPa]	2.05±0.43	2.07±0.46

The evolution of the weight fraction of Iopentol diffused into the simulated body fluid is presented in Figure 3.
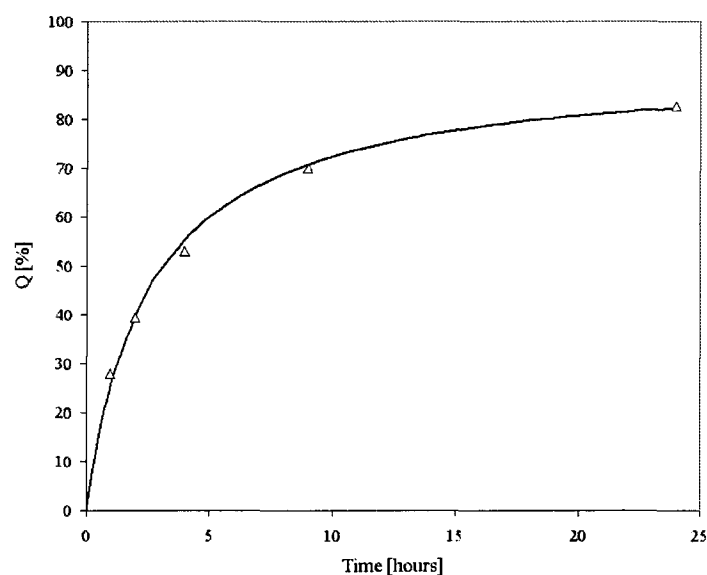
Figure 3 : Quantity of Iopentol diffused in the simulated body fluid within 24 hours.

DISCUSSION

Setting times appear not to be influenced significantly by any of the opacifiers tested here. The five cement compositions made according to reaction (1) have setting times of 24 minutes. The Iopentol and control cements of similar rheology made according to reaction (2) set in 6 minutes. This difference can probably be ascribed to the use of CSD instead of CSH. Whatever the opacifier used, no significant strength decrease is reported. However, the opacifying additives influence the porosity of the hardened cements and the completion of the setting reactions. All the opacifiers tested here tend to hinder the completion of the setting reaction (higher TCP/DCPD ratio). This should theoretically have deleterious effects on the mechanical properties, since less cementitious phase is present in the cement. However, the completion of the reaction is not the only factor affecting cement strength. Porosity is also important. It is influenced by three factors : completion of the reaction, presence of air bubbles in the paste, Solid/Liquid ratio (S/L, expressed in g/mL). In principle, the more complete the reaction is, the lower is the porosity. Porosity increases with the S/L ratio. Furthermore, for cements prepared manually as those tested here, the porosity also depends on the amount of air bubbles entrapped within the cement paste during mixing. The macroscopical defects stemming from air bubbles make it difficult to link porosity with the completion of the reaction.

Porosities of the cements appear to vary with the nature of the opacifier added to the cement. Iopamidol- and Iopentol- cements are significantly less porous than the control specimens. This probably arises from the fact that S/L (in g/mL) is actually not identical for all cements. As it was found easier in practice to measure the mass of the mixing liquids rather than their volume, S/L is identical when expressed in g/g, but differs when expressed in g/mL since the densities of the mixing liquids are different. For instance, the density of the Iopentol solution at 24°C is 1.111 g/cc, which makes S/L to increase from 2.15 (case with water as mixing liquid) up to 2.38 g/mL (Iopentol solution as mixing liquid). This is probably the main reason why the porosities of the Iopentol- and Iopamidol- cements appear to be the lowest ones.

Among the opacified cements, the Iopentol-one is that with the lowest porosity and the best completion of the setting reaction. This explains why its mechanical properties are superior to the control cement.

The $NaIO_3$-cement is the one with the poorest reaction completion, and a porosity higher than the other opacified cements. SEM micrographs of these cements show defects containing unreacted β-TCP (Figure 4). This may explain why the porosity is so high and the completion of the reaction is so low. Moreover, these defects surely act as weak points in the microstructure. Their deleterious effects on the compressive and indirect tensile strengths can be seen in Figure 2. These defects probably stem from the limited solubility of $NaIO_3$. The exact reasons for the formation of these defects are yet unclear : they are probably the result of some reaction between undissolved $NaIO_3$ crystals and the surrounding cement.

SEM micrographs of the other cements do not show obvious differences between the microstructures of the cements, and are therefore not presented here.
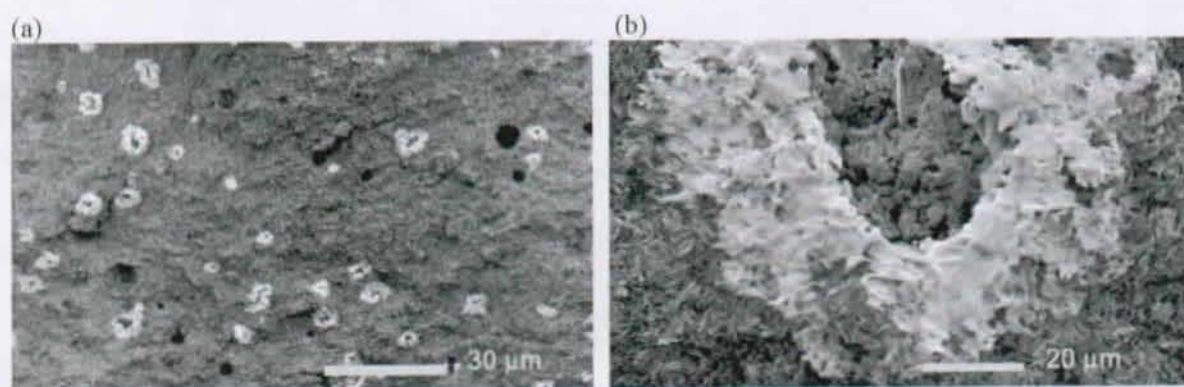

Figure 4 : SEM micrographs of the $NaIO_3$-cement.

Consistencies of the cement pastes vary with the type of opacifier used. The thicker pastes are those with Iopentol and Iopamidol, both due to higher S/L ratio (in g/mL) and higher viscosity of the mixing liquids. Control- and NaI-cements are those whose paste is more liquid. The $NaIO_3$-cement paste has a slightly higher viscosity than the latter, probably due to the higher amount of powder mixed to the liquid ($NaIO_3$ was added as a powder).

Achievement of the same paste rheology requires a slightly larger volume of mixing liquid when Iopentol is used (Table IV). This is due to the higher viscosity of the Iopentol solution compared with water. The differences between the mechanical strengths of the control cements made with CSH (reaction (1)) and those with CSD (reaction (2)) are not significant (2.11 and 2.05 MPa in diametral compression, 10.73 and 11.03 MPa in axial compression). It shows that the use of CSD instead of CSH does not affect the compressive and indirect tensile strengths of brushite cements. The Iopentol cements made with CSH have higher compressive and diametral tensile strengths than those made with CSD. This can be ascribed to the higher S/L ratio of the cements made with CSH (2.38 vs. 2.07 g/mL).

The Iopentol-cement samples prepared for study of Iopentol diffusion kinetics contain 72 mg(I) before immersion in the simulated body fluid. Within 24 hours, 83% of this amount is released in the SBF. This evolution over time can be approximated by a hyperbola, $Q = t/(at + b)$, where a equals 0.011 [1/%] and b equals 0.029 [h/%]. 1/a is actually $Q_\infty =$ 91.3%, the percentage released at infinite time, and 1/b = 35.0%/h is the initial release rate. As the SBF is renewed, concentration gradients are made to increase abruptly every time fresh fluid is added. These sudden concentration changes may not be too realistic, but they are still more representative of in vivo conditions than if no renewal at all is made. These values show that most of the Iopentol amount is released within 24 hours in these measurement conditions. This release rate is rather fast, but it is not problematic, since the role of Iopentol is only crucial during the time of injection. However, the diffusion kinetics of this molecule may be very different in in vivo conditions, since the surrounding environment would differ from the test conditions produced here.

CONCLUSIONS

This study has shown that brushite cements can be opacified with iodine-containing opacifying additives. None of the opacifiers tested here appears to alter setting times of the cements. The effect of these additives on the mechanical strengths is also minor. The only cement exhibiting a diametral tensile strength significantly higher than the control cement (without opacifier) is the one with Na-iodide. In compression, the Iopentol-cement appears to be significantly stronger than the others. The porosities of the cements made with the organic compounds are 10% lower compared to the control cement. This stems from the difference in Solid/Liquid ratios. After adaptation of the Solid/Liquid ratios to obtain cement pastes with similar rheologies, differences in compressive and diametral tensile strengths are no longer observed. The release rate of Iopentol from the cement into a simulated body fluid is found to be rather fast : within 24 hours, more than 80% of the opacifier present in the cement has been released. However, in vivo studies would be necessary to assess the diffusion kinetics in vivo and to understand how the presence of this molecule would affect the biological behaviour of the cement.

REFERENCES

[1] Vallo C I, Cuadrado T R, Frontini P M. Mechanical and fracture behaviour evaluation of commercial acrylic bone cements. Polymer International 1997;43:260-268.

[2] Chang P. Polymer implant materials with improved X-ray opacity and biocompatibility. Biomaterials 1981;2:151-155.

[3] Nzihou A, Attias L, Sharrock P, Ricard A. A rheological, thermal and mechanical study of bone cement – from a suspension to a solid biomaterial. Powder Technology 1998;99:60-69.

[4] Vazquez B, Ginebra M P, Gil F J, Planell J A, Lopez Bravo A, San Roman J. Radiopaque acrylic cements prepared with a new acrylic derivative of iodo-quinoline. Biomaterials 1999;20:2047-2053.

[5] Morcos SK, Epstein FH, Haylor J, Dobrota M. Aspects of contrast media nephrotoxicity. Eur J Radiol 1996;23:178-184.

[6] Jakobsen JA, Berg KJ, Waaler A, Andrew E. Renal effects of the non-ionic contrast medium Iopentol after intravenous injection in healthy volunteers. Acta Radiol 1990;31:87-91.

[7] Montgomery DC. Design and analysis of experiments. 3rd Ed. New York: Wiley; 1991.

[8] Pittet C, Lemaître J. Mechanical characterization of brushite cements : A Mohr circles' approach. J Biomed Mater Res (Appl Biomater) 2000;53:769-780.

ABSTRACT

A custom-made calorimeter was developed for measurement of kinetic and thermometric parameters of the cements studied. A single measurement allowed calculation of the maximum reaction rate of the setting reactions, the working and setting times of the cement pastes, the degree of conversion of the cements, and the temperature increase induced by the setting reaction.

Two of the factors studied concerned the granulometry (raw or milled) and the degree of hydration (hemihydrate or dihydrate) of one of the starting components, the calcium sulfate powder. The third factor was the presence or not of orthophosphoric acid in the mixing liquid.

The highest temperature increase recorded during setting was 14°C. It was produced by a cement made with raw calcium sulfate dihydrate, without orthophosphoric acid in the mixing liquid.

The degree of hydration of the calcium sulfate was found to have a significant influence on the kinetics of the setting reaction. The reaction is accelerated by calcium sulfate dihydrate because it provides nuclei for heterogeneous precipitation of brushite. In contrast, calcium sulfate hemihydrate was found to slow down the reaction by releasing sulfate ions in the mixing liquid. As the reaction is faster when CSD is used, heat production occurs faster and accumulates in the system. As a consequence, the temperature elevation during setting is more important.

INTRODUCTION

Calcium phosphate cements were first developed by Brown and Chow in the eighties.[1] Since then, various alternative formulations have been developed to be used as bone substitutes.[2,3,4] These cements show excellent biocompatibility, and their resorbable and osteoconductive characters favour new bone growth as they degrade. Their limited mechanical strength precludes their use in weight-bearing osseous sites. On the other hand, they are well suited to applications where the loads applied are not too high and recolonization of the implant by new bone tissue is expected, like distal radius fractures,[5] craniofacial skeletal surgery,[6,7] or prophylactic vertebroplasty.

Vertebroplasty is performed currently with acrylic bone cement, mainly for its superior mechanical properties. However, heat production during polymerization is one of the main drawbacks reported from literature dealing with surgical use of acrylic cements.[8,9] The heat released by the setting reaction provokes a temperature increase far above body temperature, so that adjacent osseous tissue undergoes thermal necrosis. This is one of the reasons why osseointegration is poor, and gap formation, often filled with fibrous tissue, is commonly observed at the bone-acrylic cement interface.

Calcium phosphate cements are known to release significantly less heat than acrylic cements upon setting. For these cements, the heat produced depends on the chemical formulation of the starting components and their relative quantities. As there are many ways of obtaining the desired final product of a calcium phosphate cement, the heat produced may also vary significantly, depending on the starting composition. To our knowledge, only one study has dealt with the thermal behaviour of calcium phosphate cements.[10] They were compared with acrylic cements, and the highest ultimate temperatures measured were 85±5°C for acrylic cements, and 44±2°C for calcium phosphate cements.

Brushite cements are calcium phosphate cements obtained by mixing monocalcium phosphate monohydrate and β-tricalcium phosphate powders in water. Calcium sulfate is generally added to the starting components to act as a setting regulator and to ensure correct in vivo behaviour of the cement. It can be used under its hemihydrate form (CSH) or its dihydrate form (CSD). It is suspected that the degree of hydration of the calcium sulfate powder, as well as its granulometry, influence the kinetics of the setting reaction and the thermal behaviour of the cement, but these effects have never been studied. Orthophosphoric

acid can also be used as one of the starting components of brushite cements. It was observed that use of this acid seems to increase the heat produced by the setting reaction. The heat produced by the setting reaction can be calculated if the reaction enthalpies are known. However, the theoretical values have never been compared to experimental ones.

The fact that calcium phosphate cements produce less heat upon setting than acrylic cements is a matter of fact. Nevertheless, the thermal behaviour of these cements needs to be documented in more details. This is why we propose to use a custom-designed calorimeter for temperature elevation measurement and for deriving thermometric and kinetic parameters of the setting reaction of various brushite cements. The effects studied are the degree of hydration of the calcium sulfate powder, its granulometry, and the presence or not of orthophosphoric acid.

EXPERIMENTAL

Experimental setup

The main body of the calorimeter used is a dewar container on which a custom-made cap is placed to ensure thermal insulation of the inner part of the calorimeter. A needle-shaped thermocouple (type T, Testo, Cat no. 0628.0027) allows temperature measurement in the heart of the cement sample, as shown in Figure 1. The samples have a 14 mm height and a 13 mm diameter.
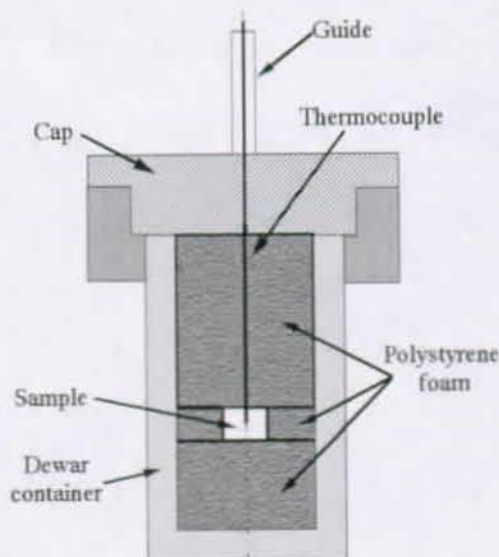

Figure 1 : Schematic drawing of the custom-made calorimeter.

Heat dissipation occurs through the metal of the thermocouple. Heat loss of the system is measured by heating a cement specimen 20°C above room temperature, placing it in the calorimeter, and measuring the decay of cement temperature for 2 hours (Figure 2). The experimental curve $\Delta T - \Delta T_0$ can be approximated by a hyperbola :

$$\Delta T(t) - \Delta T_0 = \frac{-t}{b + at} \qquad (1)$$

where t is time, ΔT_0 is the initial difference between specimen temperature and room temperature. Linearisation of the hyperbola and application of the least square method allows calculation of the curve parameters a and b. $1/a$ equals ΔT_0. Heat dissipation, defined as positive here, is expressed the following way :

$$\Delta H_d(t) = m \cdot c_p \cdot \Delta T(t) \qquad (2)$$

where m is the mass of the cement specimen (in grams), c_p its specific heat capacity (in cal/g). Derivation over time of the preceding equation gives the heat dissipation rate of the system. It is expressed as :

$$\frac{\partial \Delta H_d}{\partial t} = m \cdot c_p \cdot \frac{b}{(b + a \cdot t)^2} \qquad (3)$$

As ΔT and t are linked according to Eq. (1), Eq. (3) can be expressed as a function of ΔT :

$$\frac{\partial \Delta H_d}{\partial t}(\Delta T) = \frac{m \cdot c_p}{b} \cdot \frac{\Delta T^2(t)}{\Delta T_0^2} \qquad (4)$$

For each experimental Temperature-time curve $\Delta T(t)$, the amount of heat dissipated from the start of the experiment can be calculated by numerical integration of Eq. (4). An exemple of a heat dissipation curve is shown in Figure 5.
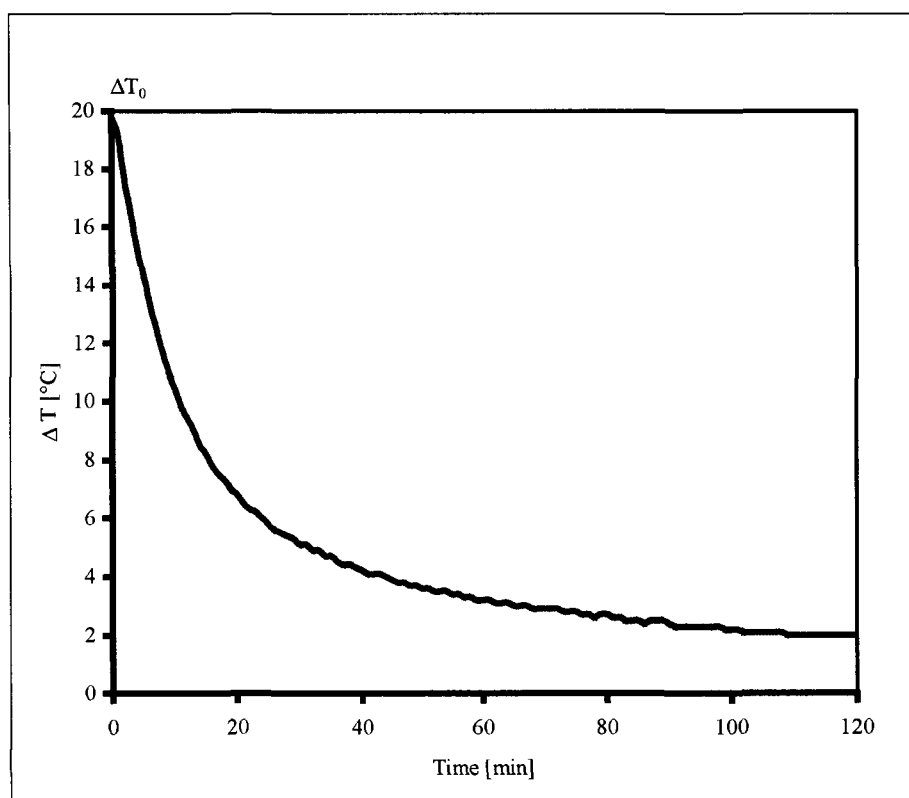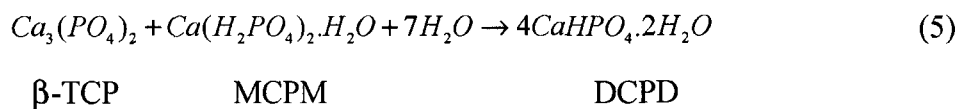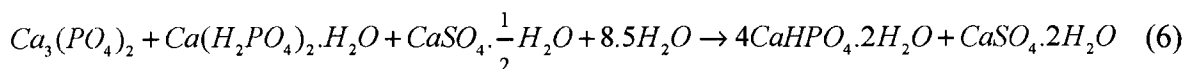
Figure 2 : Experimental Temperature-time curve for heat dissipation estimation.

Cement studied, sample preparation

The cement studied is a brushite cement, consolidating according to the following reaction :

$$Ca_3(PO_4)_2 + Ca(H_2PO_4)_2.H_2O + 7H_2O \rightarrow 4CaHPO_4.2H_2O \qquad (5)$$

$$\text{β-TCP} \qquad \text{MCPM} \qquad \text{DCPD}$$

This is the basic reaction forming the cementitious phase of the cement : brushite (DCPD). The two starting powders are β-tricalcium phosphate (β-TCP) and monocalcium phosphate monohydrate (MCPM). β-TCP is used in excess over the stoichiometric β-TCP/MCPM ratio. Upon mixing with water, the two powders react to form brushite. Calcium sulfate (CS) is generally added to the starting components. It can be used under its hemihydrate form (CSH, "Plaster of Paris") or its dihydrate form (CSD, gypsum). If Plaster of Paris is used, reaction (1) becomes :
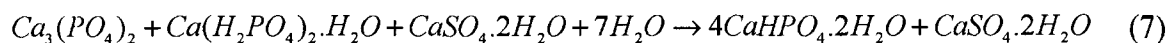
$$Ca_3(PO_4)_2 + Ca(H_2PO_4)_2.H_2O + CaSO_4.\frac{1}{2}H_2O + 8.5H_2O \rightarrow 4CaHPO_4.2H_2O + CaSO_4.2H_2O \quad (6)$$

β-TCP   MCPM   CSH   DCPD   CSD

Now if gypsum is used, the reaction is :

$$Ca_3(PO_4)_2 + Ca(H_2PO_4)_2.H_2O + CaSO_4.2H_2O + 7H_2O \rightarrow 4CaHPO_4.2H_2O + CaSO_4.2H_2O \quad (7)$$

β-TCP   MCPM   CSD   DCPD   CSD

Whatever the starting components, sodium hydrogenopyrophosphate ($Na_2H_2P_2O_7$, NaHPP, Fluka) is added as a setting regulator.

Cements are prepared from two pastes : one containing β-TCP, the other with CS, MCPM and NaHPP. Each paste is made with half the total amount of mixing liquid needed for cement preparation. The two pastes are prepared separately on a POM (polyoxymethylene) hydrophobic surface. First the TCP powder is mixed with half the mixing liquid with help of a metallic spatula, then the three other powders are mixed with the other half of the mixing liquid. After careful homogenization, the two pastes are mixed together. The setting reaction starts upon mixing of the two pastes. The resulting cement paste is molded in 1.9 mL polypropylene molds (h = 14 mm, $\varnothing$ = 13 mm), vibrated to allow easy mold filling, and then put in the calorimeter.

Experimental design

The factors tested were the hydration degree of the calcium sulfate powder, its granulometry, and the presence or not of orthophosphoric acid (OPA) in the mixing liquid. The experiments were organised in a 2^3 factorial statistical design described in Table I, and the results were analyzed with the Anova technique.[11] Each treatment was repeated 3 times.

Table I : Definition of levels of factors tested.

	CS hydration	CS granulometry	Phosphoric acid
	Hemihydrate	Raw	No
	Dihydrate	Milled	Yes

Cement compositions

Eight different cements were studied. As one of the factors is CS granulometry, it does not affect the chemical composition of the cement. Therefore, four different chemical formulations were actually tested. Their compositions are given in Table II. The amounts were calculated so as to ensure, theoretically, the same Ca/P and Ca/S ratios and the same porosity. All compositions should have a Ca/P of 1.21, a Ca/S of 7.30 and a 38.4% final porosity (assuming 100% MCPM conversion).

Table II : Nominal cement compositions - Starting components.

	CSH		CSD	
	without OPA	with OPA	without OPA	with OPA
MCPM [g]	0.980	0.803	1.007	0.825
β-TCP [g]	1.507	1.575	1.548	1.618
CSH [g]	0.427	0.426	-	-
CSD [g]	-	-	0.520	0.519
OPA 0.67 M [mL]	-	1.450	-	-
OPA 0.71 M [mL]	-	-	-	1.410
H_2O [mL]	1.360	-	1.310	-

β-TCP was synthesized in our laboratory. MCPM is from Albright&Wilson. As this powder is contaminated with some orthophosphoric acid, it was washed in ethanol. ICP analysis of the washed powder revealed a Ca/P ratio of 0.68, indicating that it is actually a blend of MCPM and DCPA, in proportions of 62.6 and 37.4 wt%, respectively. On this basis, the actual compositions were re-calculated and are shown in Table III. Presence of DCPA in the MCPM powder was confirmed by X-ray diffractions of the cements (Figure 3).

Table III : Actual cement compositions. Starting components (β-TCP, CS and mixing liquids quantities are the same as those in the preceding Table).

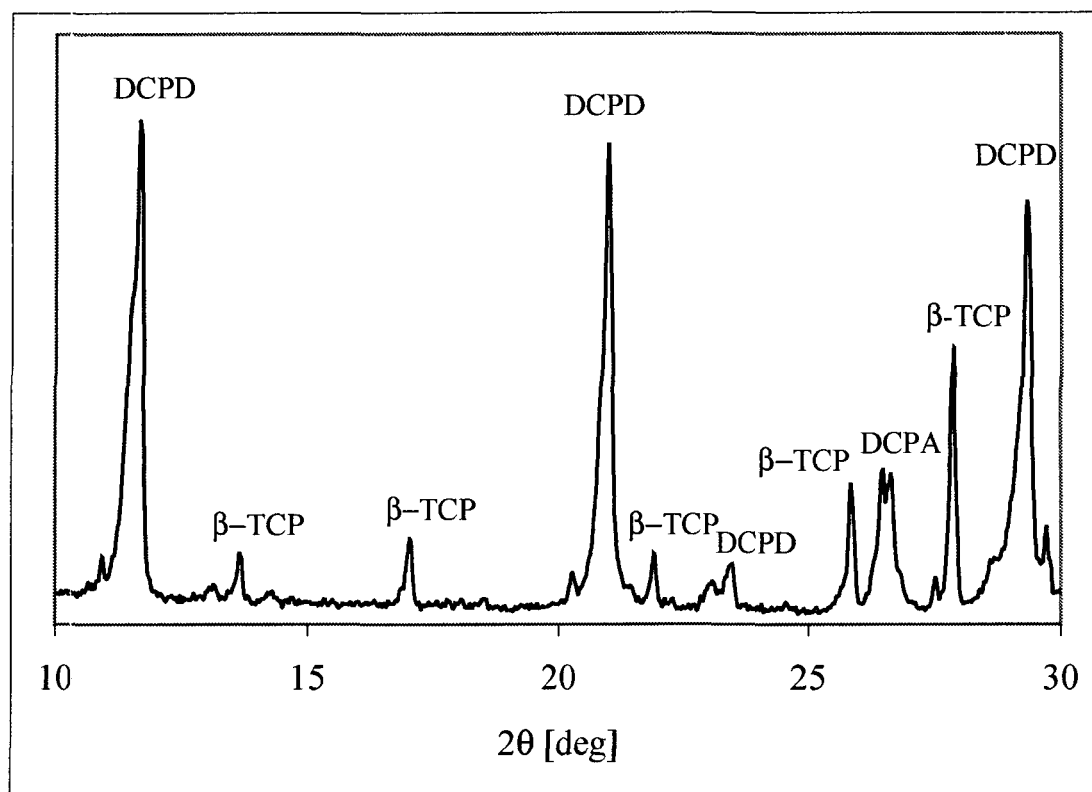|	CSH		CSD	
	without OPA	with OPA	without OPA	with OPA
MCPM [g]	0.613	0.503	0.630	0.516
DCPA [g]	0.367	0.300	0.377	0.309

Figure 3 : Typical X-ray diffractogram of cement

As the enthalpies of the reactions taking place during setting are known, the theoretical setting enthalpies of reaction can be calculated for each of the composition considered. They are shown in Table IV.

Table IV : Theoretical enthalpies of setting reaction of the four cement compositions tested.

	CSH		CSD	
	without OPA	with OPA	without OPA	with OPA
ΔH_r^0 [cal/g]	14.10	16.60	11.34	13.56

The calcium sulfate powders were used under two forms : raw or milled. The specific surface areas of these powders are shown in Table V. All calcium sulfate powders used here were derived from a CSD powder from Merck (Cat no. 1.02160).

Table V : Specific surface areas of the calcium sulfate powders (in m²/g).

	CSH	CSD
Raw	5.20	0.32
Milled	15.3	13.3

Characterization techniques

X-Rays Diffraction. XRD were performed with a Kristalloflex 805 (Siemens) diffractometer ($K\alpha$-Cu radiation), using the coupled $\theta/2\theta$ method.

SEM. Scanning electron microscopy was performed on a JEOL SM-6300F apparatus.

RESULTS

The temperature in the calorimeter was measured for an hour after the beginning of the setting reaction. The parameters derived from the Temperature-time curves are the following : the maximum temperature increase (ΔT_{max}), the degree of conversion of the setting reaction (α_{30}), the maximum reaction rate (v_{max}), the induction or working time (t_i), and the setting time (t_0). The temperature increase is the difference between the maximum temperature reached during setting and the room temperature. The other parameters are derived indirectly from the temperature-time curves. A typical curve measured during setting is shown in Figure 4.
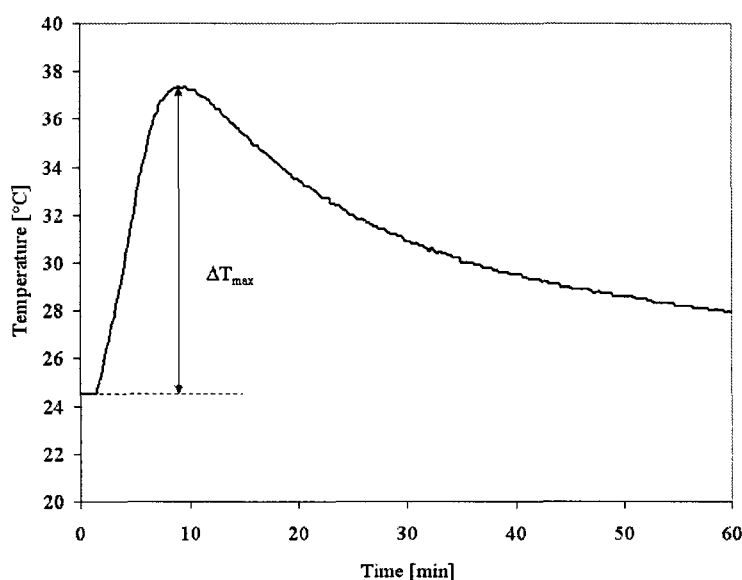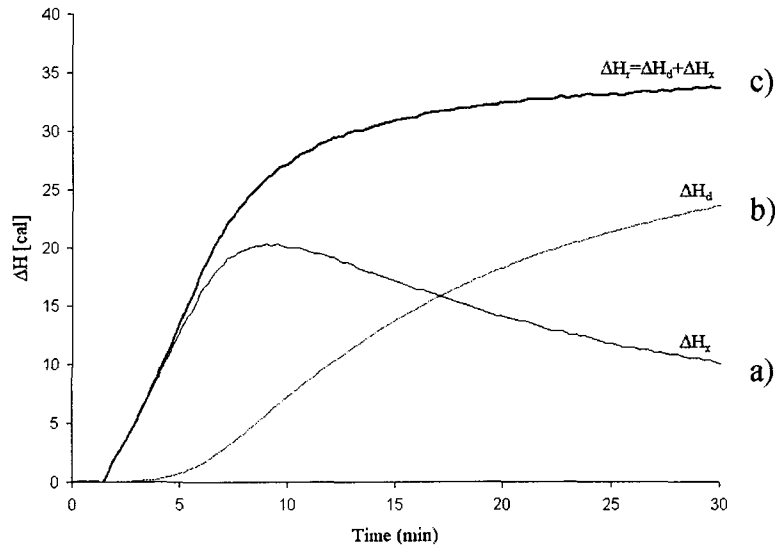
Figure 4 : Typical Temperature-time curve measured during setting.

The enthalpy actually produced by the reaction, ΔH_r, is the sum of the enthalpy measured (ΔH_x) and that dissipated by the system (ΔH_d), as shown in Figure 5. The Degree of conversion-time curve, $\alpha(t)$, is calculated as the ratio $\Delta H_r/\Delta H_{r,th}$. The theoretical enthalpies of reaction, $\Delta H_{r,th}$, are given in Table IV.

Figure 5 : Enthalpy curves. a) measured, b) dissipation, c) corrected.

The degree of conversion (α_{30}) of the reaction is the ratio between the enthalpy produced after 30 minutes, $\Delta H_r(t=30\text{min})$, and the theoretical enthalpy ($\Delta H_{r,th}$) calculated from the starting components (assuming 100% conversion, see Table IV). The first derivative of α with time can be approximated as a log-normal curve :

$$\frac{\partial \alpha(t)}{\partial t} = v_{max} \cdot \exp\left\{-\frac{1}{2}\cdot\left[\frac{\ln(t/t_0)}{c}\right]^2\right\} \tag{8}$$

Two of the three parameters describing such a curve give the maximum rate of reaction (v_{max}) and the time position of the inflection point of the $\alpha(t)$ curve. We define this time as the setting time (t_0) of the cement. v_{max} is actually the slope of the curve at setting time (see Figure 6). The induction time of such a reaction is defined as follows :

$$t_i = t_0 - \frac{\alpha_0}{v_{max}} \tag{9}$$

The correction applied to the enthalpy curves is efficient, since the corrected enthalpies reach a plateau 30 minutes after the beginning of the setting reaction, indicating that the reaction does practically not evolve any more after that period of time (Figure 5).
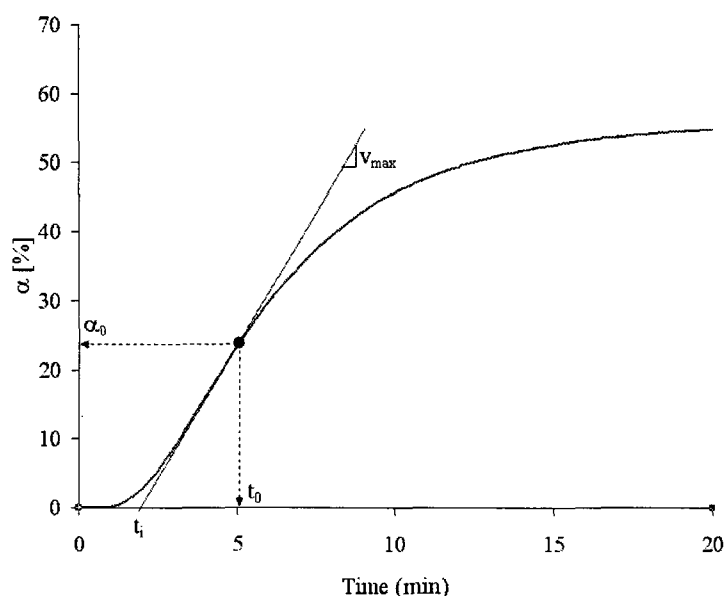

Figure 6 : Typical α(t) experimental curve, and parameters derived from this curve.

The maximum temperature elevations are presented in Figure 7. They vary between 10.8 and 14.3°C. The lower temperature increase is obtained with a cement made with milled CSH, without OPA. Cements with raw CSD without OPA produce the higher temperature increase. Use of CSD instead of CSH appears to increase significantly ΔT_{max}. This effect is stronger when the mixing liquid does not contain OPA. Milling of the calcium sulfate powder induces lower temperature increase.
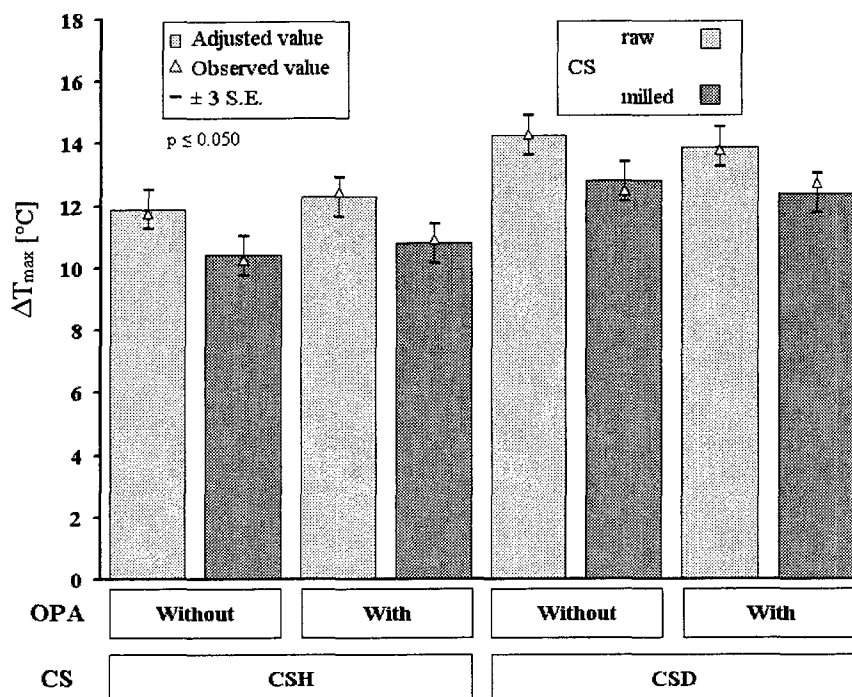
Figure 7 : Maximum temperature increases.

Setting times are shown in Figure 8. They vary between 3 and 8.5 minutes. The dihydrate form of calcium sulfate decreases the setting time, especially when the mixing liquid is free of OPA. The presence of OPA decreases the setting time of cements made with CSH, but has no significant effect when calcium sulfate is used under its dihydrate form. The effects on induction time (or working time) are the same (Figure 9).
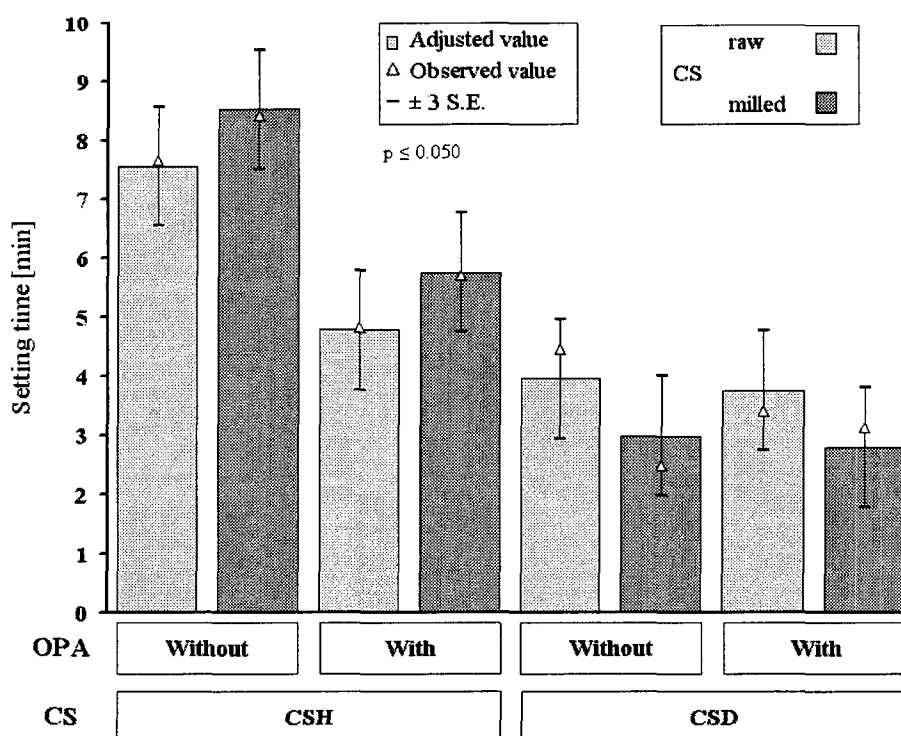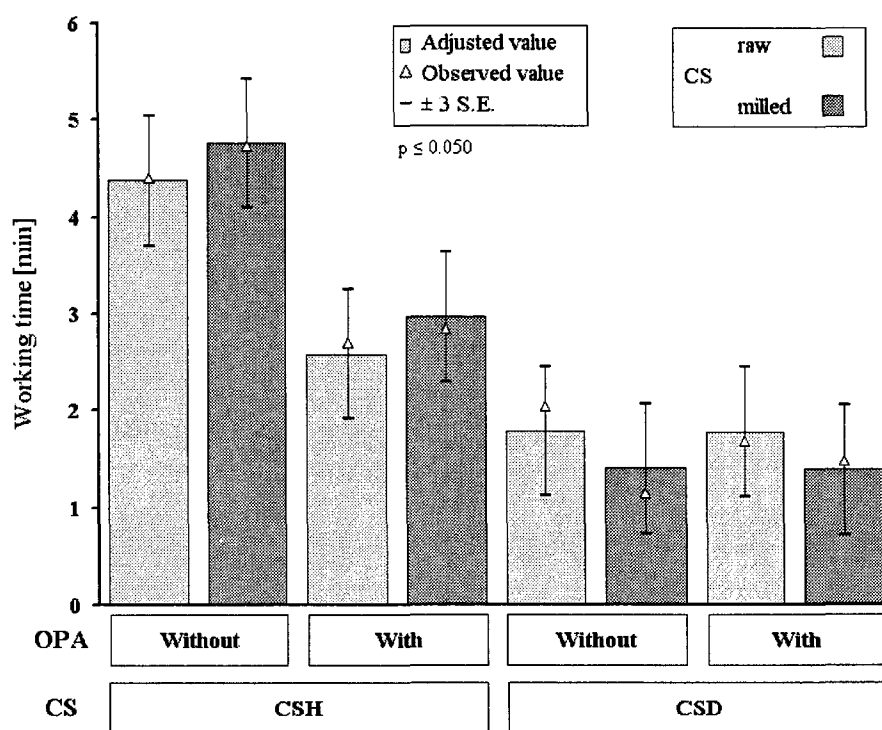
Figure 8 : Setting times.

Figure 9 : Working times.

The maximum reaction rates, v_{max}, are presented in Figure 10. v_{max} is strongly increased when CSD is used. Milling of CSH decreases v_{max}, whereas milling of CSD does not have any perceptible effect. v_{max} is not influenced by the presence of OPA in the mixing liquid.
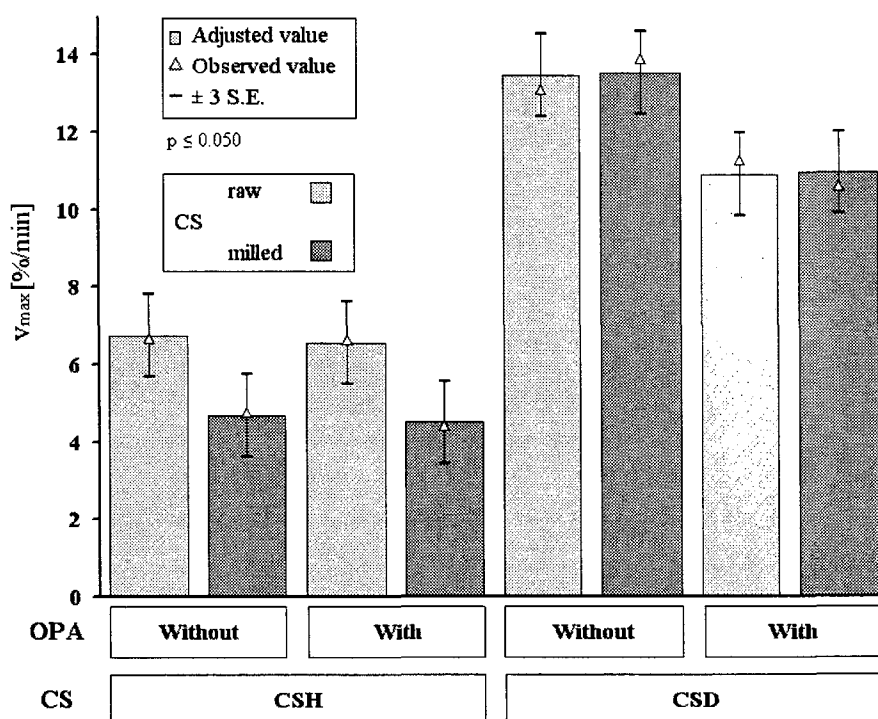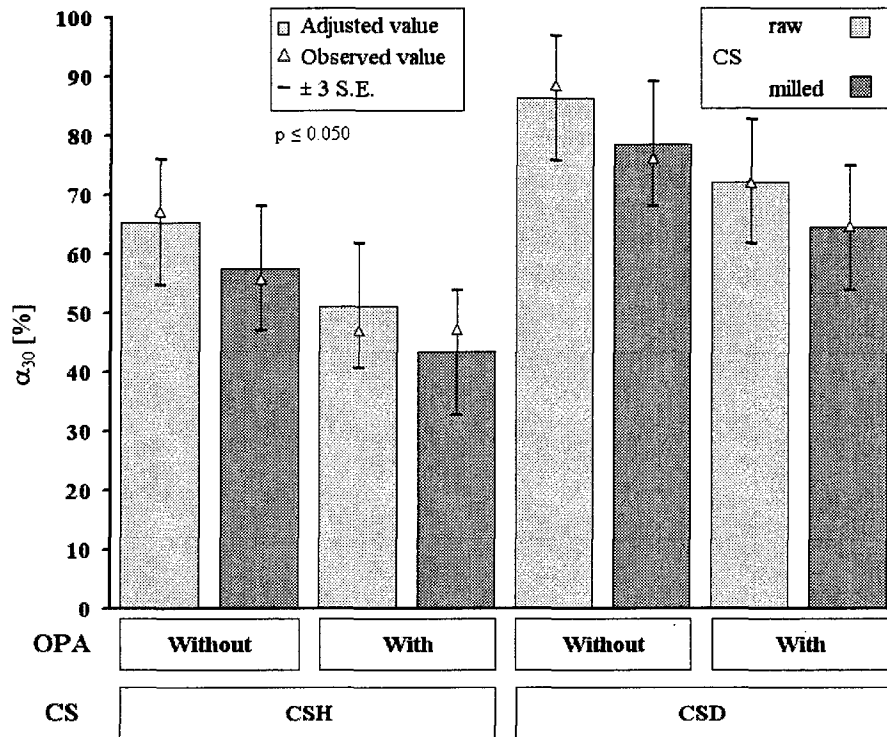
Figure 10 : Maximum reaction rates.

As shown in Figure 11, the setting reaction is found to be more complete when gypsum is used instead of plaster of Paris. Using the milled calcium sulfate powder (whatever its degree of hydration) and adding OPA in the mixing liquid both decrease the degree of conversion of the reaction.

Figure 11 : Degrees of conversion after 30 minutes.

SEM micrographs of the eight cement compositions are shown in Figure 12 and Figure 13. CSD milling appears to refine the microstructure of the cements. Among the CSH-containing cements, those with OPA appear to have a finer microstructure.
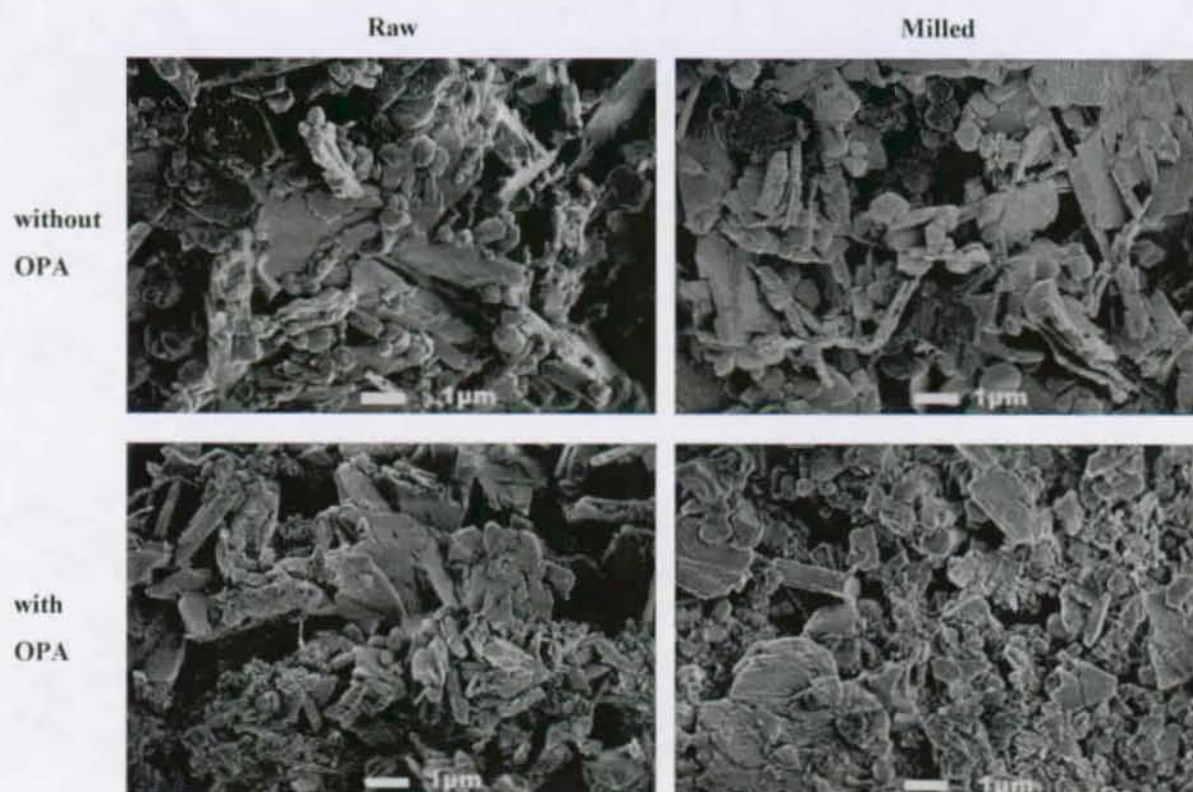
Raw Milled

without
OPA

with
OPA

Figure 12 : SEM micrographs of CSH-containing cements.
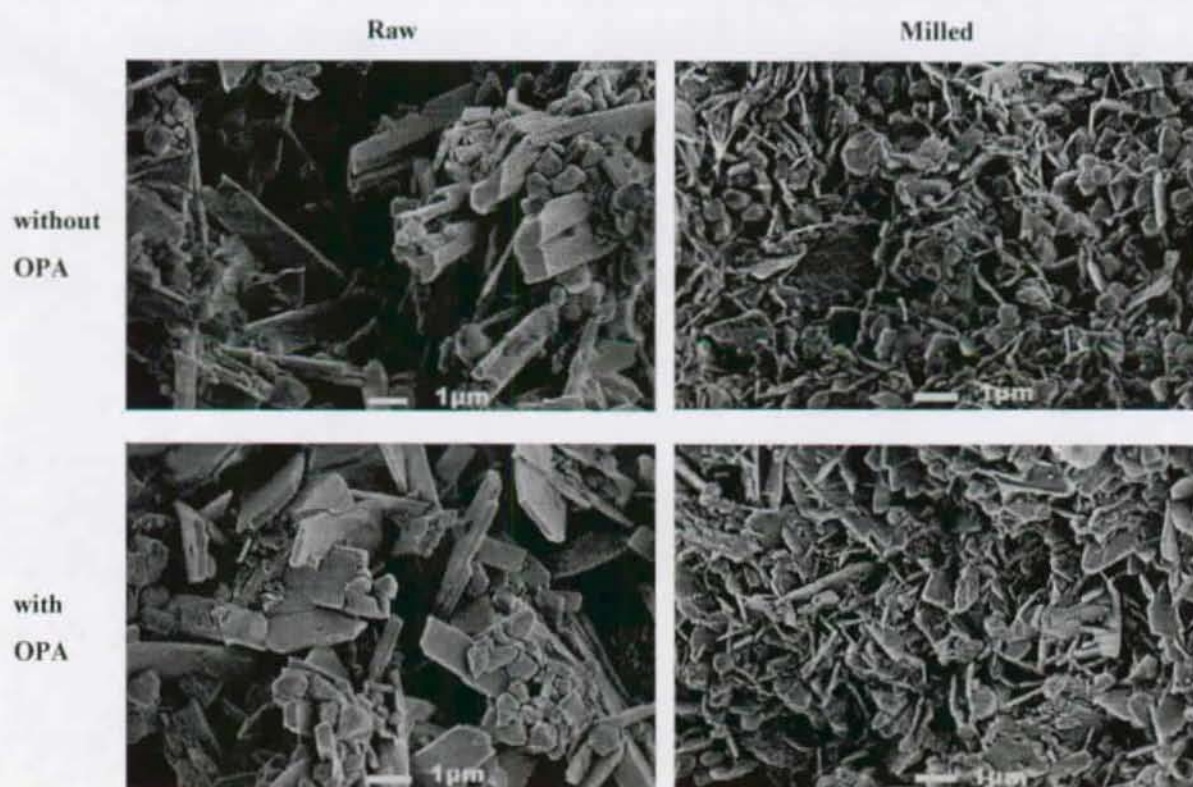
Raw Milled

without
OPA

with
OPA

Figure 13 : SEM micrographs of CSD-containing cements.

DISCUSSION

Whatever the parameter considered, the degree of hydration of the calcium sulfate powder is always the factor that has the strongest effect. Use of CSH slows down the setting reaction. This can be ascribed to the higher level of sulfate ions released in the mixing liquid (CSH is more soluble than CSD), that are known to slow down the setting reaction up to a 0.1 M concentration.[12] In contrast to CSH, CSD appears to accelerate the setting reaction (setting time decreased, v_{max} increased). There are two explanations for this phenomenon. First the solubility of CSD is much lower than that of CSH (0.01 M versus 0.08 M for CSH), so that fewer sulfate ions are solubilised to interact with the setting reaction. Second, as the crystallographic structure of CSD is very similar to DCPD, CSD particles act as heterogeneous nuclei for DCPD crystals,[12] thus accelerating brushite precipitation.

CSD-containing cements have a higher maximum reaction rate and are better converted than those with CSH. These two parameters are usually linked in that sense, since the faster the reaction, the more complete it should be after a given time.

As the gypsum powder can be considered quasi-inert, it does not contribute to the global reaction enthalpy. Therefore, cements prepared with CSD should produce less heat upon setting than those with CSH, as predicted by the results of the reaction enthalpy calculations shown in Table IV. However, the temperature increase is larger for CSD-containing cements. This contradictory finding can most probably be ascribed to faster heat accumulation in the calorimeter : as CSD shortens the setting time and increases the maximum reaction rate (Figure 8 and Figure 10), heat production occurs faster, then dissipation compensates less efficiently than with slower reaction rates. As a consequence, the temperature rise is more important.

This heat accumulation effect shows that setting time and maximum reaction rate of the cement interact with heat dissipation of the system to influence the temperature elevation measured during setting. It shows that temperature elevation is a measurable entity depending both on the cement and on its environment. In practice, the osseous site of implantation may undergo different temperature elevation depending on its characteristics, e.g. bone density or vascularization.

Milling of the CS powders is found to decrease the temperature rise during setting, although theoretically no difference in peak temperature should occur. This discrepancy can probably be ascribed to the lower degree of conversion of the reaction observed for cements made with

milled sulfate powders. The effect of milling on setting time is different whether achieved with CSH or CSD. Milled CSH appears to increase the setting time and decrease the maximum reaction rate, probably because of faster CSH dissolution. The decrease of the setting time induced by CSD milling is probably due to the fact that DCPD formation is favoured by the higher number of gypsum particles acting as sites for heterogeneous nucleation. This hypothesis is confirmed by the SEM micrographs of the CSD-containing cements, showing a refinement of the microstructure (smaller, close-packed, DCPD crystals) upon milling.

As the maximum reaction rate is not influenced by milling of CSD, the beginning of the enthalpy curve (before setting time) is simply shifted towards shorter times. This means that in this case the induction time is shorter, but once the reaction has started it takes place at the same rate. From a physico-chemical viewpoint, nucleation is favoured, but growth of the brushite crystals is not affected.

The presence of OPA does not affect greatly the maximum temperature elevation : it slightly increases the temperature rise of CSH-containing cements, and slightly decreases that of CSD-containing cements. These effects never exceed 0.5°C, and are significant at a 1.7% error risk level. However, our laboratory experience with brushite cements has already shown clear effects of OPA on temperature rise during setting. Some MCPM powders as purchased may contain up to 25 wt% OPA. Washing these powders in ethanol allows elimination of the excess acid from the powder. It was observed that OPA-containing MCPM powders produce a larger temperature increase than washed powders. In this study, the amount of OPA added may be too low to show significant effects.

CSH-containing cements have a shorter setting time when OPA is present in the mixing liquid. As OPA shifts the pH of the mixing liquid towards more acidic values. β-TCP dissolution is favoured and, consequently, saturation of the solution relative to DCPD is increased, which accelerates its precipitation and shortens the setting time of the cement. In contrast, the maximum reaction rate of these cements is slightly decreased upon addition of OPA. This suggests that growth of brushite crystals is hindered. This seems to be confirmed by the SEM micrographs of these cements (Figure 12, bottom). The slower reaction rate explains probably why cements with OPA-containing mixing liquids have a poorer degree of conversion.

Induction times are always affected in the same way as setting times by the factors discussed above. We consider that induction time can also be called working time. The latter notion is always difficult to define in practice. The physical meaning of induction time is the period after which the setting reaction starts. From this moment, the paste becomes thicker and more and more difficult to work. It may be argued that the paste can still be worked after that time. However, kneading the paste after that period should best be avoided, since it may destroy the forming structure. Induction times of the cements tested here range between 1.5 and 4.5 minutes. 1.5 minutes is probably too short a working time, whatever the application considered.

The custom-made calorimeter developed here allows several values to be obtained from a single experimental curve. The temperature increase is directly read from the experimental Temperature-time curve. All the other parameters calculated here follow from the assumption that the first derivative of the enthalpy curve can be approximated by a log-normal curve. Observation of the sum of the squares of the residuals confirms the relevance of this assumption. The temperature increase is system-dependent. In contrast, all the parameters derived from the corrected enthalpy curves should not depend on the measurement system, so long as the correction for heat dissipation is correct. Three of them describe the kinetics of the reactions : maximum reaction rate, induction time, and setting time. The two latter are parameters that are of prime importance in practice, since they have to match the surgeon's needs. Usually, setting times are estimated with a Vicat needle, but performing this measurement is tedious and time-consuming, and the times measured are less precise than those obtained from the thermometric method presented here.

CONCLUSIONS

The custom-made calorimeter developed here allows measurements of the temperature increase occurring during setting of brushite cements. Additionally, kinetic parameters like induction time of the reaction, setting time and maximum reaction rate can be derived from the enthalpy curves obtained. The degrees of conversion of the cements are calculated as the ratio between the enthalpies produced and the theoretical ones.

As heat dissipation occurs during measurement, experimental curves must be corrected for heat loss. As the corrected enthalpy curves reach a plateau after 30 minutes, the correction can be considered adequate.

The major effects that can be evidenced in this study are the opposite effects of plaster of Paris (CSH) and gypsum (CSD). The latter shortens the working and setting times because it provides nuclei for heterogeneous precipitation of brushite. In contrast, CSH increases the working and setting times by releasing sulfate ions – known as setting retardors - in the mixing liquid.

It is the first time to our knowledge that a single experiment allows determination of both thermometric and kinetic parameters of a calcium phosphate cement. Furthermore, this type of experiment appears to be very convenient in practice, and replaces advantageously the conventional methods used for determination of setting times.

REFERENCES

[1] Brown WE, Chow LC. Dental restorative cement pastes, US Patent 4,518,430, 1985.

[2] Constantz B R, Ison I C, Fulmer M T, Poser R D, Smith S T, Van Wagoner M, Ross J, Goldstein S A, Jupiter J B, Rosenthal D I. Skeletal repair by in situ formation of the mineral phase of bone. Science 1995;267:1796-1799.

[3] Knaack D, Goad MEP, Aiolova M, Rey C, Tofighi A, Chakravarthy P, Duke Lee D. Resorbable calcium phosphate bone substitute. J Biomed Mater Res (Appl Biomater) 1998;43:399-409.

[4] Mirtchi AA, Lemaître J, Terao N, Calcium phosphate cements: study of the β-tricalcium phosphate-monocalcium phosphate system. Biomater 1989;10:475-480.

[5] Sanchez-Sotelo J, Munuera L, Madero R. Treatment of fractures of the distal radius with a remodellable bone cement: a prospective, randomised study using Norian SRS. J Bone Joint Surg Br 2000;82:856-863.

[6] Costantino PD, Friedman CD, Jones K, Chow LC, Sisson GA. Experimental hydroxyapatite cement cranioplasty. Plast Reconstr Surg 1992;90:174-191.

[7] Mahr MA, Bartley GB, Bite U, Clay RP, Kasperbauer JL, Holmes JM. Norian craniofacial repair system bone cement for the repair of craniofacial skeletal defects. Ophthal Plast Reconstr Surg 2000;16:393-398.

[8] Deramond H, Wright NT, Belkoff SM. Temperature elevation caused by bone cement polymerization during vertebroplasty. Bone 1999;25:17S-21S.

[9] Leeson MC, Lippitt SB. Thermal aspects of the use of polymethylmethacrylate in large metaphyseal defects in bone. A clinical review and laboratory study. Clin Orthop 1993;295:239-245.

[10] Fernandez E, Ginebra MP, Bermudez O, Boltong MG, Driessens FCM, Planell JA. Dimensional and thermal behaviour of calcium phosphate cements during setting compared to PMMA bone cements. J Mater Sci Lett 1995;14:4-5.

[11] Montgomery DC. Design and analysis of experiments. 3rd Ed. New York: Wiley; 1991.

[12] Bohner M, Lemaître J, Ohura K, Hardouin P. Effects of sulfate ions on the in vitro properties of β-TCP – MCPM – water mixtures. Preliminary in vivo results. Bioceramics : Materials and Applications. pp. 245-259. Ed. by Fishma G, Clare A, and Hench L. American Ceramic Society, Westerville, OH, 1995.

CHAPTER 7   GENERAL CONCLUSIONS

The global objective of this thesis was to understand how the starting components of the brushite cement influence the properties relevant for its use in vertebroplasty. The work was divided into five different studies. The objectives and main results of each study are recalled here.

As a reminder, the chapters of the thesis are recalled here :

- **Chapter 1 :** General introduction.
- **Chapter 2 :** Mechanical characterization of brushite cements: A Mohr circles' approach.
- **Chapter 3 :** Influence of the starting powders granulometry on the mechanical strength of a calcium phosphate brushite cement.
- **Chapter 4 :** A model for calculations of bone cements radiopacity : Development and validation.
- **Chapter 5 :** Radiopacification of calcium phosphate brushite cements with iodine-containing additives.
- **Chapter 6 :** Influence of the starting compositions on kinetic and thermometric properties of brushite cements.
- **Chapter 7 :** General conclusions.

Chapter 2

To carry out the global objective, a test protocol was developed to characterise as fully as possible the mechanical properties of calcium phosphate cements. Two mechanical tests were performed : diametral compression (or Brazililan) and axial compression tests. The first one allows indirect measurement of the cement tensile strength, and the second one gives the compressive strength.

We tried to understand how the diametral tensile strength of our cements measured with the Brazilian test compares with their direct tensile strength. The Mohr's circles representation allowed to understand that for a material like our cement, the ultimate stress measured with

the Brazilian test must be an underestimate of the tensile strength because the compressive/tensile strength ratio is lower than 8.

From the Mohr circles representations, the intrinsic curves of the cements tested were calculated, but it appeared that no coherent true tensile strength (σ_0) value could be derived from curves calculated with the combination of the results of the Brazilian and the compression tests. Nevertheless, it appears important to perform the two tests to have a better understanding of the mechanical behaviour of a cement. Furthermore, the Brazilian test remains a test that is easy to use with brittle materials and requires simple sample shape. Therefore, it was considered as an appropriate test for our cements, even though the results it brings cannot be used to calculate intrinsic curves from the Mohr's circles representation.

Chapter 3

The objective of this study was to try to increase the mechanical strength of a brushite cement by refining the granulometry of the starting powders. The three starting powders (MCPM, CSH and β-TCP) were milled, and the effect of their granulometry on compressive and diametral strengths was studied.

The milling of MCPM and CSH was found to be beneficial both to the compressive and the diametral tensile strengths of the cements, providing a five-fold inrease in axial compression, and a three-fold increase in diametral compression. The mechanical strengths of cements made with milled MCPM and CSH were the highest measured in this thesis work : 4.1 MPa indirect tensile strength and 22.1 MPa compressive strength. For comparison, cancellous bone structures have compressive and tensile strengths that never exceed 5 MPa. In contrast with MCPM and CSH, β-TCP milling did not bring any benefits to the mechanical strength of the cements, mainly because the Solid/Liquid ratio had to be drastically decreased to produce a paste with the same rheology as the one made with raw β-TCP. Finally, this study also showed that the mechanical properties of the cement are strongly dependent on CSH granulometry and chemical purity.

Chapter 4

As X-ray opacity of cements used in vertebroplasty is always adapted in the field by clinicians so as to suit their needs, no specification regarding this cement property is available. This is why we proposed to assess the X-ray opacification a bone cement should produce to be used safely in fluoroscopic image-guided vertebroplasty. To achieve this goal, a

simple computer model was developed with Matlab[®] to calculate the linear X-ray attenuation coefficient of any material of known composition.

After validation, the computer model was used to calculate the standard attenuation coefficient a cement should exhibit to be used in vertebroplasty. It was calculated from an acrylic cement composition considered a standard in vertebroplasty, and was found to amount 2.47 cm^{-1} for the conditions simulated here.

Then, linear attenuation coefficients of various existing calcium phosphate cements were calculated. None of these was found to exhibit an attenuation coefficient as high as that of the standard one, which means that no calcium phosphate cement could be used safely in vertebroplasty in its current formulation.

Chapter 5

As the preceding study showed the necessity of opacifying calcium phosphate cements if these were to be used in vertebroplasty, we tried to make brushite cements with suitable X-ray opacity and assessed the effects of some iodine-containing opacifiers on the setting and mechanical properties of the brushite cement. The mechanical strengths were measured with the Brazilian and the compression tests.

None of the opacifiers appeared to alter the setting time of the cement or to decrease significantly its compressive or diametral tensile strengths. Iopentol seems to be the most promising opacifier, from toxicity and mechanical viewpoints.

Chapter 6

The last study dealt with thermal and kinetic properties of brushite cements. The objective was to document the thermal behaviour of these cements. It was achieved by developing a custom-made calorimeter. A single measurement allowed calculation of the maximum reaction rate of the setting reactions, the working and setting times of the cement pastes, the degree of conversion of the cements, and the temperature increase induced by the setting reaction.

Compared with CSH, CSD-containing cements accelerate the setting reaction. They also appear to provoke a higher temperature rise during setting. This is actually a consequence of the faster heat accumulation in the system, resulting in higher temperature elevation.

General conclusions and perspectives

The test protocols developed during this thesis allow us to have a better insight into the relationships between starting cement composition and mechanical, kinetic and thermal properties of the brushite cement. We showed that refining MCPM and CSH powders is a very efficient way to increase the mechanical strength of the cement, both in diametral and axial compressions. However, as the mechanical properties of the cements are strongly dependent on the granulometry of the starting powders, milling and drying routes must be under full control in order to ensure constant and precise granulometries of the resulting powders. This happens not to be the case presently, and fine tuning of these routes will be necessary to produce powders ensuring reproducible cement properties.

Calcium sulfate can be added to the cement in its hemihydrate (CSH) or dihydrate (CSD) forms. We now know what are their effects on setting time and temperature increase during setting, but it would be interesting now to analyse, in further studies, their effects on the mechanical properties of the cements. This influence will not be easy to assess, since the strength of the hardened cement depends also on the powders granulometry.

The custom-made calorimeter developed during this work seems to be an easy and precise way of measuring thermal and kinetic properties of the cement pastes. These measurements are easy to realise in practice and give reproducible results.

It was shown that the current X-ray opacity of the brushite cement is not sufficient for safe use in vertebroplasty. However, we found that incorporation of Iopentol, a contrast media commonly used in X-ray imaging applications, does not impair the mechanical properties of the cement and does not alter the setting time of the reaction either. The effect on the thermal and kinetic behaviours should be studied in the calorimeter developed in this work to assess its influence on the thermal and kinetic properties of opacified cements.

In conclusion, several properties of the cement material itself have been studied : they were mechanical, physical (radiopacity), or thermodynamic. These properties have been related to the cement compositions and the characteristics of the starting components. However, their effects on the biological behaviour of the cements remain to be clarified. Once a formulation is selected according to the criterions studied here, an in vivo experiment should be conducted on a suitable animal model in order to study its biocompatibility, osteinduction and resorption.

Christian Pittet
Rue de Champ-Fleuri 12
1022 Chavannes-Renens
phone: private +41 (0)21 691.08.34
          prof.   +41 (0)21 693.58.96
          GSM   +41 (0)78 711.34.57
e-mail : christianpittet@hotmail.com

Swiss
29 years old
Single

Education

2001	**Ph. D. Thesis** in Materials Science at EPFL
1997	**Postgraduate Diploma in Biomedical Engineering** (EPFL - UNIL). (Biomechanics, Biocomputing, Artificial organs, Medical imaging).
1997	**Engineer Diploma in Materials Science** at the Swiss Federal Polytechnical School (EPFL).
1991	Maturity Certificate type C at the Collège de Staël in Geneva, Switzerland.

Publications

Pittet C, Lemaître J. Mechanical characterization of brushite cements : A Mohr circles' approach. J Biomed Mater Res (Appl Biomater) 2000;53:769-780.

Charrière E, Terrazzoni S, Pittet C, Mordasini P, Dutoit M, Lemaître J, Zysset PK. Mechanical characterization of brushite and hydroxyapatite cements. Biomaterials 2001;22(21):2937-2945.